THE ROLE OF OSTEOBLASTIC β ADRENERGIC SIGNALING IN BREAST CANCER METASTASIS TO BONE

by

James Preston Campbell

Dissertation

Submitted to the Faculty of the

Graduate School of Vanderbilt University

in partial fulfillment of the requirements

for the degree of

DOCTOR OF PHILOSOPHY

in

Pharmacology

December, 2012

Nashville, Tennessee

Approved:

Professor David Robertson

Professor Florent Elefteriou

Professor Joey Barnett

Professor Ron Emeson

Professor Andries Zijlstra

DEDICATION

To my children Kilian and Keaton, who are my inspiration and motivation

To my wife Kathryn, who is my partner and my light

To my parents who opened my life to science

To my brother, thanks for challenging me always

To my mentor, Florent and the Department of Pharmacology that put up with my nonsense for many years

To all the scientists and friends that have come and gone in the Bone Center, thank you for making science happen

ACKNOWLEDGEMENTS

This science would not have been possible without substantial contributions from a great many people. Indeed, the entire scientific community has made this possible through a longstanding tradition of tireless and amazing discovery.

First and foremost, I must mention my mentor, Florent Elefteriou, whose enthusiasm and remarkable understanding of multiple biological systems allowed this project to succeed. He also taught me how to ‘focus!’ my science into something testable. I would like to thank my committee members: David Robertson for insight and direction about sympathetic physiology; Ron Emeson for neuroendocrine input on the chronic stress model and the infamous ‘Pharmacology Qualifying Exam’; Andries Zijlstra for invaluable and timely input about cancer biology; and Joey Barnett for offering timely and pragmatic methods for putting out so many of the academic fires I set.

I must also acknowledge the following scientists in the Bone Center for all of their help and suggestions: Julie Sterling for being a second mentor, multiple collaborations, and countless intracardiac injections; Matt Karolak for the knockdown experiments; Javier Esparza for countless sessions of troubleshooting and Spanish lessons; Heather Moss, Barbara Rowland, for invaluable technical expertise; Steve Munoz for imaging expertise, software assistance, and for playing devil’s advocate on any hypothesis; James Edwards and Josh Johnson for histological help; Rachelle Johnson, Claire Edwards, Swati

Biswas, Aubie Shaw , and Jessica Fowler for help with a thousand different cancer questions; Yun Ma for collaborations and knowledge of all things related to β2AR in bone; Dan Perrien for deep knowledge of bone and μCT; Jeff Nyman for statistics help and an engineer's view of the project; Lian Na, Weiguang Wang, Lingzhen Li, and Xiangli Yang, for their disciplined molecular insight and criticisms; and Dr. Greg Mundy for teaching the value of choosing the 'go or no go experiment'.

The amazing people in the Vanderbilt Department of Pharmacology must also be acknowledged for rigorous training I experienced during my studies: Lee Limbird for receptor theory; all the students that helped with the various qualifying exams; Karen Gieg for keeping me in line; and all the other pharmacologists that taught me the definition of agonist.

Lastly I would like to thank my family for helping me get to this point; my parents for feeding me science; my brother for invaluable support in innumerable ways; my children for inspiration and asking creative questions; and my wonderful wife Kathryn for enforcing scientific diligence and just the right balance of skepticism and support during this project.

TABLE OF CONTENTS

LIST OF FIGURES

Page

LIST OF ABBREVIATIONS

SNS	Sympathetic Nervous System
β2AR	Beta 2 Adrenergic Receptor
TGf-β	Transforming Growth Factor Beta
CXCL12	chemokine (C-X-C motif) ligand 12
SDF1	stromal derived factor 1
ALCAM	activated leukocyte cell adhesion molecule
IL-6	interleukin 6
VEGF	vascular endothelial growth factor
TLI	thymidine labeling index
SPI	s-phase index
Bcl-2	B-cell lymphoma protein 2
ECM	extra cellular matrix
RANK	receptor activator nuclear factor k-B
RANKL	receptor activator nuclear factor k-B ligand
CXCR4	chemokine (C-X-C motif) receptor 4
PTHrP	parathyroid hormone related peptide
TNF	tumor necrosis factor
TRANCE	TNF-related activation induced cytokine
OPG	osteoprotegerin
OPGL	osteoprotegerin ligand
TRAF	TNF receptor associated factor protein
JNK	c-jun N-terminal kinase
TACE	tumor necrosis factor-α-converting enzyme
MMP	matrix metalloproteinase
sRANKL	soluble RANKL
rRANKL	recombinant RANKL
cAMP	3’-5’-cyclic adenosine monophosphate
PTH	parathyroid hormone
GFP	green fluorescent protein
μCT	micro computer assisted tomography
NPY	neuropeptide Y
PGP	protein gene product 9.5
DBH	dopamine beta-hydroxylase
CB1	cannabinoid receptor 1
2AG	2-arachidonoylglycerol
CNS	central nervous system
BMD	bone mineral density
CRH	corticotropin-releasing hormone
ACTH	adrenocorticotropic hormone
PTSD	post-traumatic stress disorder
HPA	hypothalamic pituitary adrenal axis

CIS	chronic immobilization stress
CUS	chronic unpredictable stress
TrKC	tyrosine kinase receptor type 3
α-CGRP	alpha calcitonin gene related peptide
ISO	isoproterenol; isoprenaline
PBS	phosphate buffered saline
EDTA	ethylenediamine tetra-acetic acid
H&E	haemotoxylin and eosin
TRAP	tartrate resistant alkaline phosphatase
BMSC	bone marrow stromal cells
MC3T3	mouse calvarial 3T3 cells
DMEM	Dulbecco's modified eagle medium
RT-PCR	reverse transcriptase polymerase chain reaction
qPCR	quantitative polymerase chain reaction
cDNA	complimentary deoxyribonucleic acid
shRNA	short hairpin ribonucleic acid
FBS	fetal bovine serum
SEM	standard error of the mean
ANOVA	analysis of variance
IC	intracardiac
5-HT	5-hydroxytryptamine (serotonin) receptor
D2	dopamine receptor type 2
α2AR	alpha adrenergic receptor type 2

CHAPTER I

INTRODUCTION

Importance of the microenvironment in cancer

The significance of micro environmental influences on cancer metastasis was proposed by Fuchs [1] and later by Paget [2] in the “seed and soil” hypothesis of the “relation between the embolus and the tissues which receive it” more than a century ago. They proposed that the spread of malignant tumors to distant sites was not solely dictated by blood flow; that a cancer, the ‘seed’, required a fertile ‘soil’, referring to the organ-specific factors that dictate the successful establishment of a metastasis. Physicians noted that each type of malignancy had a tendency to metastasize to certain organs. For example, prostate and breast cancers had a predilection for bone, lung, and liver, while colon cancers frequently metastasized to liver but not to bone. Since each cancer had its own metastatic profile, it was obvious that each malignancy had specific characteristics that caused it to home to or prosper within a particular organ. What was not so obvious was that each organ must have had a set of characteristics that *permitted* the tumor to establish and grow. The vast majority of cancer research has focused upon creating techniques to directly inhibit cancer growth at both primary and metastatic sites- attacking the ‘seed’ so that it might not grow. Only recently has interest turned to studying the fertility of the ‘soil’ to reveal approaches that may prevent cancer growth and metastasis.

Though the concept was originally postulated with Paget's hypothesis, the words 'tumor microenvironment' appeared in the literature less than three decades ago. In the years since, the medical community has revealed a variety of means by which a tumor alters its surroundings to increase its chances of survival, encompassing every step of the metastatic process. Most of these studies however, do not address the role of the pro-metastatic microenvironment prior to the arrival of a cancer, which is at the center of our research. Specifically we have evidence that the sympathetic nervous system (SNS) can affect the bone marrow microenvironment to increase the likelihood of breast cancer metastasis to the long bones.

Metastasis accounts for virtually all breast cancer deaths and can occur in bone, lung, liver, brain and lymph nodes. Amongst these metastases, those in the bone are most common, observed in approximately 70% of breast cancer fatalities [3], and are primarily osteolytic in nature [4]. Currently available therapeutics, most of which target the cancer cells directly, are ineffective in bone metastatic breast cancer [5] and are limited to the treatment of bone symptoms and complicating fractures seen in cancer -induced bone disease. There is thus a critical need for identification of therapeutics that directly target the metastatic process and prevent the establishment of malignant foci in distant organs.

The process of cancer metastasis is multifactorial, influenced by a combination of genes, epigenetic changes, and influences of the surrounding stroma [6]. Induction of the metastatic process is dependent upon intrinsic cancer cell characteristics that dictate how cells migrate, survive and proliferate, as well as

on the cellular and cytokine profile of the tissue from which the cells initially egress. Later steps of metastasis are also governed by the microenvironment to which metastatic cancer cells ultimately home [7]. The mechanisms underlying the organ-specific nature of bone metastasis are governed by chemo-attractants (e.g. CXCL12/SDF1), attachment molecules (e.g. ALCAM, annexin II), and cytokines that regulate cell growth and angiogenesis (e.g. IL6 and VEGF) [8, 9]; what remains unclear, however, are the conditions and factors that regulate the expression or activity of these critical molecules to affect cancer cell bone colonization, establishment, tumor growth, metastatic progression, and recurrence. Characterization of these processes is critical to understanding why some people are more susceptible to skeletal metastasis and the role bone plays in chemoresistance and relapse.

Metastatic Cascade

Metastasis consists of multiple overlapping steps that must be coordinated both spatially and temporally for a cancer cell to successfully escape a primary site and establish a distant tumor. For illustrative purposes the steps of metastasis can be explained as discrete, sequential cellular and tissue level processes that result in metastasis, though this is a gross oversimplification. Initially, ample growth within the primary tumor is necessary to provide the sheer number of cells, due to chance, with the necessary sum of specific characteristics necessary for successful metastasis. The cells must then escape from the primary organ, and eventually arrest in and colonize a regional lymph

node or a distant metastatic site. What is often overlooked is that a supportive microenvironment is necessary at each step in the metastatic process. From the primary tumor where the stroma can contribute to >50% of the tumor mass [10, 11] to the distal pre-metastatic niche where stromal compliance is required for tumor establishment , [12-14] it is clear that the micro environmental influences are of central importance to cancer progression.

Growth and Proliferation

Clinically, high proliferative rate of tumor cells does not cause tumor aggressiveness but is a variable associated with it, and can be used as a prognostic factor. This suggests that the ability of tumor cells to avoid regulatory pathways which control other genes in addition to their proliferation appears to be a good index of tumor progression, rather than proliferation itself [15-18]. This is evidenced by clinical studies showing no correlation of TLI (thymidine labeling index) or SPI (s-phase index) with disease free status [15], while ki67 and certain cyclins are of prognostic value [19]. In terms of proliferation at a primary tumor, cancer cells need to avoid cell cycle arrest, proceed through S-phase, even though they contain a number of DNA mutations, and gradually accumulate more advantageous growth characteristics, all of which serve to increase the size of the tumor and the chance that a particular subset of cells will be metastatic.

Stromal contributions to primary tumor growth are also necessary for malignant progression. In vivo work has shown that gene expression profiles of the surrounding stroma can dictate whether a tumor can rapidly proliferate and

gain other malignant properties, independent of genetic changes in the tumor [20]. Tumor proliferation and growth can be mediated through stromal metabolic coupling [21], inflammation and immune modulation [22], and blood vessel recruitment [23].

Apoptosis

Apoptosis plays a slightly different role than proliferation in metastatic progression, though the two processes are often coordinated. Cancers must acquire combination of anti-apoptotic genes that allow a particular subset of tumor cells to survive, while having sufficient mutations in genes involved with other pro-metastatic pathways While proliferation serves to expand the cell population and thereby increase the numbers of cells with prometastatic changes, suppression apoptosis serves to increase the survival of aggressive cells, without necessarily increasing the number initially. Among the well-known factors involved in preventing apoptosis in malignant cells are Bcl-2 [24], p53 [25], and c-myc [26], which may also play roles in proliferation and other metastatic behaviors. Again, these and other apoptotic pathways are often subject to the whims of otherwise normal cells in the tumor's microenvironment [19, 24].

Angiogenesis

Angiogenesis is necessary for the expansion and eventual escape of malignant cells [27]. Angiogenesis requires endothelial cells in the stroma to sprout new extensions into the tumor from existing blood vessels in the stroma. This step in the metastatic cascade shows a clear necessity of stromal participation since the cancer cells themselves have not been shown create blood vessels except in rare circumstances in glioblastoma [28]. Angiogenesis is promoted by the cytokines by the tumor and tumor associated macrophages [29] as well as other myeloid lineage cells [30, 31]. Besides their role in feeding the tumor these blood vessels also provide an avenue of escape in the next step of metastasis.

Invasion

After attaining a certain size, the tumor increases the chance that a subset of its cells will have the ability to undergo the next step in metastatic progression which is invasion. In this process, tumor cells often with assistance from infiltrating immune cells such as M2 macrophages [32], dissolve certain components of the ECM (extracellular matrix) [33], become motile and invade through the basement membrane. This escape from the confines of the primary tumor/organ is achieved through changes in cancer cell morphology and motility in conjunction with MMP's and other degradative enzymes, many of which overlap with pro-angiogenic processes [34].

Intravasation

Once cancer cells have begun invading the surrounding tissue, they must then acquire a means of transportation to effectively metastasize. These travel routes are primarily veins and lymphatic vessels [35], but can also include arteries and even cerebrospinal fluid. Malignant cells migrate through the walls of and enter these vessels through a process called intravasation, much like immune cells at a site of inflammation. Yet again, stromal contributions to this process must be considered in changing the expression of invasive genes in the tumor [36, 37] to directly assisting in the intravasation of the vessel wall [38]. After entering the vasculature, metastatic cells must survive during transit to their eventual host organ. Any and all anti-apoptotic characteristics are obviously helpful for the prospective metastatic cell during this stage of malignancy.

Extravasation

Disseminated cancer cells that are durable enough to survive in circulation must arrest in and grow in a compatible environment. To accomplish this they must first adhere to the endothelial walls of the blood or lymph vessel or become imbedded in the microvasculature, and then extravasate through to the underlying tissue, in a similar fashion to leukocytes [39]. Among the factors that promote this metastatic step are chemokines like CXCL12 (sdf1) [36, 40-42], integrins [43, 44], and numerous adhesion molecules [45, 46]. Not surprisingly, this part of the metastatic cascade is also regulated by non-tumor cells in the microenvironment [46, 47].

Arrest and Distal Establishment

After extravasation through the vessel wall and into the stroma of the target organ, metastatic cells must avoid immune surveillance, then survive long enough to migrate to the proper metastatic niche within organ, proliferate, and modify the microenvironment, in agreement with the 'seed and soil' hypothesis. Again, tumor and stroma can coordinate to firmly establish a micrometastasis that eventually progresses to become lethal. Numerous stromal factors have been shown to mediate changes in the pre-metastatic niche to increase likelihood of metastatic establishment and subsequent progression. These include , but are not limited to, numerous metalloproteinases [48], multiple chemokines [49-51] , IL6 [52], and RANKL [53], which are clinically correlated with metastasis and mediate inflammation, ECM degradation, vascularization, and growth factor release which contribute to distal metastatic growth. Among other metastatic sites, these molecules are especially relevant to the skeleton.

Skeletal metastasis

Metastases from breast and prostate cancers account for approximately 70,000 deaths annually in the United States [4] , and occur most often in the skeleton, at a rate of 70-90% [54-56]. Bone lesions that result from these two types of cancers may be termed 'blastic' or 'lytic', if they form excess bone or destroy bone, respectively, or 'mixed' if they have elements of both types. Cancer -induced bone disease from breast cancer metastasis is primarily of a lytic

nature, which can cause immense pain and devastating fractures. Metastatic bone disease is incurable, thus treatment is palliative to resolve bone pain with analgesics and prevent fractures, primarily with anti-resorptive medications [57].

Among the malignancies that have a propensity to metastasize to bone are cancers of the breast, prostate, lung, kidney, and bladder [58].

As is the case with malignancies in other organs, a number of genes are associated with breast cancer metastasis to bone. Expression of receptor activator nuclear factor k-B (RANK) receptor correlates clinically with breast cancer metastasis to bone [59], though a mechanism is unclear. The expression of CXCR4 also plays a role increasing metastasis in general, though the clinical correlation specifically to bone metastasis is not as strong as with RANK [59]. At the primary tumor PTHrP expression has long been correlated with bone metastasis [60] due to its ability to induce bone resorption.

Bone Turnover

The bone is a complex structural and neuroendocrine organ responsible for maintaining ion balance, regulating metabolism, supplying stem cells and blood, storing various growth factors and manufacturing immune cells, in addition to its obvious role of providing structural support.

Bone homeostasis requires a balance of bone formation with bone resorption in order to maintain structural integrity while meeting the body's calcium and phosphorus demands. Osteoblasts, though accounting for less than 5% of total bone cells at any given time [61] are solely responsible for laying down collagen

matrix and calcifying it to produce nascent bone. After these cells imbed themselves within and calcify the surrounding extracellular matrix, they mature to become osteocytes, which are the most abundant cell type, making up more than 90% of the cells in the skeletal tissue [62]. Osteocytes form an extensive matrix of canaliculi, which they use for communication and transfer of nutrients and oxygen within avascular compact bone. Osteoclasts, which resemble macrophages, are monocyte- lineage cells responsible for dissolving both the organic and calcified portions of the bone extracellular matrix, in response to fractures or to liberate calcium. When mature, these large multinucleated cells form a seal upon calcified bone, referred to as a 'ruffled border', and secrete a plethora of proteinases and hydrogen ions in order to resorb the bone. Osteoblast precursors move into the resulting pit, or lacuna, and secrete copious amounts of type I collagen and other proteins to reform the bone which they subsequently calcify. This orderly process is severely disrupted when bone metastases are present.

RANKL

Receptor activator of nuclear factor kappa-b ligand (RANKL) is a tumor necrosis factor (TNF) family member that is central to bone turnover due to its ability to induce osteoclastic differentiation and activation. Also known as TNF-related activation-induced cytokine (TRANCE), RANKL is necessary for organogenesis of lymph nodes [63], development of mammary glands during pregnancy [64] and is expressed by both T-cells and B-cells [65, 66], all of

which, along with its role in bone turnover gives this ligand a central role in breast cancer metastasis to bone.

RANKL was initially dubbed osteoprotegerin ligand (OPGL) [63], as it was found to bind osteoprotegerin (OPG) as well as RANK during the studies that discovered its important role in bone resorption. Osteoblasts [67], osteocytes[68], and immune cells[69] can all express RANKL within the bone to stimulate subsets of monocytic cells in the bone to differentiate and undergo multinucleation to form mature osteoclasts [70], and subsequently prevents their apoptosis [71]. This cytokine also activates existing osteoclasts, causing them to begin resorption of calcified bone [72].

As with many other TNF family members, RANKL forms a trimer [73] in order to bind and activate its receptor, which is also a trimer [74]. Signal transduction in osteoclasts occurs via TRAF1,2,3,5 and TRAF-6, followed by subsequent activation of IKK and NFK-b, C-src and Akt, and to a lesser extent, JNK and p38 [75, 76], resulting in the aforementioned cellular functions of RANKL in bone remodeling. Initially it was believed ligand binding was limited to direct cell-cell contact of the ectodomain of membrane-bound form of RANKL , as was seen with osteoblast-osteoclast interactions [77]. Later studies revealed that a soluble form of the ligand, cleaved by TACE or other MMP's [78], is also active and can signal differently than its membrane bound form [78, 79]. In addition to its roles in bone metabolism , soluble RANKL (sRANKL) has been shown to induce migration of many types of cancer cells [80-82]. These observations along

with the clinical correlation of RANK in bone metastatic breast cancer [59] make RANKL an attractive molecular target for bone metastasis research.

Denosumab is a clinically prescribed mAb against RANKL, used in the treatment of osteoporosis and cancer induced bone disease. It is a first line antiresorptive treatment with an efficacy similar to, zoledronate [83], which is the most potent of the bisphosphonates [84]. Given the clinical data regarding RANK/RANKL in breast cancer metastasis, Denosumab also has the possibility of directly inhibiting breast cancer metastasis to bone, giving it an advantage over bisphosphonates, which solely target bone resorption.

Vicious cycle

Within the bone, osteolytic breast cancer metastases enter a well-characterized 'vicious cycle', consisting of cyclical bone destruction and tumor growth. In this feed-forward process, metastatic breast cancer cells secrete PTHrP into the bone stroma, where it stimulates osteoblasts' PTH receptors, increasing cAMP levels and secretion of RANKL. This stimulation is analogous to the bone's response to PTH which results in calcium release. The RANKL acts upon osteoclasts and their monocytic precursors to increase differentiation, fusion, and resorptive activity. Osteoclastic resorption of bone allows for the release, cleavage, and activation of matrix-embedded growth factors such as TGFβ. These active growth factors then stimulate the cancer cells to increase their proliferation and number, resulting in more PTHrP to perpetuate the cycle [85].

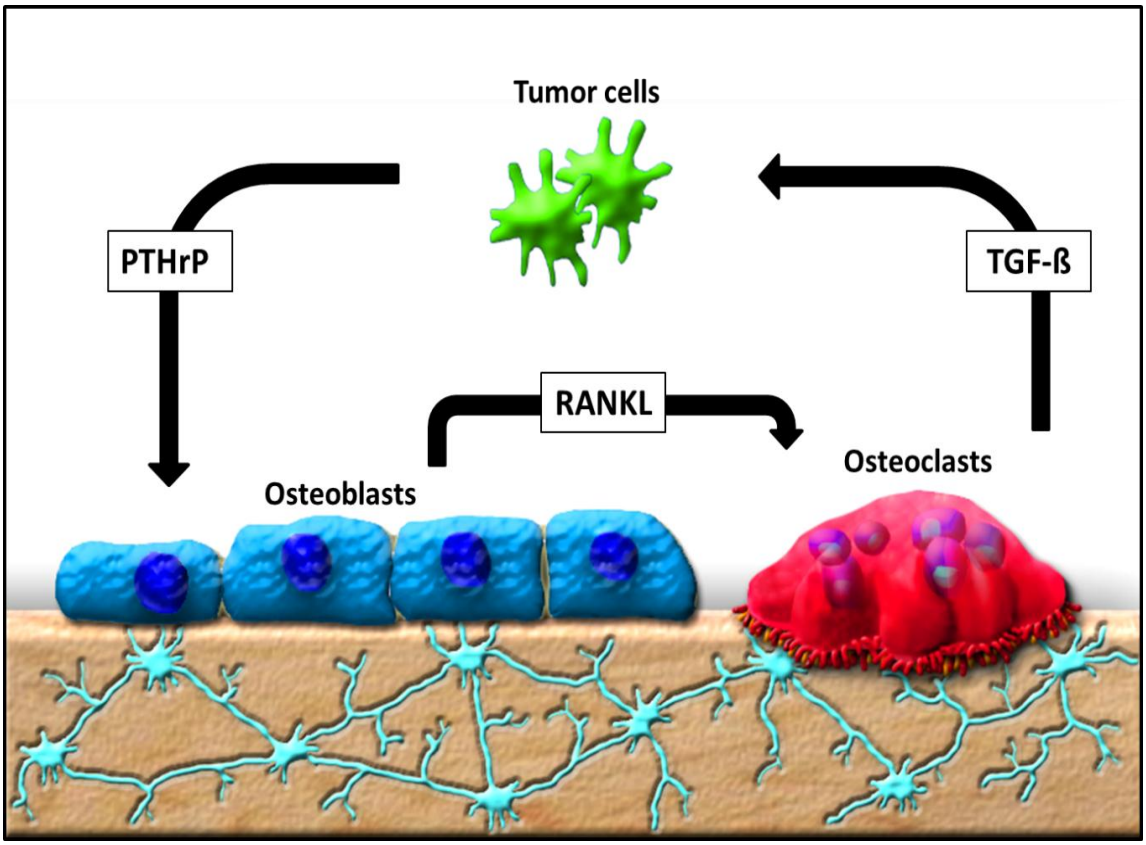

Figure 1. The osteolytic 'vicious cycle'. In cancer-induced bone disease, **(A)** Tumor cells secrete parathyroid hormone related peptide (PTHrP), which stimulates PTH receptors expressed on osteoblastic cells, increasing RANKL production. **(B)** RANKL increases resorptive activity of osteoclasts. **(C)** Growth factors are release from the resorbed bone matrix which fuel the growth of the tumor.

Models of Bone Metastasis

Bone metastases are a common occurrence in several malignancies, including breast, prostate, and lung. Once established in bone, tumors are responsible for significant morbidity and mortality [86]. Thus, there is a significant need to understand the molecular mechanisms involved in the establishment of tumors within bone. In order to study these events, multiple *in vivo* models have been established that each have specific benefits. The most commonly used model utilizes intra-cardiac injection of tumor cells directly into the arterial blood supply of athymic (nude) BalbC mice. While this procedure can be applied to many different tumor types (including PC-3 prostate cancer, lung carcinoma, and mouse mammary fat pad tumors), in this manuscript we will focus on the breast cancer model, MDA-MB-231. This model utilizes a bone-specific clone that was derived originally in Dr. Mundy's group in San Antonio [87], and has since been fluorescently labeled and re-cloned by our group [88]. While intracardiac injections are most commonly used by bone groups [87], in certain instances intratibial [89] or mammary fat pad are more appropriate.

Intracardiac injection of human tumor cells allows monitoring of the cells' ability to metastasize to and establish within bone. If a study is focused upon the effects on bone post tumor cell establishment, then this is often best addressed with intratibial injections. This method is the quickest and most direct method of studying tumor interactions in the bone since it utilizes direct injection of cancer cells into the bone, underneath the growth plate. Alternatively, if the desired aim is to monitor primary tumor growth or metastasis from the primary site, mammary fat pad inoculations are most appropriate. However, very few tumor cells will

metastasize to bone from the primary site, with 4T1 bone-specific clones being the exception [90, 91].

Studies of tumor-induced bone disease rely on several animal models, of which the two most commonly used are intracardiac and intratibial. While the intracardiac model is in many cases the best option for studying metastasis to bone, it nonetheless fails to represent the full metastatic process. Towards that aim, mammary fat pad or other orthotopic injections are the ideal approach, but for most studies using human cells, tumor cells do not metastasize readily from the primary site; when this does occur, they primarily metastasize to the lungs. Some strains of 4T1, such as the 4T1-592 subclone will metastasize to bone [90, 91], but the lesions are smaller and the cells are of mouse origin, which do not resemble human osteolytic metastases. Other models of tumor-induced bone disease, such as myeloma, utilize tail vein injections [92]. However, this approach will not work for solid tumor metastasis; it will seed tumors to the lungs and the mice will die of lung disease before developing quantifiable bone metastases. The intratibial injection method is generally viewed less favorably than the other methods, as it does not represent a model of metastasis, but rather of later established bone disease, and the procedure creates substantial local inflammation. However, in the case of most prostate models it is the only approach that allows for tumor growth in bone, which is a severe limitation to prostate and bone cancer studies [89].

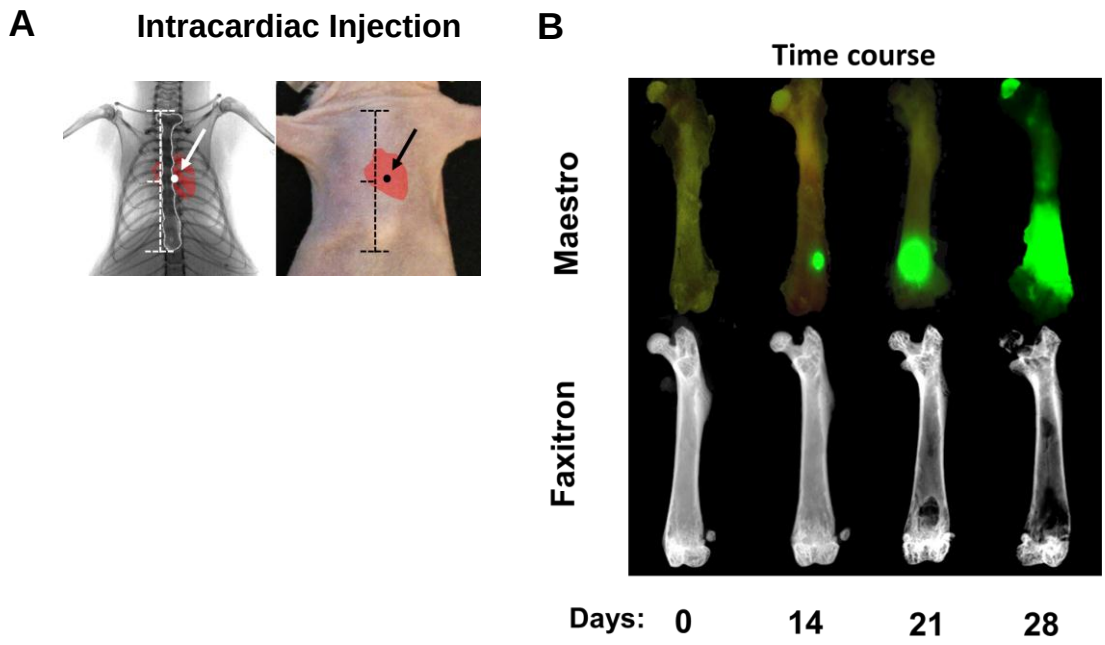

Figure 2: Intracardiac Model of Bone Metastasis. Ventral radiographic view **(A)** of adult mouse thorax showing proper placement of needle in the 4th intercostal space and into the left ventricle for intracardiac inoculation. Anatomical landmarks are shown with horizontal dashed lines on the sternum (outlined in white). On the mouse's skin the sternal notch and xyphoid process serve as landmarks, the needle is inserted slightly left of the sternum. Time course of intracardiac MDA-MB-231 model **(B) Top Row:** *Ex vivo* Maestro image showing GFP fluorescence at day 0, 14, 21, and 28 after intracardiac injection of MDA-MB-231. Note that tumor foci at day 14 are only visible in ex vivo after soft tissue removal. **Bottom row:** Ex vivo Faxitron images of the same femora illustrating osteolytic bone lesions. Note that bone destruction is not usually visible until 3 weeks after cardiac injection.

Imaging Modalities

Quantification of in vivo bone metastasis studies requires specialized techniques for hard tissues. The most commonly utilized are radiography and fluorescence for longitudinal disease monitoring, and histology and micro-computer assisted tomography (μCT) for end point analysis. Bioluminescence is also widely used in studying bone metastasis, but we have observed more consistent osteotropic phenotypes with our green fluorescent protein (GFP)-expressing clones when compared to our luciferase expressing cells. We see some technical benefit with fluorescence vs. luminescence imaging with better anatomic detail for x-ray co-localization, superior resolution with the available equipment, and more precise and defined tumor margins. Improved sensitivity is often touted as an advantage when using luciferase instead of GFP expression, but direct comparison between bioluminescence and fluorescence modalities did not yield a significant difference for early detection of metastases in bone in our studies.

Bone metastasis researchers also employ a variety of *ex vivo* imaging techniques that are tailored specifically for calcified tissues. Due to the opacity of bone and interference from overlying soft tissues *in vivo*, it is helpful to perform imaging techniques after bones have been removed and cleaned. This allows for highly detailed radiographic and sensitive fluorescence analysis to detect small metastasis and bone anomalies that are not visible in vivo and difficult to find through serial histology. Osteolytic lesion number area is routinely quantified via x-rays since it corresponds to the most routinely used method for detecting bone

metastases in the clinic. The most accurate bone volume and bone destruction data is obtained via micro-computer assisted tomography (μ-CT). While this technique is performed similarly to studies of normal bone, the analysis of tumor-bearing bones requires specialized scripts and knowledge since tumor-induced bone destruction frequently eliminates or disrupts the growth plate and cortical bone which typically serve as landmarks for orientation and contouring. Bone analysis with μCT gives yields detailed information about bone structure that can reveal the exact 3D location of an osteolytic tumor, details about cortical vs. trabecular resorption, and subtleties about bone formation. Histological analyses are also nuanced in tumor-bearing bearing bones, since a decalcification step or plastic embedding is required before sectioning, both of which alter most routine stains. Much information about tumor-bone interactions including osteoclast number and activity, immune cell recruitment, vascularization, necrosis, osteoblast number, and bone formation rate are elucidated from various histological techniques here, making it a powerful tool for elucidating mechanisms in bone cancer. Bone volume can also be assessed via histology but is less reliable than μCT, due the inherent error and technical limitations of 2D histological measurements when compared to continuous 3D histomorphometry [93].

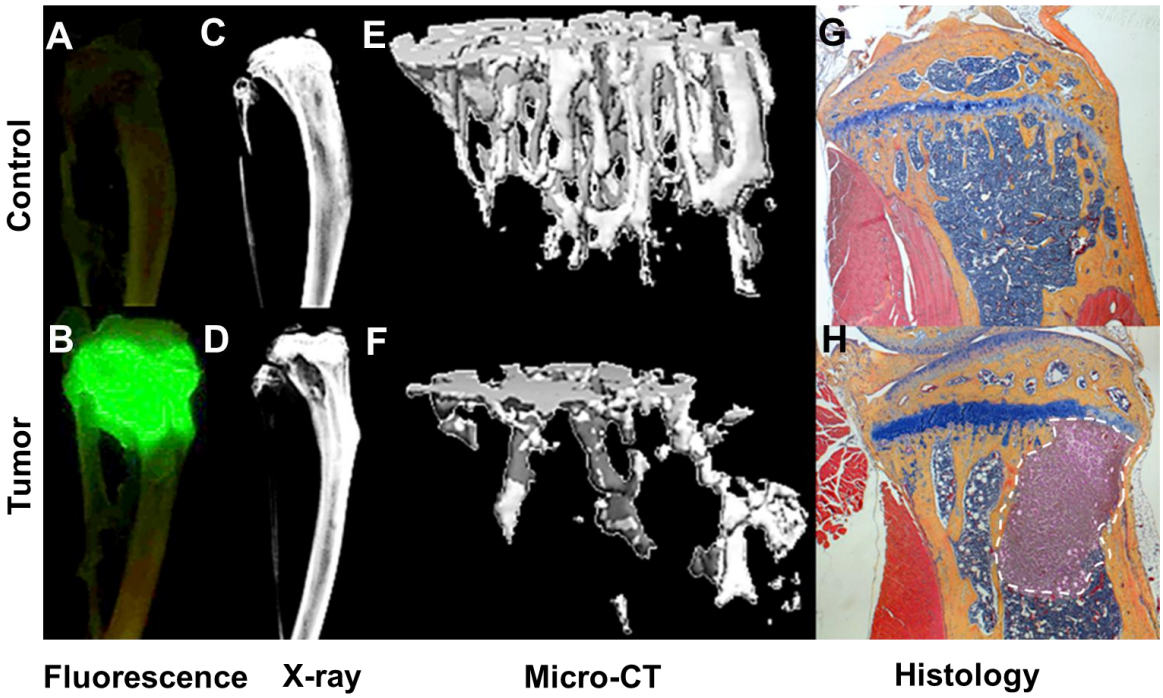

Figure 3: Quantification of bone metastatic progression. GFP+ tumor as visualized by Maestro™ imaging ex vivo of tibiae of a non-tumor bearing mouse **(A)** and a mouse 4 weeks after intracardiac injection of a GFP expressing MDA-MB-231 sub clone **(B).** Tumor foci correlate with areas of bone destruction as shown by Faxitron **(D)** compared a bone without tumor **(C).** Further bone and tumor detail is seen in corresponding Haematoxylin, eosin, orange G, phloxine stained histological sections **(E & F).** Bone structural and mineral data from μCT measurements is rendered as 3d images of a healthy bone **(G)** and a tumor bearing bone **(H)** where areas of bone destruction are shown as void area.

Bone Sympathetic Innervation

Autonomic innervation of the skeleton is documented at the gross anatomical and histological levels, with both long and flat bones innervated by myelinated sensory and unmyelinated sympathetic nerve fibers [94-96]. Retrograde tracing and axotomy experiments have demonstrated that these intraosseus nerve fibers are structurally and functionally connected to primary afferent neurons in dorsal root ganglia and paravertebral sympathetic ganglia [97]. Although the terminal nerve branches feeding the bones at this point remain largely unstudied, they are likely derived from the overlying muscle innervations. Postganglionic fibers, arising from the cervical sympathetic ganglion and glossopharyngeal nerve, innervate external and internal bones of the skull. The long bones of the upper extremities receive nerve supply from the brachial plexus, which then branches to the median nerve, in turn innervating the humeral as well as the ulnar and radian nerves, which supply the forearm bones. Osseous innervation of the flat rib bones is achieved via the anterior branches of the twelve pairs of intercostal nerves. Sympathetic innervation of the lower limbs originates in the lumbar plexus, which supplies the femoral and deep saphenous nerves to the femur, as well as the tibial, medial, and popliteal nerves to the tibia and fibula. Basivertebral nerves in the spine supply intraosseus autonomic innervation of the vertebral bodies [98].

Due to the technical difficulties inherent to working with osseous tissue, little research exists concerning the development of bone innervation. In rats, nerves penetrate uncalcified osseous tissues relatively late, after gestational day 17, and

continue to develop more fully after birth [97]. These nerve fibers parallel blood vessels and grow into the bone, presumably in response to bone marrow expression of neurotrophic factors [99] , although this has yet to be demonstrated in vivo. Despite their presence in developing embryonic tissues, it is still unclear whether sympathetic nerves have a functional role in early bone developmental processes. The lack of obvious bone developmental or morphogenesis abnormalities in mutant mouse models lacking dopamine β-hydroxylase, the β1, 2 and 3-adrenergic receptor, NPY or the Y1, 2 or 4 receptors, for instance, argues against a major role of sympathetic nerves during development, despite the demonstrated need for norepinephrine for embryonic cardiovascular development [100].

The first detailed description and histology of bone innervation was given by de Castro (1930), who developed a silver staining technique that demonstrated ramification of neurons with mesenchymal cells in bone. Subsequent research has shown that intraosseus nerves express tyrosine hydroxylase (TH) [101], indicating catecholamine synthesis, PGP 9.5, vasoactive intestinal peptide, calcitonin-related gene product, and substance P, denoting both sensory and autonomic innervation (see [102] for review). The location of these neural markers illustrate that neurosteal fibers can be divided into two major groups: marrow innervation and periosteal innervation (Figure 4A). Most nerve fibers in

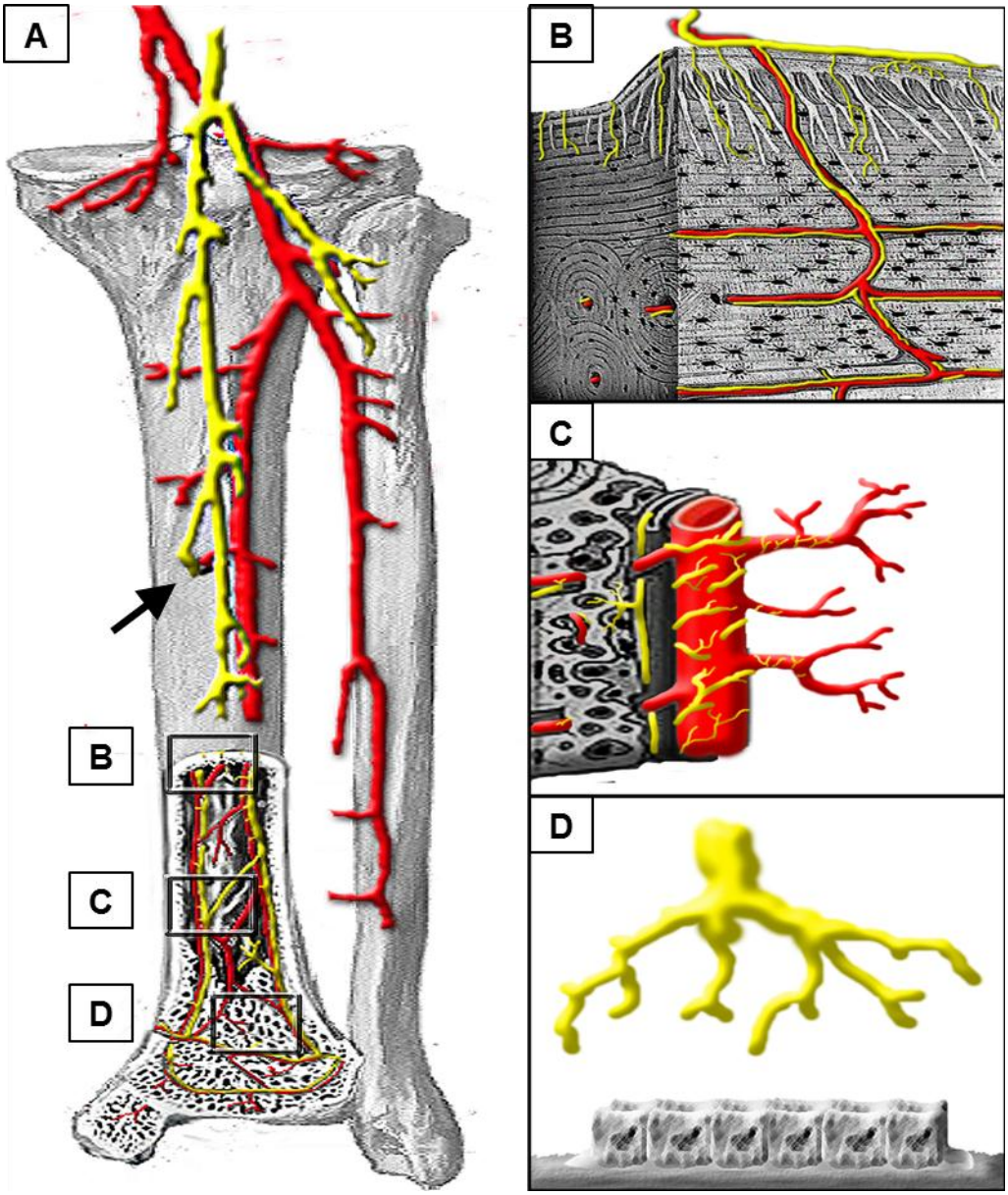

Figure 4.**Innervation of Bone.** Branches of the tibial nerve supply the bones of the lower limb (A) alongside the posterior tibial and peroneal branches of the popliteal artery (red). Blood vessels and nerves enter the bone shaft via the nutrient foramen (arrow). Neurosteal fibers in the periosteum run parallel with Sharpey's fibers and throughout the canaliculi of the cortex (B). Most nerve fibers in the central canal are perivascular vasomotor nerves (C) though some branch into the bone. Sympathetic fibers ramify near mesenchymal cells such as osteoblasts (D), but whether these derive from periosteal or perivascular nerves is unknown.

the periosteum are sensory, but autonomic TH-positive fibers are also present. These sympathetic nerves branch around the periosteum and enter the cortical bone, where they are organized parallel to the long axis of the bone in the Haversian canals or perpendicular, alongside Sharpey's fibers, which anchor the periosteum to the cortical bone (Figure 4B). In the marrow, nerves accompany blood vessels through a nutrient foramen into the bone's interior where they can be seen to branch and make vascular and cellular contacts (Figure 4C). The majority of these nerves are perivascular, forming spiral patterns around blood vessels, and can be categorized as vasomotor, controlling the vascular hemodynamics in the bone marrow. Schwann cells are also present in the marrow though they are believed to accompany sensory nerves rather than the sympathetic axons. Electron microscopy studies have shown nerve fibers in the proximity of osteoblasts but have not likewise demonstrated the presence of synapses (Figure 4D)[103].

Effect of sympathetic nerves on bone remodeling

The cells that comprise bone and govern its constant remodeling during adult life include osteoblasts, the bone-forming cells of mesenchymal origin, osteoclasts, the bone -resorbing cells of monocytic origin, and osteocytes, which are fully matured bone matrix-embedded osteoblasts. Both osteoblasts and osteoclasts express the β2AR and are thus responsive to catecholamines [103]. Catecholamines and adrenergic receptor agonists potently increase intracellular cAMP levels in osteoblasts and trigger changes in gene expression for

osteoclastogenesis (RANKL) and proliferation-related genes (G1 cyclin and Ap1) [104, 105].

In agreement with these cellular effects, isoproterenol administration in rodents causes severe bone loss attributed to increased bone resorption and decreased bone formation [103, 106]. On the other hand, pharmacological blockade of the βAR by propranolol increases bone mass in mice and rats by inhibiting bone resorption and promoting bone formation [103, 107]. The use of mutant mouse models verified these findings, with the demonstration that genetic lack of dopamine β-hydroxylase (DBH) or of the β2AR in mice causes an increase in bone mass [103, 104].

In addition to their structural function, bones are also hematopoietic tissues that host a wide variety of immune cells, most of which express βARs, and are at distinct stages of differentiation. The fact that immune cells are involved in the complex regulation of bone remodeling is increasingly recognized, and the effect of sympathetic nerves on both lineages, hematopoietic and mesenchymal, is likely to be interrelated. The recently identified effect of sympathetic nerves on hematopoietic stem cell egress from the bone marrow, mediated by osteoblasts, supports this hypothesis [108].

NPY is co-released with NE from sympathetic nerves and a role of this neuropeptide in the regulation of bone remodeling is also well established [109]. The Y2 receptor expressed by hypothalamic neurons exerts an inhibitory influence of bone formation, as demonstrated by the high bone mass phenotype of mice lacking the Y2 receptor specifically in these neurons [110]. On the other

hand, the Y1 receptors expressed by bone stromal cells appear to regulate the number of mesenchymal stem cells in bone, downstream of NPY signals from bone sympathetic nerves [111]. Surprisingly, NPY is also expressed by osteocytes, which are fully differentiated osteoblasts embedded within bone matrix [112].

Relevance of sympathetic nervous system in bone and pathophysiology

Despite the fairly well-established nature of these findings in murine models, it is still unclear to what extent sympathetic nervous system (SNS) signaling regulates bone mass or contributes to human bone pathologies. Most studies in humans have been restricted to the effect of β-blockers on bone mineral density and tend to support a protective effect of this class of drugs on bone mineral density [113]. The pharmaceuticals or conditions that influence sympathetic outflow or responsiveness remain to be investigated.

Sympathetic signaling in bone may be regulated by several physiological and/or pathological signals. Activation of the cannabinoid receptor 1 (CB1) by 2-arachidonoylglycerol (2AG) may represent such a signal, since it regulates sympathetic signaling at the pre-synaptic level in bone nerve endings by reducing NE release as well as the anti-osteogenic effect of the sympathetic nervous system [114]. Glucocorticoids, however, may promote sympathetic responsiveness of osteoblasts to induce bone loss, by their action on β2AR expression and signaling [115]. The effect of thyroid hormones on bone may involve a similar mechanism, although this has not been demonstrated yet.

Sympathetic outflow is also regulated centrally, particularly by brainstem and hypothalamic centers that control major bodily homeostatic functions, including body weight and reproduction. In mice, the finding that β-blockade by propranolol or β2AR deficiency prevented the bone-catabolic effect of hypothalamic leptin administration clearly linked hypothalamic neurons to the regulation of bone remodeling, and functionally positioned the skeleton as a target organ of central neurons, via the sympathetic nervous system [104] (Figure 5). Severe stress and depression are two pathological conditions of the central nervous system (CNS) that may stimulate sympathetic outflow and exert effects on bone via this mechanism, as suggested by a study in mice [116] and by the association between clinically-diagnosed depression and low bone mineral density (BMD) [117].

Lastly, the skeleton is increasingly recognized as a true endocrine organ, the secretory activity of which is controlled by sympathetic nerves. Osteocalcin secretion by osteoblasts regulates glycemia and testosterone production and is in turn mediated by catecholamines [118, 119].

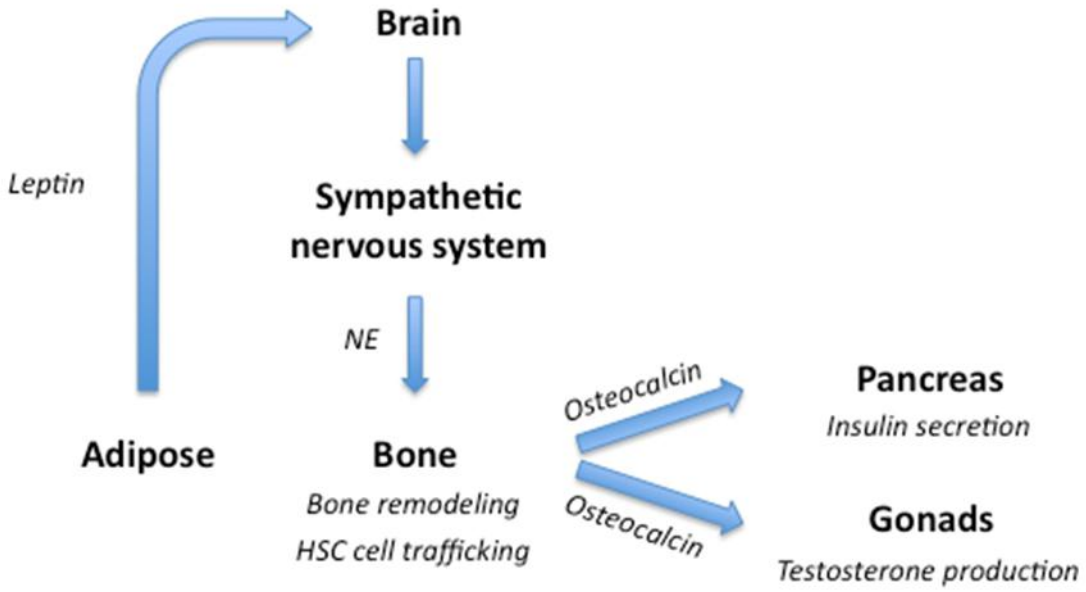

Figure 5. SNS in bone and metabolism. The sympathetic nervous system links central neurons to bone cells and regulates the endocrine function of the skeleton.

Effects of Chronic Stress

In the broadest biological sense, stress is any stimulus that pushes a system away from homeostasis. At an organismal level, stress has been defined as the "...response of the body to any demand placed upon it" [120]. Functionally, this concept can be defined in terms of a *stressor* (input), which can be any stimulus sensed by an organism, usually via the central nervous system, and the subsequent endocrine *response* (output), which attempts to bring the organism back to equilibrium. The classic 'fight or flight' neuroendocrine stress response consists of sympathetic nervous system (SNS) activation that results in the systemic release of catecholamines and corticosteroids. Neurons in the cerebral cortex and the limbic system send stress input from situational alarm, anxiety or other heightened emotional states to the locus coeruleus and the hypothalamus, which integrates these inputs and starts the proper neuroendocrine cascade. The most rapid cascade occurs from hypothalamic efferent stimulation of the greater splanchnic nerve. The preganglionic sympathetic fibers release acetylcholine directly to chromaffin cells in the adrenal medulla, resulting in the release of norepinephrine and epinephrine. Simultaneously, norepinephrine from the locus coeruleus prompts the hypothalamus to release corticotropin-releasing hormone (CRH) from parvocelluar neurosecretory neurons. CRH stimulates the release of adrenocorticotropic hormone (ACTH) from the anterior pituitary. ACTH is carried by the blood to the adrenal cortex where it stimulates the secretion and production of glucocorticoid steroid hormones from the zona fasciculata.

Acute effects of sympathetic activation increase the ability of an organism to defend itself or escape. These include the adrenergic effects of elevated blood pressure and cardiac output, pupil dilation, increased thrombogenic potential of blood, increased respiration, and mobilization of energy sources. In the short term, catecholamines also increase immune surveillance via mobilization of natural killer cells and effector T-cells [121, 122]. All of these changes are limited to a matter of minutes and are followed by a slower and longer-acting glucocorticoid signaling phase.

During the next several hours following a stressful event, glucocorticoids are released from the adrenal cortex, which can help an organism recover from some of the consequences of abrupt adrenergic signaling. Cortisol, the most active glucocorticoid in humans (corticosterone in mice) [123], plays its most well-known role by decreasing inflammation and immune cell activity, which serves to counteract the increased immune activity from adrenergic signaling. This immunosuppressive effect works in conjunction with cortisol's ability to mobilize nutrients, in order to repair tissue damage that might have occurred during a stressful event [124], though high dose and long term glucocorticoid treatment prevents wound healing [125]. Glucocorticoids also increase surface expression of adrenergic receptors which have been desensitized from the binding of catecholamines [126]. In addition, metabolism is greatly influenced by cortisol, accounting for the 'gluco' prefix in this class of steroids. While catecholamines increase breakdown of glycogen in the muscles and liver for use in escaping

danger, cortisol stimulates production afterward to replenish the short term energy stores lost during a ‘fight or flight’ response.

In the short term, sympathetic stress cascades tend to be self-limiting, from receptor desensitization [127, 128], negative feedback from glucocorticoid receptor signaling in the hypothalamus[129], and parasympathetic recovery [130]. Such elegant balance is not the case during chronic stress. Long term activation of the HPA axis produces a variety of adverse health consequences, including immune suppression [131, 132], ulcers [133], fatigue [134], arrhythmias [135], headaches, obesity [136], wasting [137], and bone resorption [138]. States of chronic stress are not limited to situations with obvious external stressors such as war or severe socioeconomic distress, but also include complex emotional states like depression and post-traumatic stress disorder, which makes these conditions challenging to study *in vivo*.

Depression and Stress

Clinical depression, also known as major depressive disorder is a complex syndrome of neurological and emotional dysfunction characterized by decreased mood, motivation, and energy. Despite these outward symptoms, major depression is associated with increased SNS outflow [139, 140] and parasympathetic hypoactivation [140]. Though clinical depression has a strong genetic basis, stressful life events play a substantial role in the progression of this disease [141]. Indeed chronic psychosocial stress, hostility, fear, and anxiety can all contribute to major depression and other debilitating mood and

stress disorders such as post-traumatic stress disorder (PTSD) [142-145]. Elevated emotional stress also results activation of the HPA axis to the point of hypercortisolism [146, 147], which can cause depression [148, 149] leading some researchers to postulate neuroendocrine cycle of stress related conditions that can exacerbate symptoms of clinical depression [150] and lead to relapse [150]. Autonomic dysregulation from major depression and other stress disorders correlates with significant mortality and comorbidity in a variety of clinical disease from cardiovascular disease [140, 151] to cancer [152].

Beta Blockers

In 1958 , pharmacologist and physician James Whyte Black developed the first clinically successful beta blocker, propranolol, which revolutionized cardiology and lead to his Nobel Prize (along with his work with cimetidine). This compound, a 'non-selective b-blocker', prevents the binding of norepinephrine and epinephrine at the $\beta 1$ and $\beta 2$ adrenergic receptors. By preventing b-adrenergic stimulation of cardiac muscle, propranolol is able to decrease the heart's demand for oxygen, decrease blood pressure, an prevent angina and cardiac arrest. Lipophilic b-blockers like propranolol and metaprolol can also cross the blood-brain barrier and prevent adrenergic feedback in the brain, which results in increased sympathetic tone, and increasing peripheral norepinephrine, which binds alpha-1 adrenergic receptor ($\alpha 1$AR). The net result is two mechanisms of the drug's cardiovascular effects by stimulating $\alpha 1$AR (via NE) and directly blocking the $\beta 2$ AR, whose vascular effects oppose those of the

α1AR. Propranolol also increases HPA activation and subsequent cortisol levels which may be a mechanism for the published adverse effects of b-blockers on memory [153] . Other central nervous system effects of propranolol are an increase in some symptoms of major depression [154] but a decrease of stress and anxiety [155] that is often found in these patients.

Models of chronic stress

Scientists have demonstrated a remarkable capacity for discovering new and creative ways to distress rodents. These animal models have been well characterized and used extensively for evaluating innumerable anti-depressants, cardiac medications, and anti-anxiety drugs over the last half century. Each model has a particular ability to induce physical or psychological stress signal glucocorticoid levels, and various changes in neurological functioning and behavior ; researchers must be careful in selecting the appropriate method. The following paragraphs give a brief description of some of the more commonly used models and are by no means exhaustive.

Predatory Stress

The threat of being killed and/or eaten is likely to elicit severe stress, especially in mice, which tend to be near the bottom of the food chain. The most fundamental function of the 'fight or flight' response is to prevent this kind of adverse life event so that an organism can propagate. Thus, exposure to a natural predator is an effective anxiogenic method. Substantial variation exists in

these models including placement of a natural predator, such as a cat, near the rodent's cage (Figure 6A), exposure to predator feces, spraying of predator urine or pheromones near the rodent, or placement of rodent and predator in the same cage with a barrier [156, 157]. Significant anxiety is seen in this model, which can be rescued with CCK [158] blockade, and with propranolol [159] indicating significant activation of both the HPA and SNS. Though predator exposure is sufficient to produce a strong acute stress response, it is of only limited use in chronic stress models after the rodent learns that it is in no real danger, and cumbersome to implement without a dedicated facility for stress studies.

Cold Water Immersion and Cold Isolation

The sudden and imminent threat of drowning or freezing has been shown to induce a strong stress response in rodents [160, 161] and in humans [162]. In this model, animals are dropped into a container of cold (Figure 6B) water and forced to swim (or sink). The rodent's thermogenic response to cold water combined with fear and physical exertion yields a substantial neuroendocrine stress response. A major disadvantage of this model is that a research subject can actually drown. A safer alternative calls for the isolation of the rodent in a dry 4^{o}C container for 15 minutes. Again, the temperature decrease stimulates an adrenal response which is enhanced by the sudden change of environment. Though this model is effective in inducing SNS outflow, it is complicated by the numerous metabolic changes that occur in low temperature exposure.

Light-Induced Stress Models

As a primarily nocturnal prey animal, mice are sensitive to changes in light. Numerous models are built around this idea including using excessively bright lights in the cage, rapid flickering (strobe) lights, and changing the timings of light cycles [163] The last strategy serves to alter the circadian rhythm and sleep-wake cycle of the rodent, which results in significant psychological and physical changes [164]. This model is also subject to desensitization, which can be remedied by continuous alteration of the timing of the light.

Social Isolation

Laboratory mice are social animals and frequently engage in social grooming and huddling. Separation of a rodent from its cage mates induces a stress response [165] of sufficient magnitude to cause a variety of health problems [166, 167]. For this model of stress, a mouse is simply placed in an empty cage, usually without a cardboard shelter or nesting materials, for an extended period of time. Isolation from the other mice and lack of a place to hide (open field exposure stress) creates a combination of depression and anxiety in the mouse [168].

Loud Noise

In humans, noise above 90 decibel (dB) is considered a stressor and chronic exposure to such induces a variety of negative effects on calcium metabolism, oxidative stress, etc. [169] In murine sound stressor models a speaker is placed above the rodents' cage, which plays a continous 100dB sound anywhere in the 1-100khz range that mice are able to heart [170]. The noise is played for 15-240 minute intervals for 0-15 days. Sound at 100dB may be excessive since vacuum cleaners in the animal room may even be stressful [170].

Chronic Immobilization Stress (CIS)

CIS, also known as restraint stress is one of the most widely used models for chronic stress [171-173]. Most commonly, rodents are trapped inside a small tube, with sufficient ventilation to breathe, for a period of 1-4 hours. Understandably, this situation creates a great deal of panic in the animal resulting in a robust sympathetic stress response. Another variation uses a series of Plexiglas chambers that can be adjusted to decrease the space available to the animal, thereby increasing the stress response [174] Yet another method requires the researcher to physically restrain each limb of the rodent by binding them to a board with tape or straps for several hours. These methods are relatively safe and reliable for up to 3 weeks of stress response before desensitization.

Chronic Unpredictable Stress

An obvious approach to rodent habituation and desensitization in a stress model is to vary the stressor. In the case of Chronic Unpredictable Stress (CUS), a combination of several of the aforementioned stress models are applied to the rodents, but each on a different day. Thus, the animal does not know what to expect, which keeps the neuroendocrine stress response high for an extended period of time and induces a helpless, depressive state[175]. A variation of this model applies a series of less severe stressors, like social isolation and predatory exposure with similar neuroendocrine changes, though smaller in magnitude [176]. Though these models can be more effective than using single stressors, they introduce the problem of standardizing multiple stress treatments for a single experiment and generate other logistic challenges.

Genetic Models

Multiple transgenic mouse models have been created that can recapitulate some of the neuroendocrine and psychological changes seen in chronic stress and depression. Hypertensive mice [177], mice that overexpress neurotrophic tyrosine kinase receptor type 3 (TrKC) [178], and mice with altered corticotropin-releasing hormone (CRH)-binding protein [179], and α-CGRP deficient mice [180] are all models with elevated SNS outflow. Other models, such as β2AR knockout, can alter adrenergic signaling outside of the SNS, to block stress effects in a responsive tissue. Other genetic models have been developed where

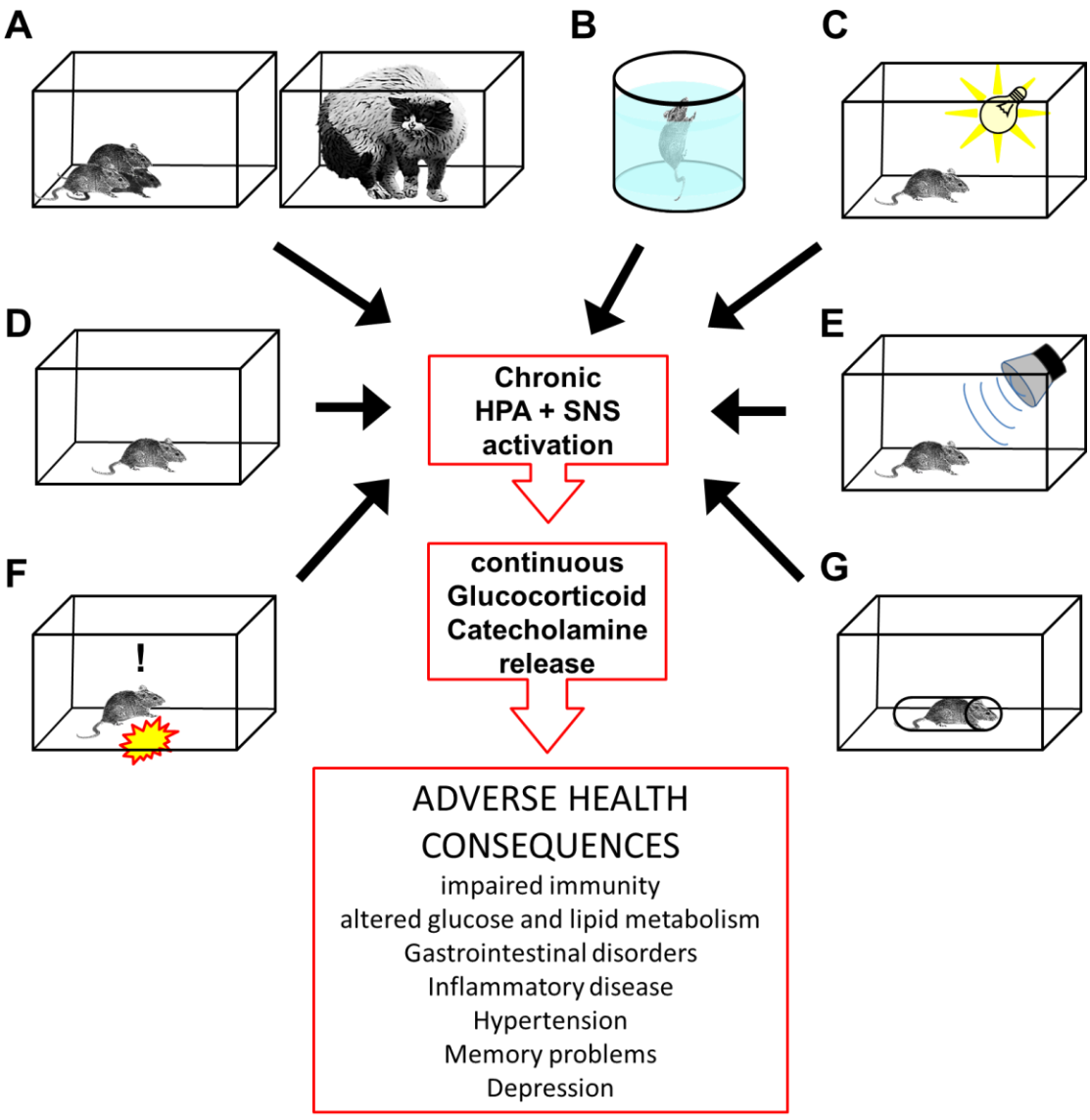

Figure 6. Models of Chronic Stress. A wide variety of established methods exist with which researchers can simulate stress and depression in rodents. These disparate models have very similar neuroendocrine effects. **(A)** Predatory Exposure. **(B)** Immersion in Cold Water. **(C)** Light Induced Stress. **(D)** Social Isolation. **(E)** Loud Noise **(F)** Foot Pain (shock or thermal). **(G)** Chronic Immobilization Stress (CIS) also known as 'Restraint Stress.

the genes involved are unknown, but the animals have a phenotype with enhanced stress response and anxiety [181].

Psychosocial Stress and Cancer

Emotional stress and depression have been linked to malignant diseases since Hippocrates first coined the term for cancer, *karkinos* , meaning crab, two thousand years ago. He believed the underlying cause of tumor formation was a buildup of *melankolia* black bile, referring to emotional depression. This hypothesis linking psychosocial stress to cancer has persisted through the ages but only recently has research demonstrated the nature of this relationship. Though prolonged psychosocial stress does not seem to affect overall tumor incidence, it is associated with shorter patient survival and increased recurrence of breast cancer, which suggests that sympathetic signaling may contribute to breast cancer metastasis [152, 182]. Further supporting a link between 'stress' and cancer are mouse models that reveal a linkage of neuroendocrine signaling to increased tumor vascularization, invasiveness, and metastasis in soft tissues, via a direct effect on ovarian or breast tumor cells [183, 184].

Activation of the sympathetic nervous system (SNS), from prolonged or severe emotional stress, causes the release of peripheral catecholamines, which enter the bone in the form of norepinephrine sourced from dense innervation of the bone or from epinephrine in the bone's rich vascular network. These catecholamines stimulate the β2AR's on osteoblast lineage cells, resulting in profound changes in the bone marrow microenvironment. Among the affected

bone processes are inflammation, cell trafficking and bone resorption, all of which are also central to bone metastasis and progression. Additionally, cytokines involved in soft tissue metastasis are affected by catecholamine activity [185]. SDF1 has been clearly implicated in the mechanisms underlying the homing of metastatic cancer cells [186], including breast and prostate carcinomas [187, 188], and RANKL is increasingly recognized as a crucial factor for cancer cell motility [189, 190], in addition to its well-established role in tumor-induced osteolysis [85]. As mentioned previously, current data concerning SNS signaling and cancer demonstrate a direct effect on the malignancy, but the data presented in this work indicates that emotional stress could *indirectly* control the behavior of metastatic cancer cells by acting on host bone marrow stromal cells, incidentally affecting the 'seeds' by controlling the fertility of the 'soil'.

CHAPTER II

MATERIALS AND METHODS

Drugs/compounds :

Isoproterenol, a nonspecific βagonist, also known from Isoprenaline (Sigma Aldrich, USA)

Guanfacine hydrochloride, also known as Tenex, N (Aminoiminomethyl)-2,6-dichlorobenzeneacetamide, is a sympatholytic, selective α2A receptor agonist (Sigma Aldrich, USA)

Atipamezole, also known as Antisedan is a selective α2A receptor antagonist (Sigma Aldrich, USA)

Propranolol, nonselective β antagonist (Sigma Aldrich, USA)

Animal models

Wild type BalbC mice were used with experiments involving 4T1 subclones and athymic BalbC $^{nu/nu}$ mice were used with MDA-MB-231 sub clone experiments. All procedures were approved by the Institutional Animal Care and Use Committee at Vanderbilt University Medical Center. Mice were group housed in plastic cages (n = 5/cage) under standard laboratory conditions with a 12-h dark, 12-h light cycle, a constant temperature of 20 C, and humidity of 48%. Mice

were fed a standard rodent diet (Pharma Serv, Purina Rodent Laboratory Chow 5001; Framingham, MA). Nude mice were housed in sterile conditions and fed autoclaved standard chow. Isoproterenol (ISO) treatment was given as daily intraperitoneal injections (3mg/kg in 100uL sterile PBS). Control mice were not given injections or given injections of PBS. Propranolol groups received propranolol ad libitum (0.5g/L) via drinking water.

Chronic Immobilization Stress

Chronic Immobilization (CIS), restraint stress, was carried out by placing mice in 50mL laboratory conical tubes, perforated for adequate air supply, for 2 hours daily. Published methods include multiple perforations in a clear cylinder or a transparent restraint rack system. Perforations must be large or numerous enough to allow ample ventilation. Walls of the restraint tube must be clear to allow monitoring for signs of distress beyond those within the scope of the experiment. For our experiments, using a clear plastic cylinder requires the researcher to coax the rodent head first into the tube, and then promptly affix the lid, which can take quite some time depending on the temperament of the mouse. To remedy this problem we developed a slight modification of the single restraint tube in order to lessen the time it takes to restrain 40 mice each day. Using a soldering iron, we cut a narrow, lengthwise slit along a 50mL conical tube. This allowed us to place a mouse into the tube by grasping the tail and pulling them in backward, similar to a device for tail vein injections. While holding the tube containing the mouse in one hand, with the tail firmly gripped, we can

then use the other to apply the perforated cap to the tube. By cutting the slit in the tube with a soldering iron, we melt the edges, making them smooth, which prevents any injury to the mouse's tail upon gently pulling them backwards into the tube.

In vivo tumor growth assay

Subcutaneous growth: 4-6 week old Fox3p$^{-/-}$ BalbC (nude) mice were inoculated subcutaneously with 100uL of PBS solution containing 1x 10^6 MDA-231 at the dorsal midline between the scapulae. Measurements of tumor dimensions were made every 2-3 days with calipers or via Maestro GFP imaging of the tumor mass at multiple angles.

Mammary Fat Pad Tumors-

For 4T1-592, 50uL of a PBS solution containing 5 x 10^3 cells were injected into the 4th mammary fat pad. Tumor size was assessed longitudinally with caliper measurements or volume and post-mortem by weighing on a balance.

Radiographic Analysis

Osteolytic lesions were quantified bilaterally in the humeri, femora, and tibiae at end point from Faxitron images. Presence of tumor within the bones was confirmed with GFP imaging or by histology. Lesion area was calculated as the average of total osteolytic area per mouse (sum of all 6 bones counted). Lesion number was calculated as total number of long bones with a visible lesion per

mouse, e.g. 0/6, 1/6, etc. Data were double-blinded and calculated by at least 2 independent researchers.

Microcomputed tomography (μCT) analysis

Tibiae from each animal were dissected, cleaned, and fixed for 48 hours in 10% formalin/PBS, transferred to 70% ethanol, then loaded into 12.3-mm-diameter scanning tubes, and imaged (μCT 40; Scanco Medical, Bassersdorf, Switzerland). The scans were integrated into three-dimensional (3-D) voxel images. A Gaussian filter (sigma = 0.8, support = 1) was used to reduce signal noise, and a threshold of 300 was applied to all analyzed scans. Scans were done at 12 μM resolution (E = 55 kVp, I =145 μA). 200 transverse slices of the proximal tibia were taken from the growth plate and extending distally. All trabecular measurements were made by manual determination of appropriate slices to exclude growth plate, and automated contouring using voxel counting and sphere-filling distance transformation indices.

Histology

Following μCT scanning, bones were decalcified in 20% EDTA pH7.4 at room temperature for 3-4 days. Decalcified samples were then dehydrated and embedded in paraffin. A modified H&E-phloxine-Orange G stain was used to quantify tumor burden and tumor number in 4-5um paraffin sections. Metastatic tumor foci were identified by morphology and pink staining in contrast to blue bone marrow cells. Tumor number was counted as number of long bones

present with a tumor. Tumor burden was quantified using the Bioquant system imaging software (Nashville, TN) as total tumor area per combined area of the 6 long bones averaged from 3 sections per bone. Osteoclasts were visualized and counted following Tartrate Resistant Acid Phosphatase (TRAP) staining using a standard protocol and the Bioquant system.

Migration assays

MDA-231VU used in this study were derived from MDA-231SA, a highly bone metastatic GFP-tagged clone developed by Dr. T. Yoneda by *in vivo* passage via intracardiac injection and subsequent culture of tibial metastases. MDA-231VU cells were then FACS sorted for GFP to enrich for GFP-positive cells. MDA-231VU cells were detached with trypsin and resuspended in 10% FBS for 1 hr. prior to assay. Cells were plated in serum-free DMEM in the top well of a 96 well Boyden chamber apparatus (Neuroprobe), and allowed to migrate through a semipermeable (8µM pore size) membrane towards 2.5% FBS DMEM in the bottom chamber for 4-6 hours. Co-culture migration assays were conducted with two separate transwell systems: a 24 well format using Corning 8um pore transwell inserts, and a 96 well Boyden chamber (Neuroprobe). Primary BMSCs or MC3T3 osteoblasts were grown to confluence in 24 or 96 well tissue culture plates. 24 hours before migration, fresh 2.5% FBS DMEM containing 10uM isoproterenol or PBS was added to the cells. On the day of migration, semipermeable membranes were added to the plates, on top of which MDA-231 cells were plated in serum-free media. In both types of assays,

“unmigrated” cells were removed from the top of the membrane with a wet Kim wipe, and then subsequently fixed with 10% PBS buffered formalin and stained with crystal violet. Total cell area per well was then quantified with an area scan on a 96 well plate reader (Synergy2, Biotek).

Growth Assays

MDA-231VU and 4T1-592 cell growth was assessed in phenol-free DMEM containing 2.5% serum, in a 96- well format. Medium was changed daily with fresh isoproterenol or PBS. Cell number was quantified daily by GFP signal measurements (MDA-231VU cells) or crystal violet staining and OD_{592} reading after fixation (4T1-592), using a Synergy2 plate reader (Biotek). Growth curves were normalized against day0. Each treatment contained 8 replicates. Dose-response was calculated based on cell number after 4 days of growth. For coculture growth assays, BMSCs, MC3T3, or NIH3T3 cells were grown to confluence in 96 well plates in 10% FBS DMEM. 2.5×10^3 MDA-231VU cells were then plated onto these cells in phenol-free DMEM containing 2.5% serum, which was changed daily along with treatment. Total GFP signal per well was quantified with a Syngery2 plate reader. Total counts at each time point were reported as raw numbers or normalized against day0 reading as indicated.

Gene Expression Assays

For all gene expression assays, cDNA was generated using the High Capacity Reverse Transcriptase Kit (Applied Biosystems #438814) using TRIzol extracted RNA from tissues or cells. Real-time PCR was performed using TaqMan gene expression assays on a BioRad CFX96 Real Time System. TaqMan probes/primers were from Applied Biosystems [*Adr*β*2*, Mm02524224_s1; CXCR4, Hs00237052_m1; Cxcr4 *Mm01292123_m1; Cxcl12(Sdf1), Mm00445553; RANK (TNFRSF1), Hs00187192_m1; Rankl*, Mm00441908_m1; *18s* RNA (DQ) MIX probe dye: FAM-MGB, 4352655; *Hprt1*, Mm00446968_m1]. Results were analyzed using standard curve quantification or ddct methods. RT-PCR for βAR1-3 expression was performed as described previously [104].

Knock down

MDA-231 (1 x 10^6) cells were transfected with HuSH-29 (Origene, Rockville, MD) shRNA silencing vectors against human *RANK* (*TNFRSF11A*) 5'GGAAAGCACTCACAGCTAATT3' or scramble control: 5'GGAATCTCATTCGATGCATAC3'. Transfections were carried out with the shRNA Nucleofection Kit (Lonza, Walkersville, MD) per manufacturer's instructions. Selection and maintenance of stable clones was performed with 1ug/μL puromycin.

MDA-231 intracardiac bone metastasis model

MDA-231VU cells were cultured in 10% FBS DMEM with 1% penicillin streptomycin. Cells were trypsinized at 70-90% confluence, rinsed and re-suspended in cold PBS at 10^7 cells/mL. Athymic nude fox3p$^{-/-}$ female mice aged 4-6 weeks were anesthetized and injected in the left cardiac ventricle with 100uL of cell suspension (10^6 MDA-231VU cells). Bone metastasis was assessed weekly for 4 weeks with Maestro *in vivo* fluorescence and Faxitron radiographic imaging.

Statistics

All data are presented as means ± SEM. Statistical analyses were performed using one-way ANOVA for multiple comparisons and two-tailed Student's *t* tests, either paired or unpaired with Welch's correction for two-group comparisons. For all analyses, a $P < 0.05$ was considered significant.

CHAPTER III

CHRONIC STRESS INCREASES METASTATIC COLONIZATION OF BONE

Propranolol blocks the stimulatory effect of CIS on breast cancer colonization of bone

Metastasis to bone is a multistep process starting from the egress of metastatic cells from the primary tumor, contingent upon their subsequent survival in the bloodstream, followed by arrest within the bone capillaries, and colonization of the bone marrow microenvironment. We utilized an established model of bone metastasis in which GFP-tagged MDA-MB-231 human mammary carcinoma cells (called MDA-231 cells herein) are inoculated via intracardiac injection (IC) into athymic nude mice [191]. This model is relevant to the late stages of the bone metastasis process, at which point metastatic cancer cells egress from the blood capillaries and reach the bone marrow microenvironment. Elevated SNS activity is seen in conditions of psychiatric disturbance such as PTSD [192] and major depression [193] which are correlated with increased cancer mortality [152]. To simulate the physiological consequences of these conditions in mice we used chronic immobilization stress (CIS) since this model is easily reproducible and known to increase endogenous sympathetic activation [183] and depression [194] in rodents. In this experimental paradigm, mice are submitted to bodily restraint for 2 hours a day, 6 days a week, for the duration of the experiment. When mice experience 6 weeks of CIS treatment, including 2

week of CIS treatment prior to tumor cell inoculation, a 2-fold increase in the number of osteolytic lesions (and lesion area) is seen by X-ray analyses in the restraint-stressed group (CIS) when compared to control (no CIS) (Figure 7A,B,E). Endogenous sympathetic activation also significantly increased bone tumor number (2.5-fold increase), measured by serial histological examination of the long bones (Figure 7D). Upon propranolol administration, no significant decrease in bone lesion area and number was observed in control (no CIS) mice. By contrast, in mice subjected to CIS treatment, propranolol significantly decreased the number of osteolytic lesions and the lesion area (Figure 7B,C), indicating that the effects of SNS are mediated through SNS activation and adrenergic signaling rather than the HPA and glucocorticoids. These data indicate that endogenous sympathetic activation by chronic stress in mice can exacerbate metastatic bone disease, and that β-blockers have the potential to inhibit this effect. Furthermore, the increase in tumor number indicates an additional effect of β-adrenergic signaling on the successful establishment of bone metastases.

ISO treatment increases tumor cell colonization of bone by acting on the host bone marrow environment.

To elucidate the mechanism whereby chronic stress increases bone colonization and tumor growth, we used isoproterenol as a surrogate for sympathetic stress,

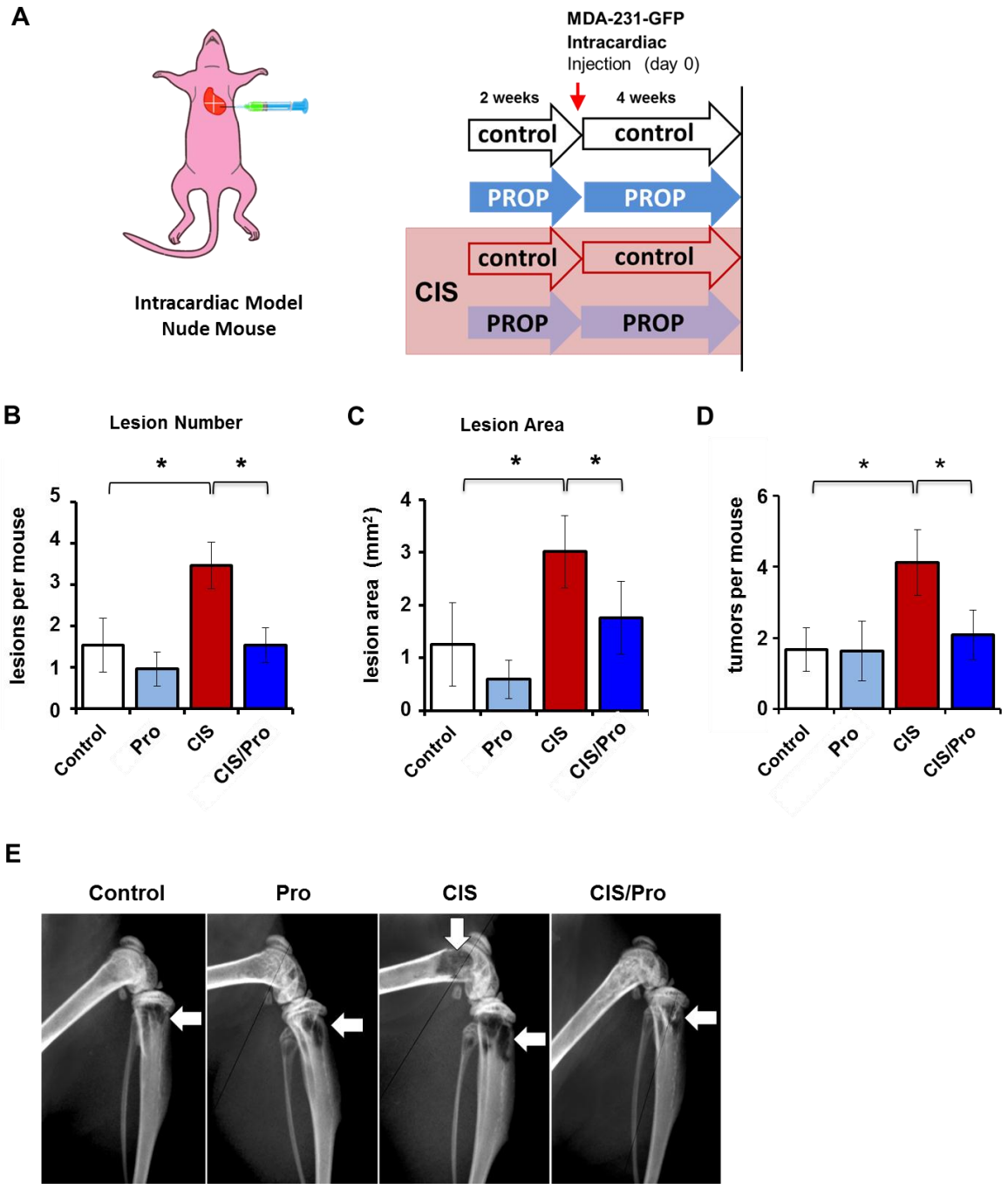

Figure 7. Propranolol inhibits CIS-induced bone metastasis A) Mice were given propranolol (Pro) in the presence or absence of 2hr daily chronic immobilization stress (CIS). **(B)** Bone lesion number and **(C)** lesion area in the femurs, tibiae, and humeri of nude mice, measured by Faxitron analysis (n=10). **. (D)** Bone tumor number as quantified from histological analysis of hind limb sections **(E)** Representative Faxitron images of hind limbs 28 days after tumor inoculation, showing osteolytic lesions (white arrows). Data are plotted as means ±SEM ; ***** p<.05.

as its use precludes glucocorticoid involvement and its effects have been well studied in our research group. This compound stimulates both β1 and β2 adrenoreceptor subtypes, but based on previous data [102], we hypothesized that ISO would exert its effects in the skeleton via the β2AR, rather than having any effect on cancer. Daily intraperitoneal injections of ISO (3mg/kg) were given to nude mice before MDA-231 cell intracardiac inoculation ("pre" treatment for 2 weeks) or after MDA-231 cell inoculation ("post" treatment for 4 weeks) (Figure 8A). We reasoned that if sympathetic activation promotes cancer cell colonization in bone via an indirect effect on the stroma, treating mice with ISO *prior* to tumor inoculation (with no further treatment afterward) may increase the incidence of tumors in bone and possibly the number of osteolytic lesions, whereas treating mice *after* tumor inoculation should promote bone resorption and increase the area of osteolytic lesions, but not bone colonization.

In tumor bearing bones, ISO treatment for 4 weeks post-MDA-231 cell inoculation significantly increased tumor burden, but not tumor number, as measured by histomorphometry (Figure 8 B-D). Accordingly, ISO "post" treatment also increased the size, but not the number, of osteolytic lesions, assessed by radiographic analyses (Figure 9 B-D). In contrast, ISO "pre" treatment increased bone lesion and tumor areas, but also increased bone lesion and tumor numbers. More metastatic tumors and bony lesions were thus formed in the "pre" ISO treatment group, even though MDA-231 cells were never directly subjected to ISO stimulation, indicating that ISO promotes metastasis to bone via its effect on the bone marrow environment and not the tumor cells themselves.

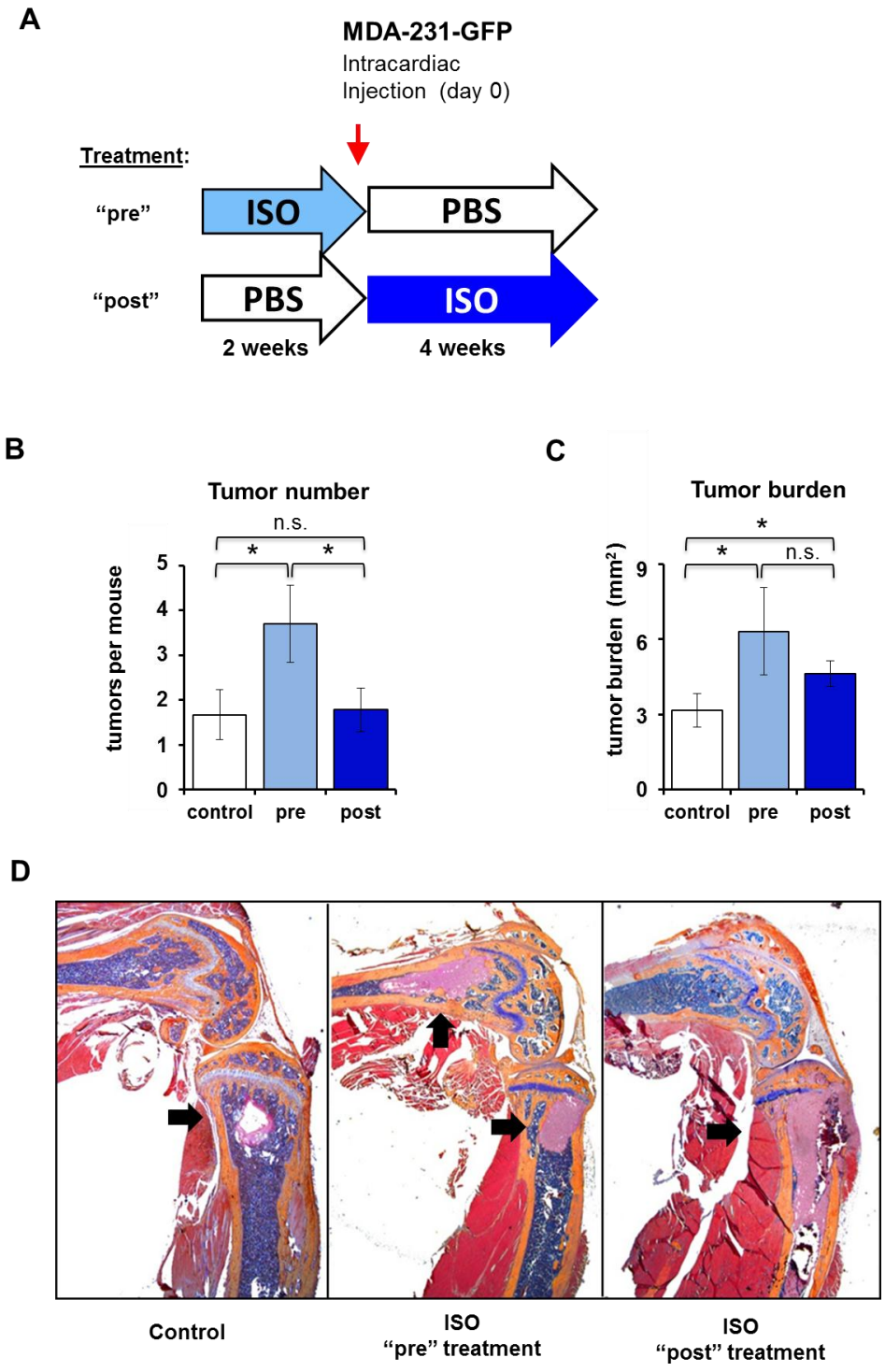

Figure 8. Isoproterenol treatment of bone increases tumor colonization

(A) Athymic (Foxn1^{nu} BalbC) mice were treated daily with ISO (3mg/kg) for two weeks prior to or for 4 weeks after intracardiac injection of MDA-231 cells. **(B)** Tumor number counted in femora and tibiae by histology (n= 8) **(C)** Total bone tumor burden per mouse by histology (n=8). **(D)** MDA-231 tumors appear as pink masses in the metaphysis as seen in representative images (modified H&E). Data are plotted as means ±SEM ; ***** p<.05; ****** p<.005.

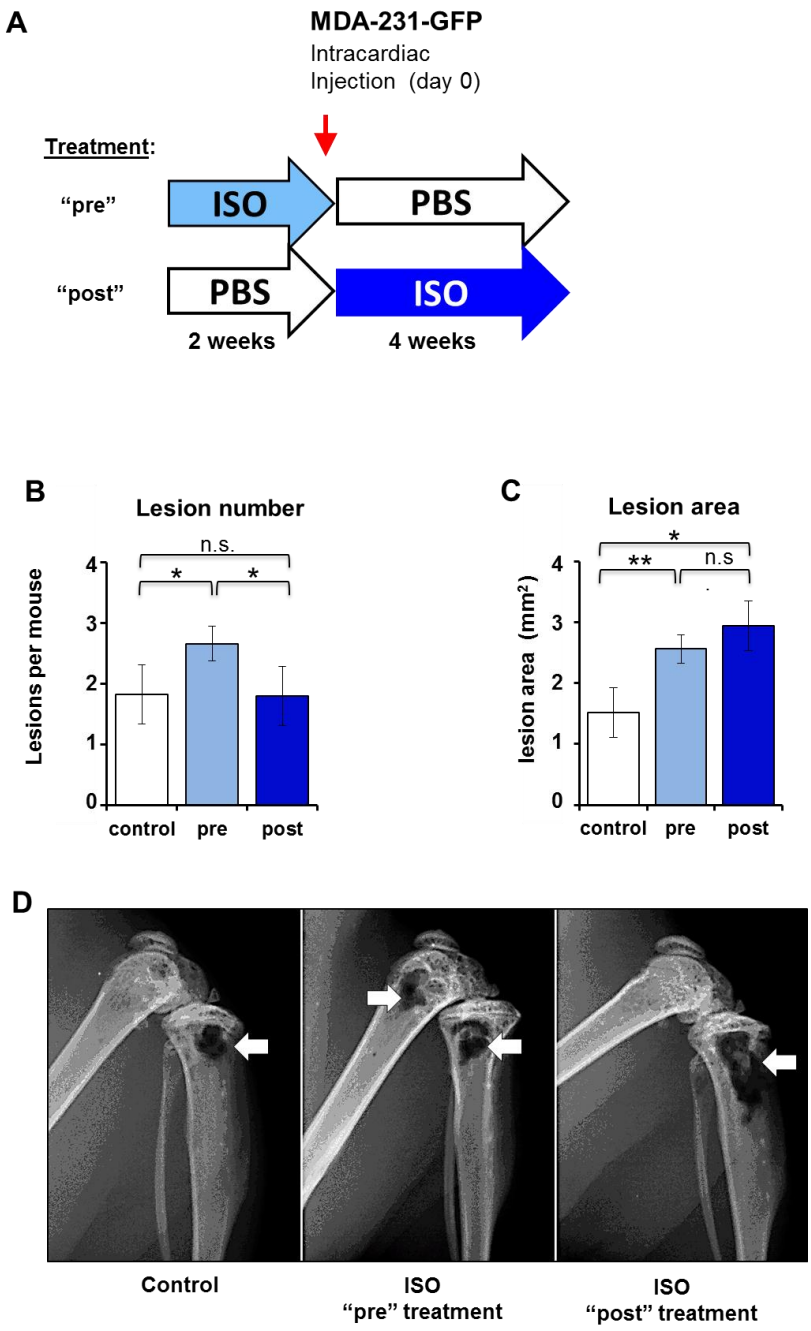

Figure 9. β2AR signaling differentially affects lesion number and size. **(A)** Athymic (Foxn1^{nu} BalbC) mice were treated daily with ISO (3mg/kg) for two weeks prior to or for 4 weeks after intracardiac injection of MDA-231 cells. **(B)** Number of osteolytic lesions per mouse as quantified from Faxitron radiographs at d28 in humeri, femora, and tibiae (n=8) **(C)** Total osteolytic lesion areas visible per mouse, as assessed by Faxitron (n=8). **(D)** Representative Faxitron images of hind limbs at d28. Lesions (white arrows) are visible as dark areas in the bone. Data are plotted as means ±SEM; ***** p<.05; ****** p<.005.

Mechanistically, the observation that ISO has a similar effect to CIS is evidence that sympathetic activation, rather than activation of the hypothalamic-pituitary-adrenal axis, triggers these effects of CIS on tumor metastasis**.** These results indicate that sympathetic activation alters the bone marrow environment to make it more hospitable for breast cancer cell metastatic colonization, establishment and growth, thus priming the "vicious" cycle of bone destruction induced by cancer cells, and exacerbates this cycle once tumor burden increases, stimulating osteoclastogenesis and bone resorption.

β2AR signaling in osteoblasts does not increase cancer growth *in vitro*

When mice were treated with ISO only prior to cancer inoculation ('Pre'), the number of bone tumors was increased, indicating that the effects of β2AR stimulation on metastasis occurred through changes in the bone microenvironment rather than through effects of ISO directly on the cancer. To test whether ISO increased the production of bone factors that could stimulate growth of metastasis at critical early phases and account for the increase in metastasis, we performed a series of in vitro growth experiments using conditioned media from osteoblast cultures. When we treated BMSC cultures with ISO for 24 hours and used this media to grow MDA-231 or 4T1 592 cells we saw no increase in cell growth, as measured by GFP+ cell number or crystal violet staining, from ISO stimulated bone cells that could account for the

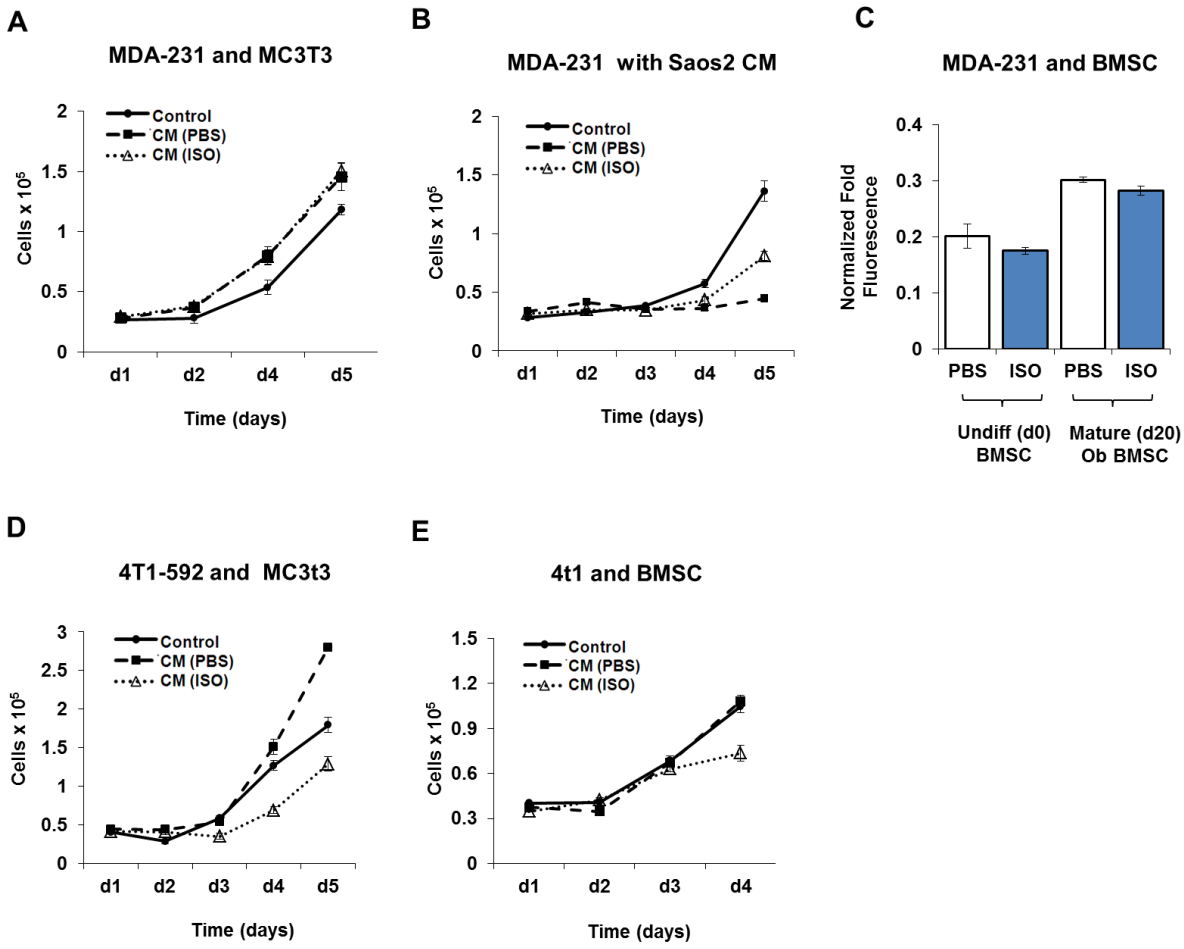

Figure 10. ISO treatment of bone stroma does not increase cancer cell growth through soluble factors. MDA-231 cell growth in the presence of Media from confluent MC3t3 **(A)** with or without ISO treatment. **(B)** Media from a human osteosarcoma SAOS2 decreased cell growth of MDA-231 with or without ISO treatment, as quantified by counts of crystal violet stained cells. **(C)** Media collected from confluent Bone Marrow Stromal Cell cultures with or without 20 day differentiation with Ascorbic acid did not affect MDA-231 growth after ISO treatment. 4T1 cell number at specified time points with CM collected from confluent MC3t3 **(D)**or primary BMSC **(E).** Data are plotted as means ±SEM

increase in bone tumors in vivo. Since osteoblasts are the major transducers of β2 AR signaling effects in bone we repeated the conditioned media experiments with osteoblast-like MC3T3 and again saw no increase in cell number in either 4T1 592 or MDA-231. If we differentiated BMSC to mature osteoblasts with ascorbic acid for 20 days, then treated with ISO, we still saw no effect on MDA-231 growth, demonstrating that ISO does not increase growth of MDA-231 via soluble factors from either immature or mature osteoblasts. Finally, using a conditioned media from a human osteogenic cell line, Saos2, we also failed to observe an increase MDA-231 growth. These negative data on growth suggest that CIS or ISO increases bone colonization by some other mechanism(s).

Duration of action of ISO in Foxn1$^{nu/nu}$ mice

Another possibility to explain the observed increase in bone metastasis following CIS is that β-adrenergic stimulation could increase cardiac output and peripheral vasodilation that would affect cancer cells' likelihood of extravasation into the bone marrow, and account for the increase in bone colonization. Since ISO treatment is stopped 18-24 hours before injection of the cancer cells, we needed to know whether β1-induced tachycardia, elevated blood pressure, and β2–mediated vasodilation could persist until the time of cancer inoculation and affect bone cancer metastasis.

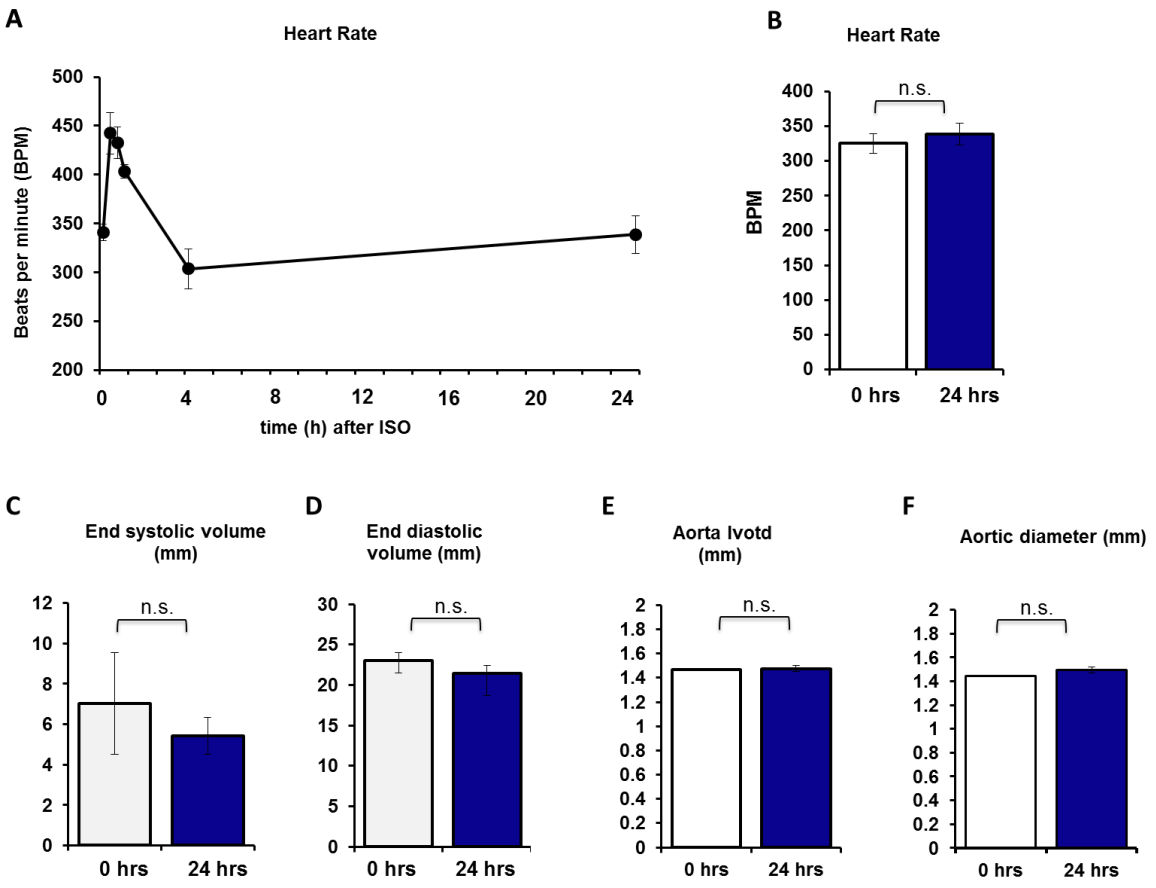

Figure 11. Duration of ISO effects in the nude mouse. Isoproterenol does not affect hemodynamic parameters after 24 hours in athymic mice. Time course of isoproterenol effects on heart rate shown in **(A)** and **(B)**. Systolic **(C)** and diastolic **(D)** ventricular volume using((4/3)*(⌈])) *(D/2)³ ventricle as a sphere. Aortic parameters of left ventricular outflow tract during systole **(E)** and aortic diameter **(F).** Measurements were taken with Visualsonics Vevo770 ultrasound on anesthetized athymic mice (n=3).

Isoproterenol has a half-life *in vivo* of <1 minute [195], but the duration of action in athymic mice is unknown. Since this agonist is central to our experiments, we performed cardiac pharmacodynamics experiments to ascertain the duration of isoproterenol's hemodynamic effects in vivo in athymic mice. For these experiments, we measured multiple cardiac parameters (Figure 11A-F) before and after intraperitoneal injection of 3mg/kg isoproterenol. In agreement with published data in other rodents [196], the cardiac effects of isoproterenol were rapid onset and peaked within 1 hour, as measured by echocardiogram. Tachycardia lessened over the next 3 hours and heart rate diminished to a level below baseline at 4 hours post injection (Figure 11A) and returned to baseline levels by 24 hours (Figure 11B), as did aortic diameter and blood pressure (not shown). As anticipated, these data show that isoproterenol has a relatively short half-life and duration of action in vivo in athymic BalbC mice. Since cancer inoculations in our experiments were performed 18-24 hours after ISO treatment, the short duration of action of ISO precludes the possibility of hemodynamic effects during intracardiac injection that could account for the increase in bone metastasis after SNS activation.

β2AR signaling in bone marrow osteoblasts increases the migration of mammary carcinoma via RANKL

To further investigate a mechanism by which SNS activation increased the metastatic colonization of bone, we looked into the effects of β2AR stimulation of

the motility of MDA-231 cells, using a series of transwell migration assays. When MDA-231 cells were plated in the transwell filter without osteoblasts in the bottom chamber, ISO treatment did not increase their migratory properties (data not shown). Contrastingly, in co-culture transwell assays, primary BMSCs plated in the bottom chamber increased the migration of MDA-231 cells plated on the transwell filter, and ISO treatment significantly exacerbated this effect (Figure 12). ISO treatment of osteoblasts, prior to the addition of propranolol-treated MDA-231 cells to the transwell filters (in order to block β2AR signaling specifically in cancer cells), did not inhibit cell migration indicating that the effects of ISO on the migration of MDA-231 cells are mediated by β2AR stimulation in osteoblasts.

RANKL is a cytokine well-known for its osteoclastogenic properties and for being a critical mediator of the feed-forward cycle of bone destruction induced by bone metastatic cancer cells. It is also expressed by normal mammary gland epithelial cells, contributing not only to the development of the lactating mammary gland during pregnancy [64] but also to cancer cell migration in melanoma [81]. In agreement with other reports [81, 197], we found that parental and non-osteotropic breast carcinoma-derived ATCC MDA-231 cells express *RANK*, the receptor for RANKL, but at a lower level than bone metastatic MDA-231 cells (Figure 13E). In contrast, *RANK* mRNA expression was not detectable in non-metastatic MCF-7 cells (Figure. 13E). These results, coupled with the observation that ISO strongly increases the expression of *Rankl* in bones to a

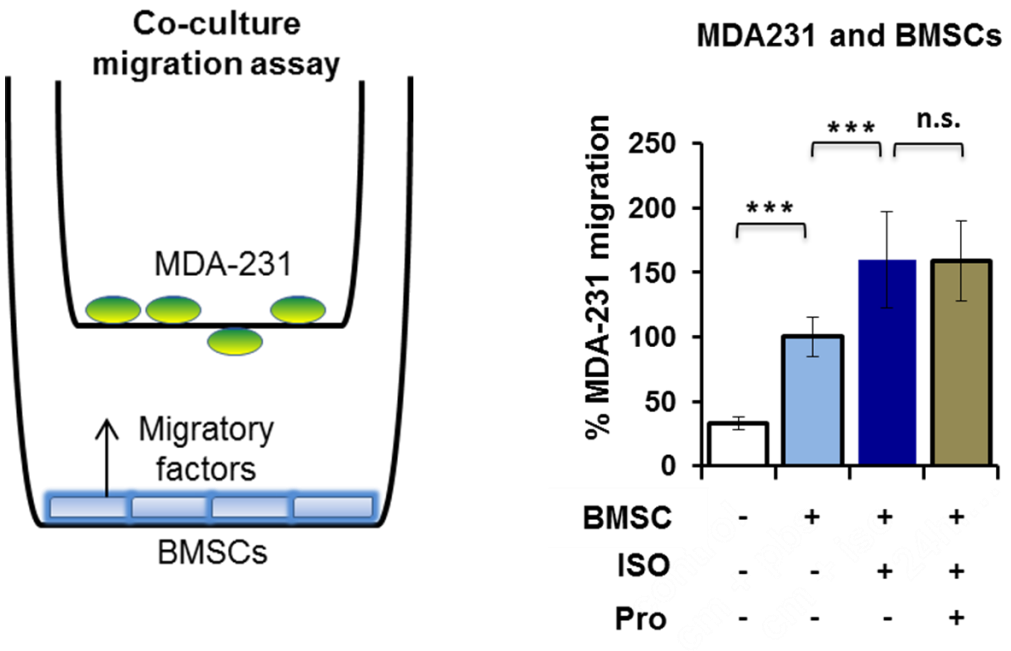

Figure 12. β2AR signaling in bone cells increases cancer cell migration via soluble factor(s). (A) Schematic of the osteoblast-MDA231 co-culture transwell migration assay. **(B)** Transwell migration assays of MDA-231 cells toward BMSCs (n=3), in the presence of 10uM ISO (n=3) or Pro (10uM) treatment (n=2). Data are plotted as means ±SEM ; ******* p<0.001.

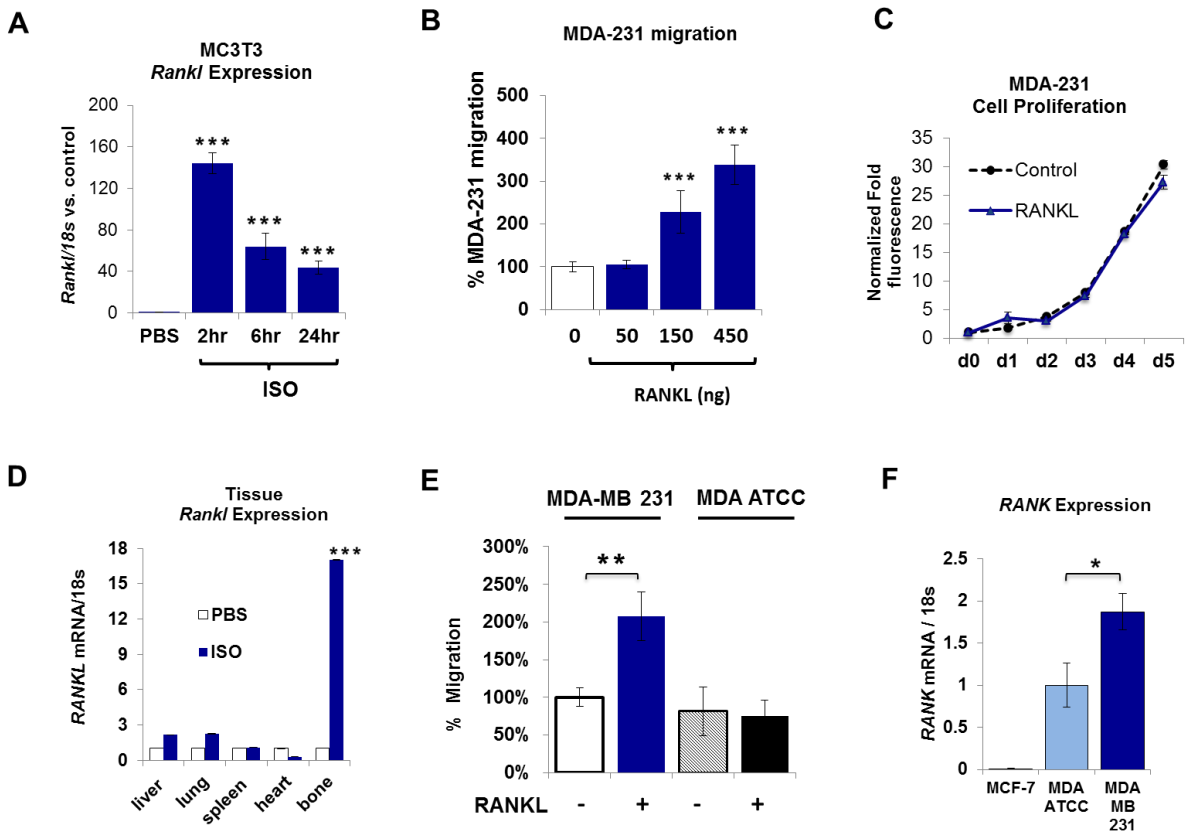

Figure 13 . Osteoblast-derived RANKL promotes the migration of osteotropic cancer cells.**(A)** *Rankl* expression in ISO-treated MC3T3 osteoblastic cells as measured by qPCR. **(B)** MDA-231 transwell migration assay in response to soluble rRANKL (n=3). **(C)** Cell growth as measured in vitro over 5 days by recording GFP fluorescence, with or without 250ng/mL rRANKL. **(D)** Whole bone (tibia and femur) *Rankl* expression in response to ISO treatment (3mg/kg) *in vivo* compared to other soft tissues measured by qPCR (2h treatment, control bone vs. ISO bone (n=4). **(E)** Migration of osteotropic clone vs. non osteotropic MDA ATCC in transwell assay in response to rRANKL, 200ng/mL (n=3). **(F)** *RANK* mRNA expression in the MDA-231 bone metastatic sub-clone compared to MCF-7 and parental MDA-MB-231 (ATCC) as measured by qPCR (n=3) All *in vitro* assays repeated at least 2 times. Data are plotted as means ±SEM ; *p<.05; **p<.01; ******* p<0.001.

greater extent than in any other organs tested (Figure 13 D), led us to explore whether this cytokine contributes to the effect of sympathetic activation on breast cancer metastasis to bone.

As observed in bone *in vivo* (Figure 13 D), ISO significantly increased *Rankl* expression in primary bone marrow stromal cells cultured *in vitro* (BMSCs, Figure 24B) as well as in MC3T3 osteoblasts (Figure 13A), which suggests that among mesenchymal bone marrow cells, the osteoblast lineage represents a main target. Addition of recombinant soluble RANKL (rRANKL) dose-dependently stimulated the migration of MDA-231 cells (Figure 13 B), and consistent with the above observations, high *RANK*-expressing MDA-231 cells, but not low RANK-expressing parental ATCC MDA-231 cells, responded to rRANKL with a significant increase in migration (Figure 13E). Since mammary epithelia require *Rankl* for proper mammary function during lactation, we examined whether RANKL could affect MDA-231 proliferation in vitro, but observed no change (Figure 13C).

We then set out to confirm functionally that RANKL is the pro-migratory soluble factor released in response to ISO treatment of BMSC. Using transwell BMSC/MDA-231 coculture assays, we found that addition of recombinant osteoprotegerin (OPG), a soluble decoy receptor for RANKL, blocked the effect of ISO on MDA-231 cell migration, indicating that RANKL is the primary cytokine involved in ISO-mediated stimulation of MDA-231 cell migration toward BMSCs (Figure 14 B). Similar results were obtained by co-culture of MDA231 cells with

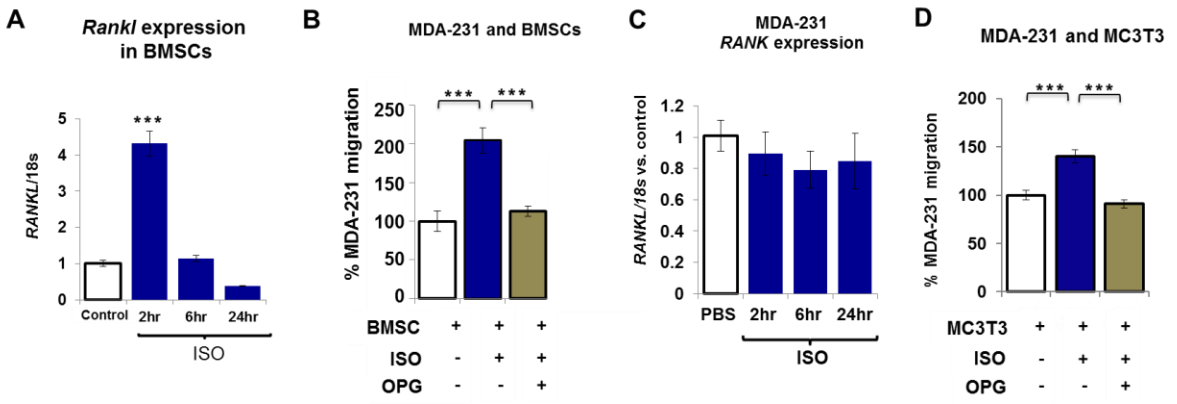

Figure 14 ISO increases MDA-231 migration via stromal RANKL. (A) *Rankl* expression in ISO-treated BMSCs measured by **(B)** Transwell migration assays of MDA-231 cells toward BMSCs in the presence of ISO or OPG (1ug/mL) treatment (n=2). **(C)** Expression of *CXCR4* and *RANK* mRNA after ISO treatment in MDA-231 cells, measured by qPCR (n=2). **(D)** Transwell Migration of MDA-231 toward MC3T3 with ISO and OPG (1uG/mL). Data are plotted as means ±SEM ; ******* p<.001.

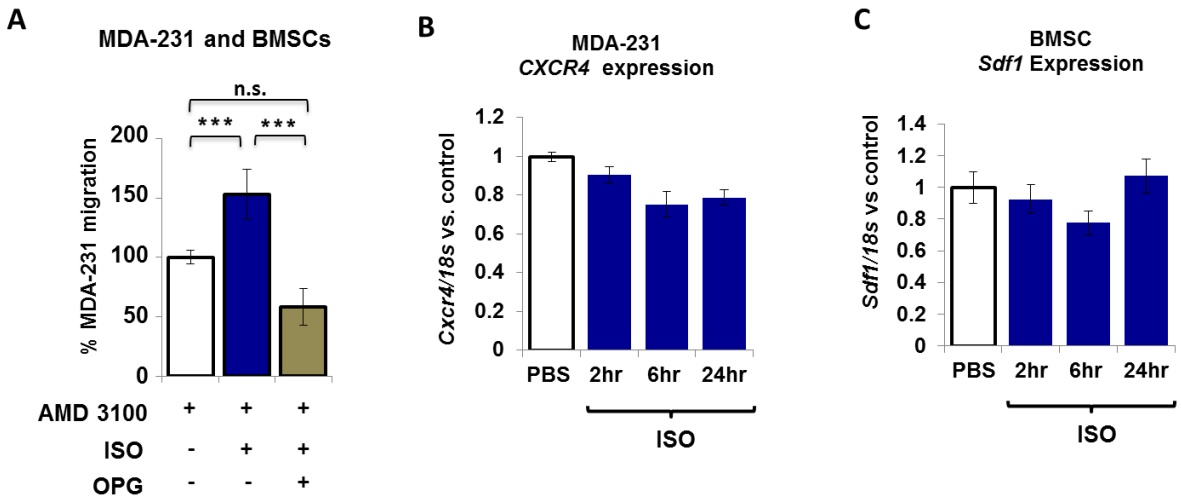

Figure 15 . Stromal β2AR signaling increases MDA-231 migration independent of CXCR4 axis.
(A) Transwell migration assays of MDA-231 toward BMSCs in the presence of ISO or OPG or AMD 3100 (10ng/mL) treatment (n=3). **(B)** Expression of *CXCR4* and mRNA after ISO treatment in MDA-231 cells, measured by qPCR (n=2). **(C)** *Sdf1* mRNA expression in bone stromal cells after ISO treatment, measured by qPCR (n=2).

MC3T3 osteoblasts (data not shown). Since cancer cells *in vivo* would be exposed to β2AR stimulation, we tested whether or not RANK could be upregulated by ISO, which could account for increased RANKL-induced migration, but we observed no effect (Figure 14C). Inhibition of SDF1-CXCR4 signaling by AMD3100, a CXCR4 antagonist, did not block the ISO-induced increase in MDA-231 cell migration, but further reduced migration when used in combination with OPG (Figure 15 A). These data are in agreement with the observation that pharmacological blockade of the SDF1-CXCR4 axis by AMD3100 does not fully prevent bone metastasis in vivo [81]. BMSC expression of *Sdf1*, a major cytokine promoting breast cancer cell migration, was unaffected by ISO treatment for 2, 6 or 24h (Figure 15 C); in breast cancer cells treated with ISO, the expression of the receptor for SDF-1, *CXCR4,* remained unchanged as well (Figure 15 B). These results demonstrate that β2AR stimulation in osteoblasts *in vitro* promotes breast cancer cell migration via RANKL and via an SDF1-independent mechanism.

RANK shRNA knockdown prevents ISO induced migration and bone metastasis

To address whether the pro-migratory activity of RANKL observed *in vitro* contributes to the stimulatory effect of sympathetic activation in breast cancer metastasis to bone *in vivo,* we used a loss-of-function strategy to specifically block RANK expression in metastatic MDA-231 cells. The advantage of this strategy, compared to using a RANKL blocker like OPG, was that it allowed us to

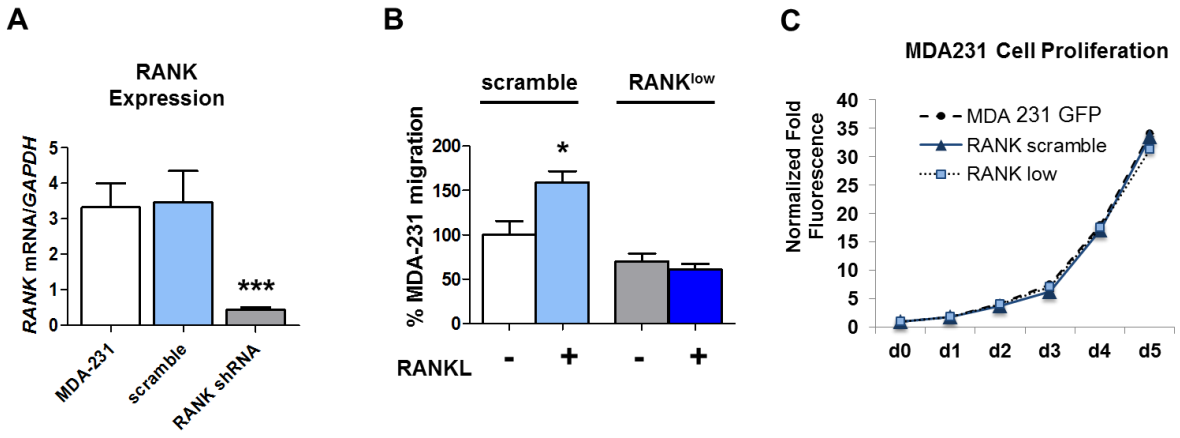

Figure 16. RANKL-induced migration is rescued by RANK shRNA knockdown.
(A) *RANK* mRNA expression in the MDA-231 bone metastatic sub-clone compared to MCF-7 and parental MDA-MB-231 (ATCC) as measured by qPCR (n=3) **(B)** Transwell migration assay in response to rRANKL, 200ng/mL (n=3) **(C)** In vitro cell proliferation assays comparing MDA-231 controls cells, $Rank^{scramble}$ cells or $Rank^{low}$ cells (n=3). Data are plotted as means ±SEM ; ***** p<.05. ; ***p<.001.

assess whether sympathetic activation promotes breast cancer bone colonization via the pro-migratory effect of RANKL on metastatic cancer cells or via an indirect stimulatory effect on bone turnover, since sympathetic activation increases bone remodeling, potentially increasing the expression, activity, and/or availability of other cell or ECM-derived cytokines promoting cancer cell bone colonization, establishment and growth. A shRNA knockdown approach was used to generate stable clones of MDA-231 cells expressing reduced levels of RANK. We selected a clone whose *RANK* expression was decreased by 85% ($RANK^{low}$) compared to scramble shRNA control ($RANK^{scramble}$) (Figure 16). To determine effects of the clonal selection process or RANKL signaling on growth of MDA-231 we performed in vitro cell growth assays. No difference in cell proliferation was detected between MDA-231 $RANK^{scramble}$ control cells and $RANK^{low}$ cells, treated or not with rRANKL (Figure 16). We also observed no change in *PTHrP* expression that might affect the vicious cycle and subsequent tumor growth. In contrast to these negative results on growth parameters, RANK knockdown significantly reduced MDA-231 cell migration in response to rRANKL in a transwell assay (Figure 16), demonstrating the necessity of a functional RANKL-RANK signaling pathway for the migratory properties of MDA-231 cells. We then inoculated MDA-231 $RANK^{scramble}$ control cells or $RANK^{low}$ cells via intracardiac injection to nude mice treated daily with ISO for 6 weeks to mimic sympathetic activation. Confirming the first set of results, when control MDA-231 $RANK^{scramble}$ cells were used, ISO treatment significantly increased the incidence of GFP-positive tumors in bone, the number and area of bone lesions measured

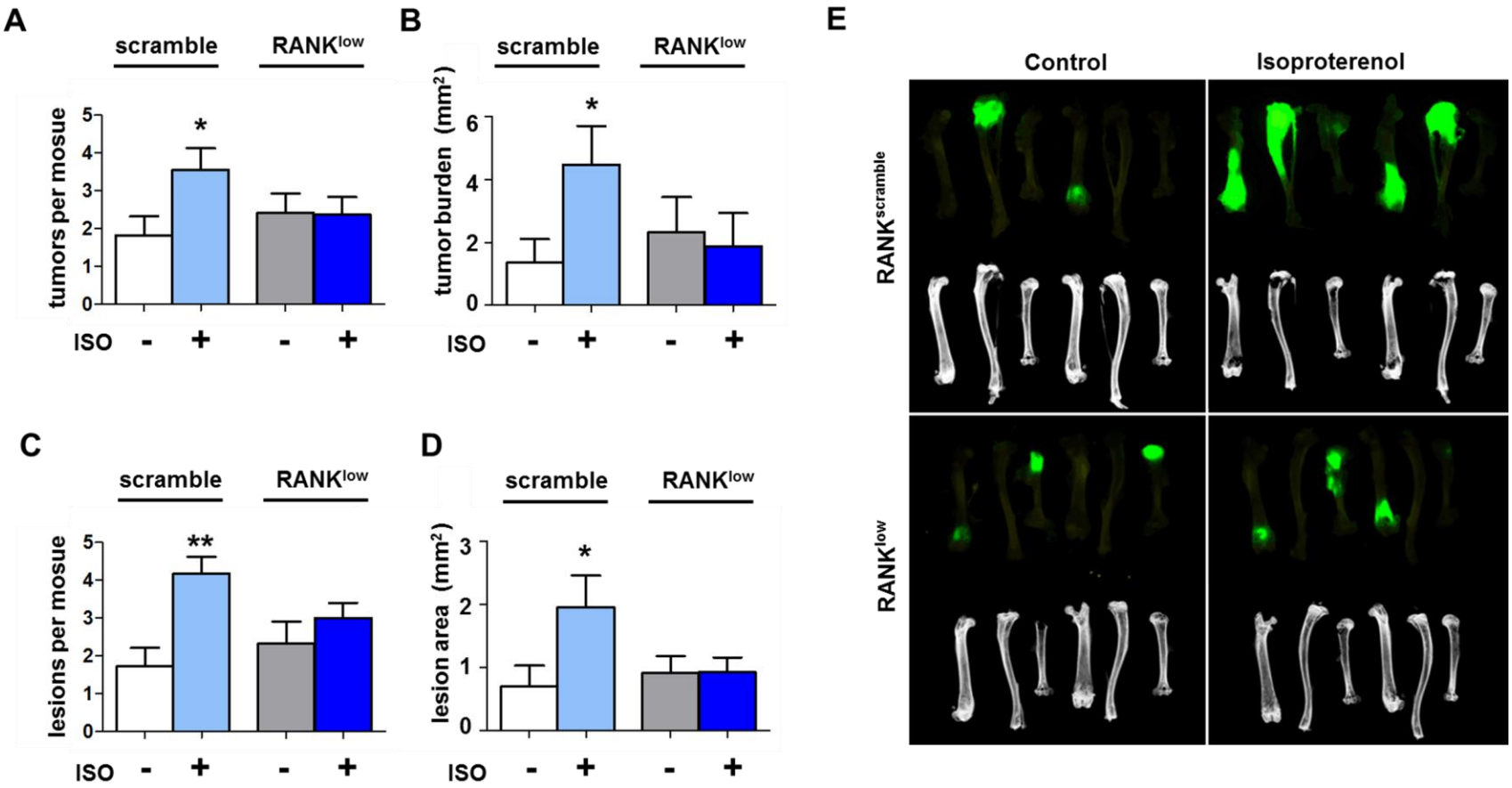

Figure 17. RANK knockdown prevents increased bone metastasis induced by ISO treatment. **(A-B)** Quantification of GFP+ bone tumor number and tumor burden per mouse from Maestro imaging (n=9). **(C-D)** Number and area of osteolytic lesions visible in Faxitron images at 4 weeks (n=9) . **(E)** Representative images of GFP-positive long bones correlating with osteolytic lesions after 4 weeks in ISO-treated mice that were inoculated with $Rank^{scramble}$ or $Rank^{low}$ MDA-231 cells . Data are plotted as means ±SEM ; ***** p<.05; ****** p<.005.

by Faxitron, and bone tumor burden measured by histomorphometry, when compared to PBS-treated mice (Figure 17). In contrast, selective inhibition of RANK expression in MDA-231 $RANK^{low}$ cells blunted the effect of ISO on each of these parameters. No significant difference was observed between the two clones in absence of ISO treatment. These results demonstrate that RANK expression in breast cancer MDA-231 cells, independently of increased bone turnover, is required for their migratory response toward RANKL-expressing bone cells *in vivo* in response to sympathetic activation.

Isoproterenol Increases Bone Tumor Burden and Bone Destruction

We observed that SNS activation, via β2AR, can increase both bone tumor colonization and subsequent growth. The first effect was mediated by RANKL which increased migration in vitro and tumor number in vivo by acting on the RANK receptor expressed on MDA-231. Since the 'post' treatment mouse model experienced ISO only two days after the MDA-231 cells were seeded in the marrow, we hypothesized that the increase in tumor growth was due to some other mechanism beside RANKL-induced migration. To investigate this and confirm the effect of ISO in inducing tumor growth after establishment bone destruction, athymic mice were given daily intraperitoneal injections of 3mg/kg ISO for 2 weeks before and 4 weeks after intracardiac injection of 10^5 GFP expressing MDA-231 cells. After a total of 6 weeks of chronic intermittent β-adrenergic stimulation, we observed a substantial increase in both bone tumor

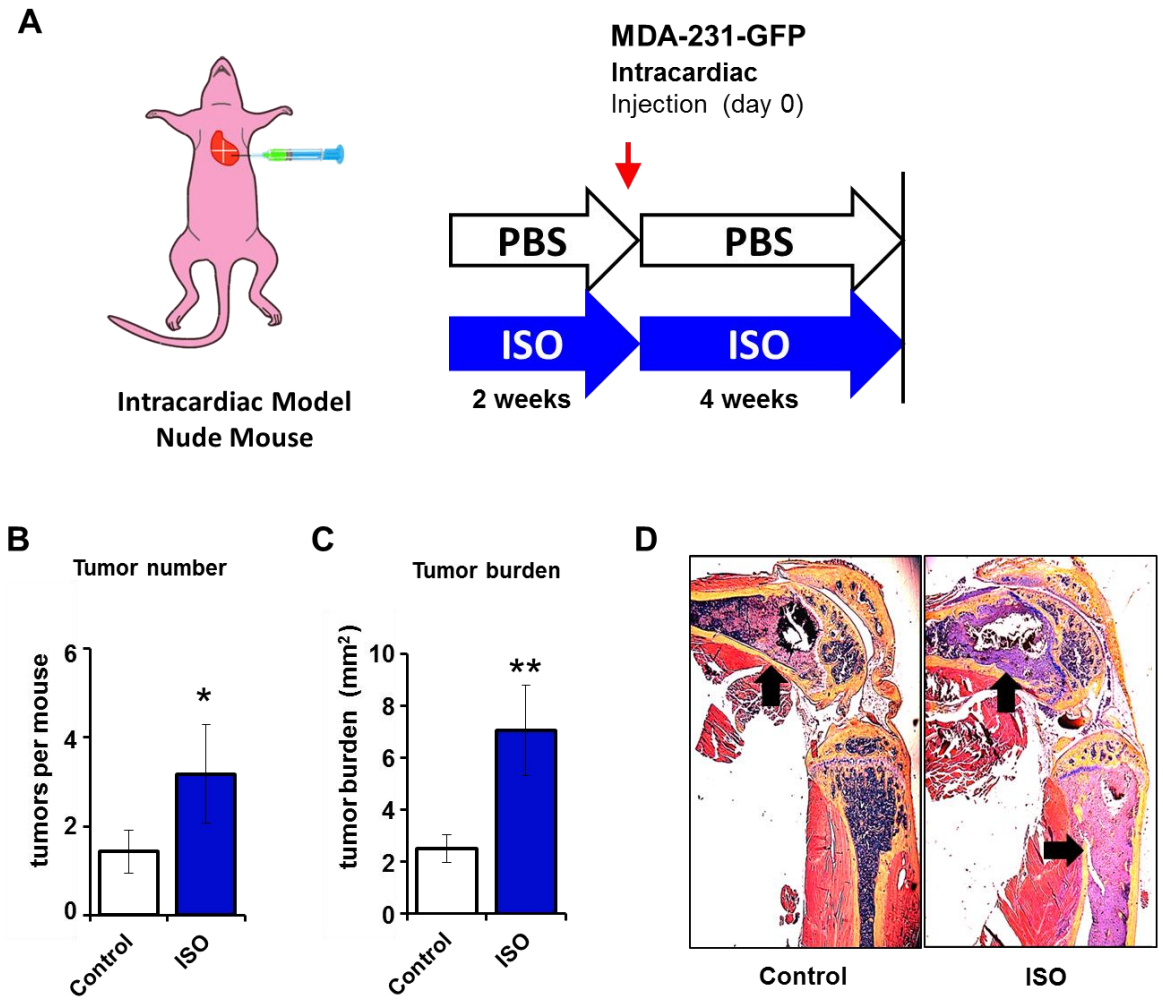

Figure 18. β2AR signaling increases number and size of bone tumors. (A) Fox$^{nu/nu}$ BalbC mice received daily treatment with 3mg/kg Isoproterenol (ISO) for 2 weeks before and 4 weeks after inoculation with GFP-expressing MDA-231. Quantification of and total number **(B)** and size **(C)** of bone tumors in H&E stained hind limbs 28 days after tumor inoculation (n=8). **(D)** Representative histological images of modified H&E, phloxine, orange G stained paraffin sections. Tumors (black arrows) are identified by pink staining. Data are plotted as means ±SEM ; ***** p<.05; ****** p<.01.

number and tumor burden compared to control mice (Figure 18B-C), as quantified by histology, demonstrating that adrenergic signaling can increase metastasis to the skeleton. In agreement with the increase in bone tumor number, there was a significant increase in both the number and size of osteolytic lesions, as shown by radiographic analysis (Figure19A-C) of Faxitron images. The increase in both the number of tumors and the area of the osteolytic lesions confirmed that there are indeed two distinct effects of β2AR signaling: one on tumor establishment and another on tumor growth after establishment. The notion that there is an additional effect of SNS outflow on bone tumor establishment independent of RANKL mediated colonization was further supported when we compared 'pre' treated mice to 'pre-post' treatments and saw that the size of each tumor increased with additional ISO treatment after establishment of tumor Figure (20A-E) .

Since we know that chronic β2AR stimulation with ISO increases bone resorption and subsequent bone loss in nude mice, we assumed that accelerated bone loss could play a role in increasing the rate of tumor growth in this model of cancer-induced bone disease. Indeed, the amount of bone loss in tumor bearing mice treated with ISO was much greater than that in the non-tumor bearing control (Figure19 D, E). The parallel increase in bone destruction and increased tumor burden together suggest that SNS signaling may exacerbate metastatic bone disease by accelerating the vicious cycle of tumor-induced bone destruction, but when treated MDA-231 with 10uM ISO, we observed no change

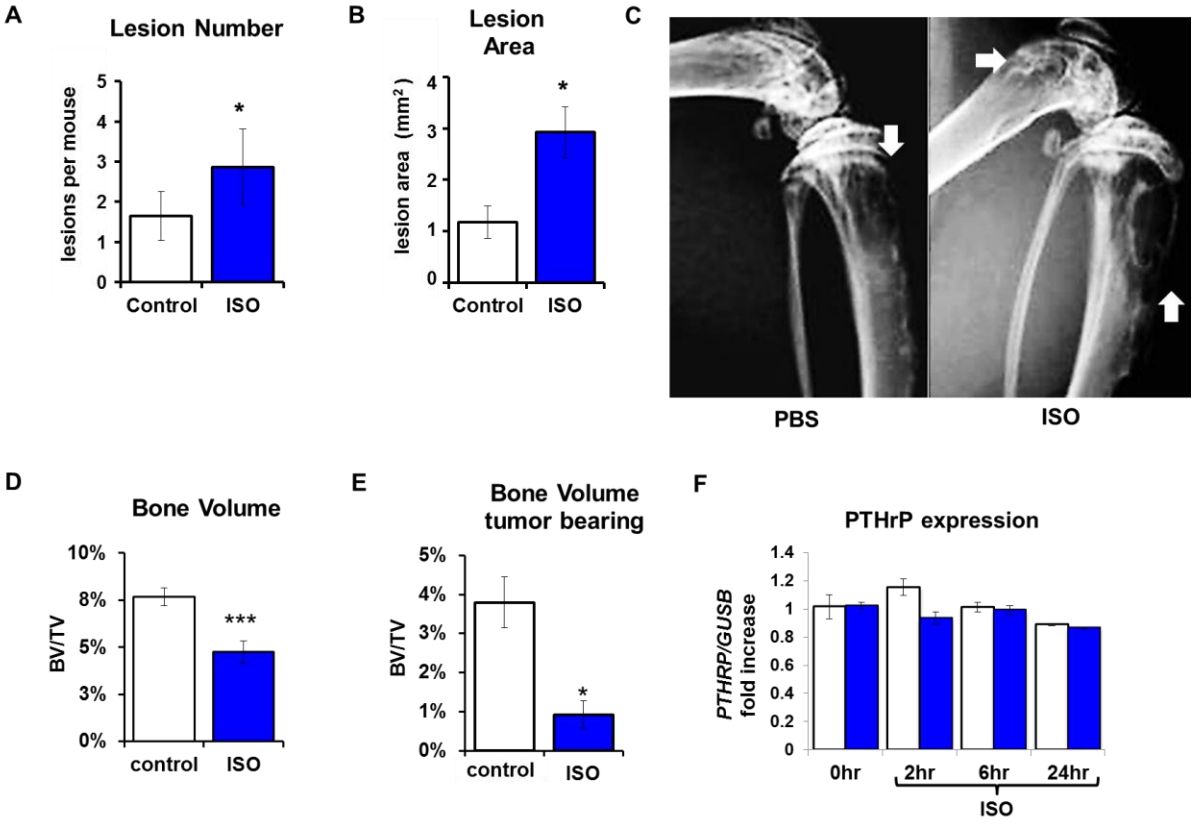

Figure 19. □2AR signaling increases osteolytic lesion number and area. Fox$^{nu/nu}$ BalbC mice received daily treatment with 3mg/kg Isoproterenol (ISO) for 2 weeks before and 4 weeks after inoculation with GFP-expressing MDA-231. Quantification of osteolytic lesion number **(A)** and area **(B)** of 2D radiography of femora and tibiae 28 days after tumor inoculation (n=8). **(C)** Representative Faxitron images of hind limb bones at d28. Lesions (white arrows) are identified by dark areas. Decrease in bone volume observed in micro-CT scans of trabecular bone in the tibia due to ISO treatment in tumor bearing and non-tumor bearing **(D and E).** PTHrP levels are unaffected in ISO treated osteoblasts **(F)**. Data are plotted as means ±SEM; ***** p<.05; ******* p<.001.

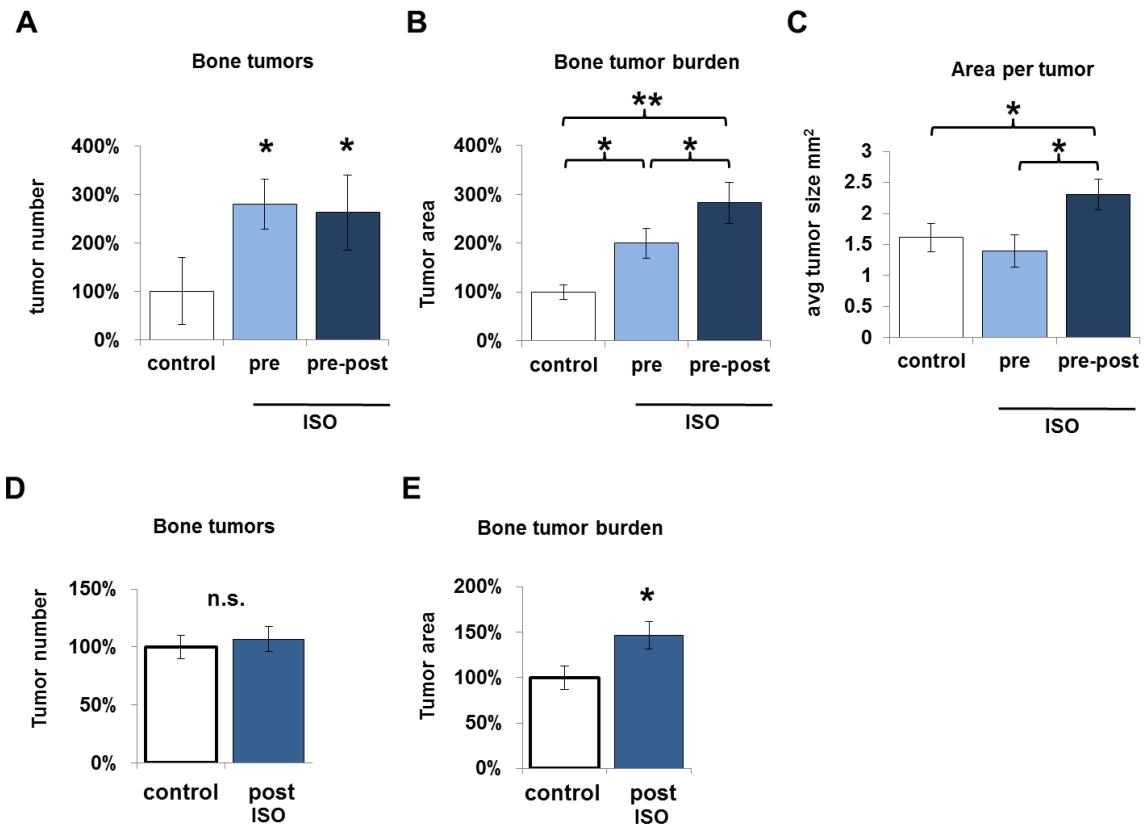

Figure 20. Isoproterenol increases growth of metastatic bone tumors Differential effects on numbers and size of bone tumors were seen in mice that received daily treatment with 3mg/kg Isoproterenol (ISO) for 2 weeks before (pre) and 4 weeks after inoculation (pre-post) with GFP-expressing MDA-231. Quantification of and total number **(A)** and size **(B)** of bone tumors in H&E stained hind limbs 28 days after tumor inoculation (n=8). **(C)** Size of each bone tumor from histologic sections **(D)** Number of bone tumors in mice treated only for 4 weeks after tumor inoculation (E) Size of bone tumors in post treated animals. Data are plotted as means ±SEM ; ***** p<.05; ****** p<.01.

in PTHrP expression that could account for the increase in tumor growth or bone resorption.

β2AR stimulation of breast cancer cells decreases extraskeletal tumor growth.

Both osteoblasts and breast cancer cells, including MDA-231 and 4T1-592 cells, express the β2AR (Figure 21A). Therefore, the stimulatory effect of sympathetic activation on breast cancer cell metastasis to bone may be mediated by a direct effect on cancer cells, or by an indirect effect through host bone cells. To assess a possible direct effect of adrenergic stimulation on cancer growth, we first treated MDA-231 and 4T1-592 tumor cells (an osteotropic clone derived from 4T1 cells [91]) with ISO (1uM), then measured cell number over a 4 day period. Surprisingly, ISO decreased MDA-231 and 4T1-592 cell numbers over time, in a dose-dependent manner (Figure 21B-E). We then used an *in vivo* model of tumor growth to further assess the direct effect of β2AR stimulation in breast cancer cells. In this subcutaneous model, MDA-231 cells will be exposed to treatment, as in the in vitro experiment, but with a more relevant environment to determine effects of *direct* stimulation of the β2AR on cancer cells. In athymic nude mice inoculated subcutaneously with 10^6 MDA-231 cells and treated daily with ISO for 3 weeks, tumor volume was not increased but rather decreased compared to the PBS control group (Figure 22A). Furthermore, no increase in tumor growth was observed in wild type (WT) BALB/c mice that received mammary fat pad

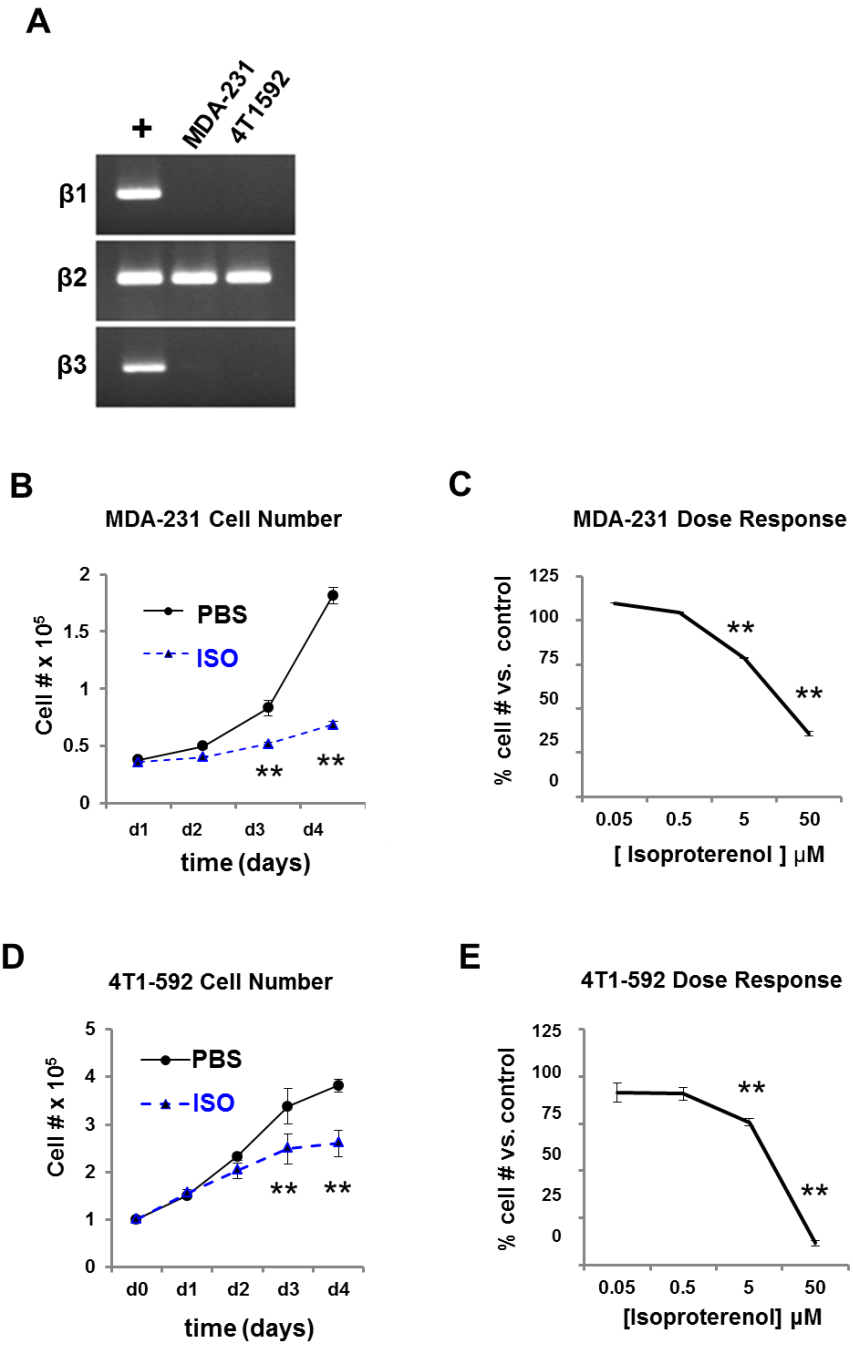

Figure 21. β2AR stimulation directly decreases tumor cell growth *in vitro* (A) β2AR expression in two bone metastatic mammary carcinoma lines MDA-231 and 4T1-592 assessed by RT-PCR. **(B)** *In vitro* effects of ISO (1 μM) on MDA-231 cell number over 4 days (n=3). **(C)** ISO treatment dose-response on MDA-231 cell number vs. control (n=3). **(D)** 4T1-592 cell number *in vitro* in response to ISO vs. control (n=3). **(E)** ISO treatment dose-response on 4T1-592 cells (n=3). Data are plotted as means ±SEM; ****** p<.005.

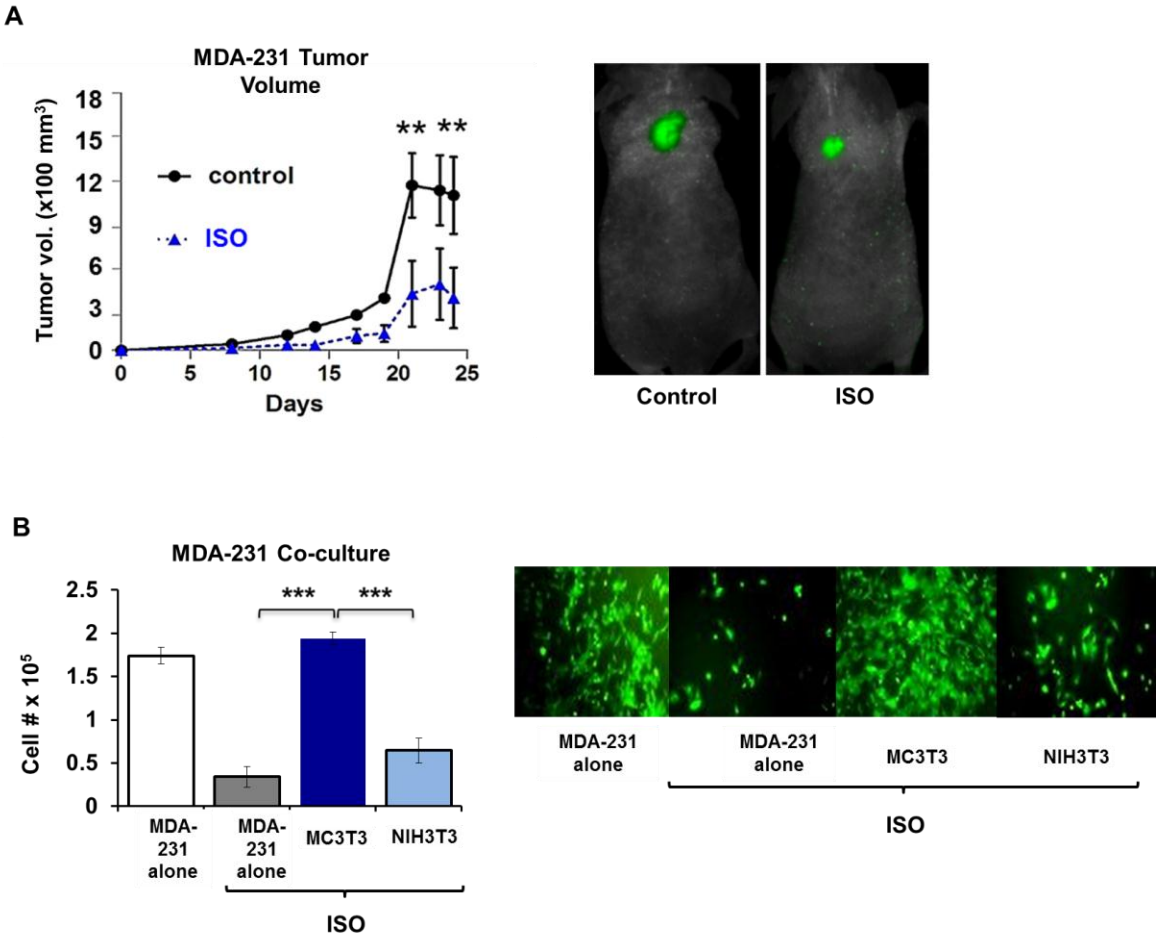

Figure 22 Osteoblastic cells prevent ISO-inhibited cancer cell growth. **(A)** Subcutaneous MDA-231 cell growth quantification (tumor volume) following daily PBS (control) or ISO injections (n=6). **(B)** Effects of ISO on MDA-231 cell proliferation when cells were grown on tissue culture plastic (MDA-231 alone) or on cocultures with MDA 231 plated on monolayers of osteoblastic MC3T3 or fibroblastic NIH3T3 cells (n=3). Data are plotted as means ±SEM ; ******* p<.001.

inoculations of 5 x 10^3 4T1-592 cells and subsequent ISO treatment for 4 weeks (Figure 24B). This ISO-induced reduction in cell number was abolished when MDA-231 cells were co-cultured with MC3T3 osteoblasts, but not control NIH3T3 fibroblasts (Figure 22B), suggesting that osteoblastic cells may protect cancer cells at early stages of metastatic colonization, and that this may contribute to bone selectivity of some cancer cell lines. These results also suggest that direct adrenergic stimulation of breast cancer cells inhibits their growth or promotes cell death in extraskeletal sites, and that the increase in bone tumor lesion and number observed *in vivo* following CIS treatment is not due to the promotion of cell proliferation, but rather to an effect of sympathetic nerves on bone colonization.

β2AR signaling decreases bone mass in athymic mice

In C57BL6 mice, it has been thoroughly demonstrated that β2AR signaling regulates bone turnover via RANKL [102, 198-200]. For the purpose of studying breast cancer and bone, however, C57BL6 mice are unsuitable since bone metastatic models generated on this background are not currently available, and primary immune response to cells from human tumors or other mice strains would make metastasis improbable. For our studies, BalbC WT mice and BalbC Nude mice were chosen since well characterized metastatic mammary carcinoma cell line exist for both of these murine lines. The effects of β2AR signaling on bone have not been characterized in athymic mice, which is of critical importance when considering the role of T-cells and B-cells in RANKL

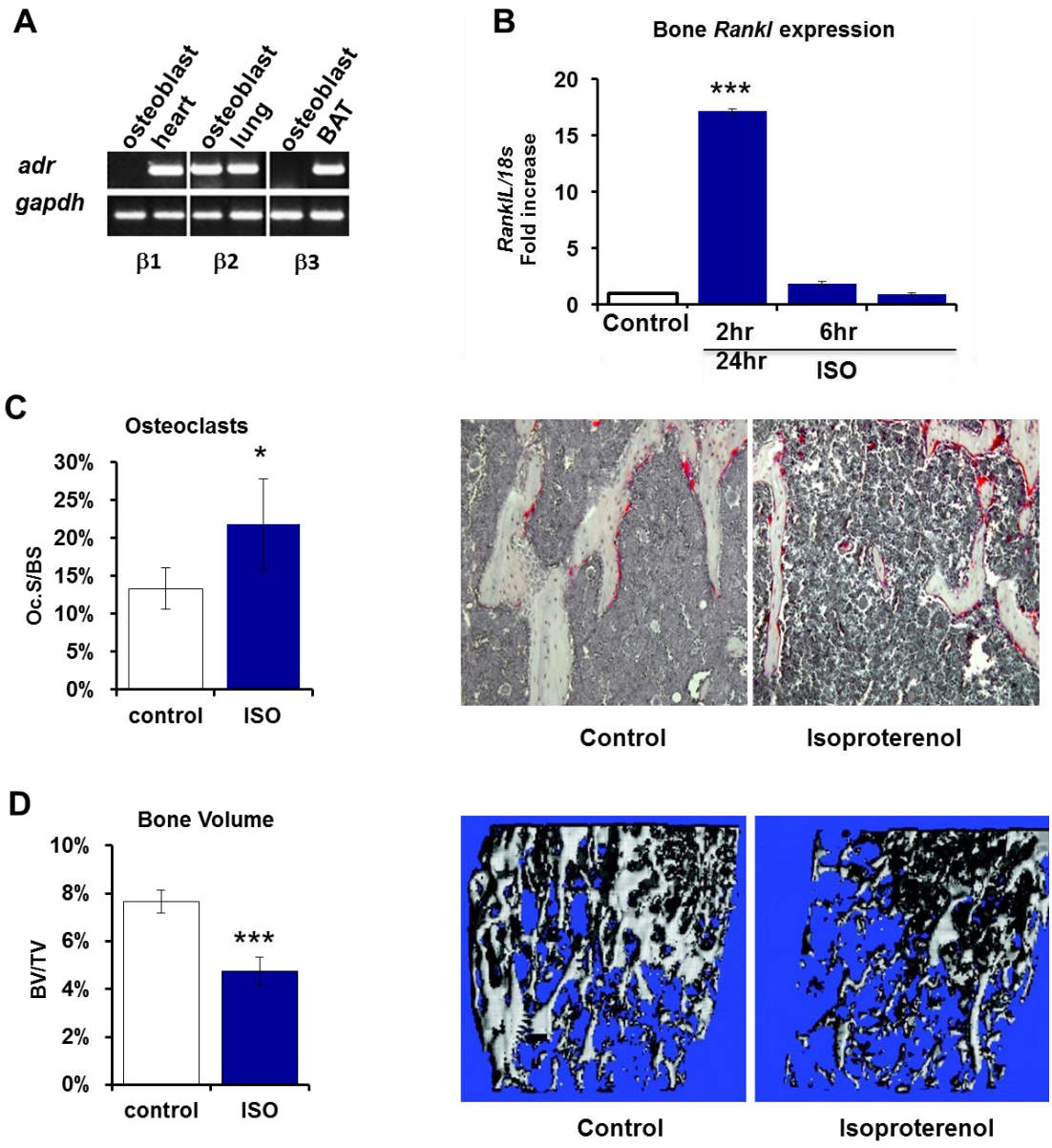

Figure 23. β2AR stimulation increases bone resorption in athymic mice. (A) PCR of cDNA extracted from mouse osteoblasts, showing expression of the β2AR **(**B) Bone *Rankl* mRNA expression assessed by qPCR (n=4,p<.001). (C) Osteoclast surface per trabecular bone surface (Oc.S/BS) in non-tumor bearing tibiae (n=9,). (D) Tibial Bone Volume/Tissue Volume (BV/TV) of non-tumor bearing athymic mice treated daily with ISO for 4 weeks(n=9). (Data are plotted as means ±SEM ; * p<.05; *** p<.001

production and bone turnover [66, 201]. Murine osteoblastic cells highly express only the β2 adrenoreceptor and not the β1 or β3 subtypes as evidenced by RNA expression (Figure 23A). Upon treatment with isoproterenol (3mg/kg), a dramatic increase in RANKL expression is seen in the long bones of athymic mice (Figure 23B), which parallels previous data in other euthmyic mice strains [104] . In agreement with other studies, the increase in RANKL corresponds with a significant increase in osteoclast surface in relation to bone surface (Figure 23C) and a subsequent decrease in the volume of mineralized bone normalized to tissue volume (Figure 23D), thus demonstrating that athymic BalbC mice are susceptible to deleterious bone effects from chronic β2AR stimulation. These data indicate along with the increased lesion area indicate that ISO can enhance bone destruction in the presence of a tumor via osteoblastic β2AR and increased RANKL, and that this accounts for the increased tumor growth seen in 'post' and pre-post' treated mice.

CIS accelerates tumor-induced bone destruction

Endogenous sympathetic activity from restraint stress increased the number and size of lytic lesions, which is rescued with propranolol, suggesting that CIS exacerbates the vicious cycle via β-adrenergic signaling and RANKL. When we measured RANKL expression in whole bones of mice treated with CIS, we observed a significant increase in RANKL expression (Figure 16A), in agreement with data from ISO treated animals, indicating that this is β-adrenergic

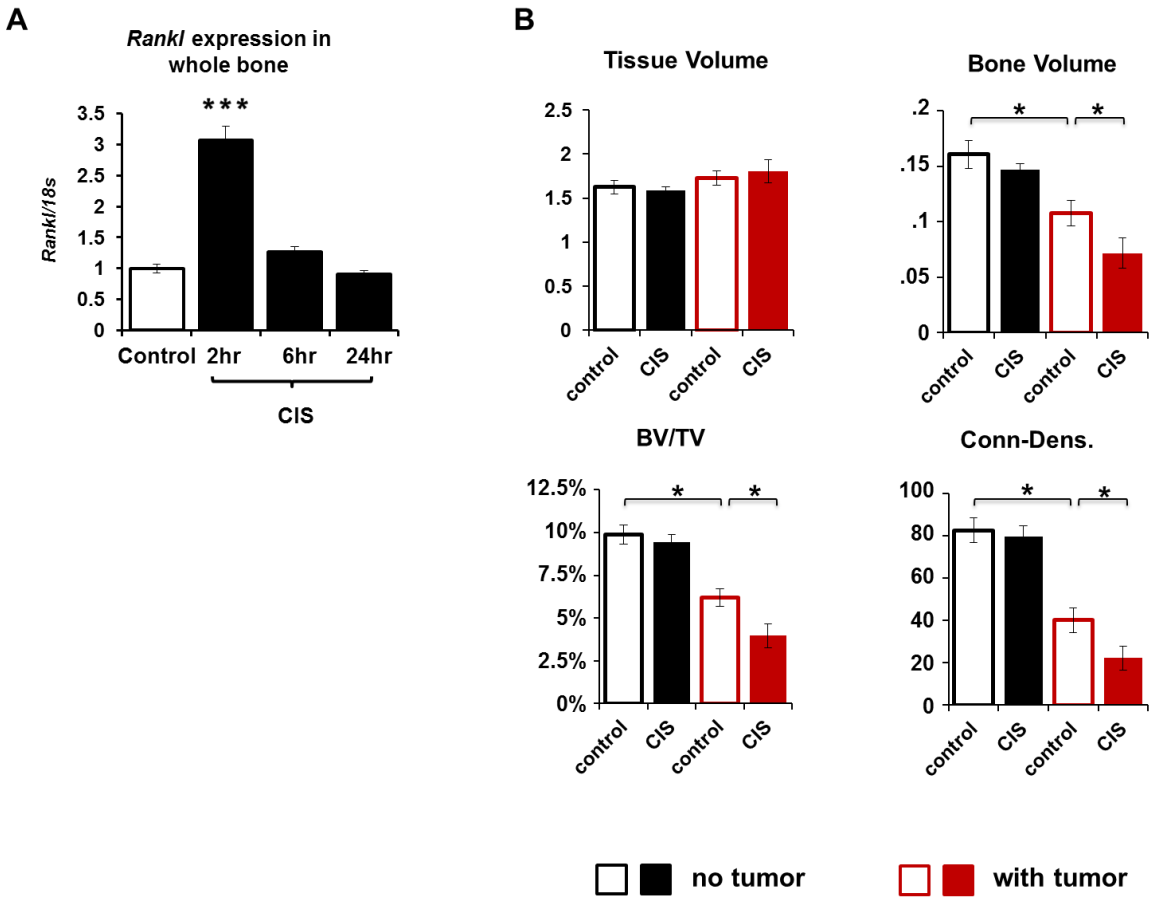

Figure 24. **CIS increases bone destruction in tumor bearing mice. (A)** *Rankl* expression time course in long bones from mice subjected to daily restraint stress for two weeks (CIS)(n=3)from total bone extracts by qPCR. Bone parameters as assessed by micro-CT (B) in CIS treated tumor bearing (red) and non-tumor bearing mice (black). Data are plotted as means ±SEM ; ***** p<.05.

mechanism. The increase in RANKL in CIS treated mice corresponded to a decrease in BV/TV in the presence of a tumor (16B), which along with the ISO post treatment data, suggests that chronic stress, via osteoblastic β2AR and RANKL, feeds into the vicious cycle and can accelerate tumor growth and bone destruction in cancer induced bone disease.

ISO increases metastasis and bone destruction in a mammary fat pad model

To further test the influence of β2AR signaling on breast cancer to bone metastasis, we sought to replicate the findings of the intracardiac model in an immune competent model with a primary tumor. We chose a bone metastatic sub clone of the widely used 4T1 mammary carcinoma cell line called 4T1-592 [91]. Since 4T1 cells were derived from a BalbC mouse, we were able to use a wild-type BalbC for this syngeneic model. As in the MDA-231 model, we injected mice with 3mg/kg ISO for 2 weeks before inoculation with cancer cells. In these experiments however, we were able to inject into the 4^{th} mammary fat pad, instead of an intracardiac route, to more fully replicate the metastatic process. As was the case with the 'pre-post' treatment in the intracardiac experiments, we observed an increase in both lesion number and lesion area due to ISO treatment (Figure 25A-D) demonstrating for the first time that β2AR signaling can increase the spontaneous metastasis of breast cancer from a primary tumor to the bone. An increase in the number of long bones with osteolytic lesions (Figure 25C), but not an increase of growth at the primary tumor (Figure 25B),

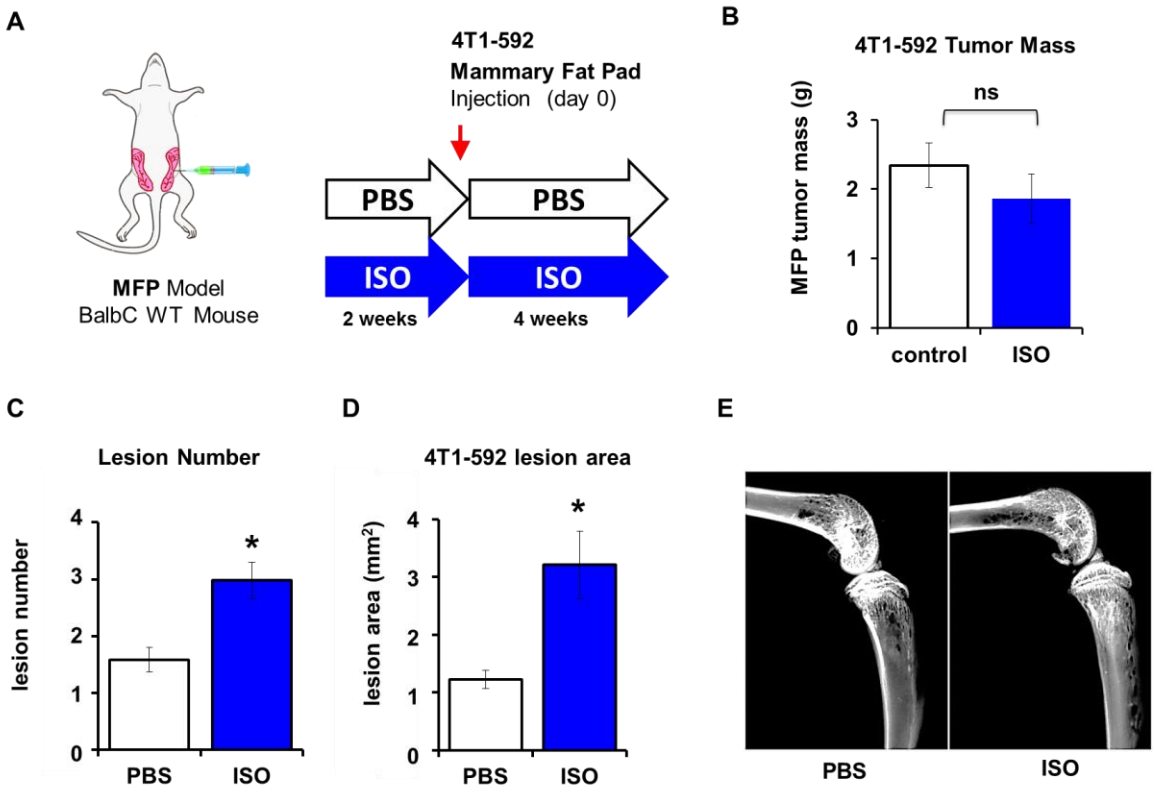

Figure 25. **Isoproterenol increases bone lesions in 4T1592 MFP model.** Wild-type BalbC mice were injected with 1 x 10^6 4T1-592 cells into the 4^{th} mammary fat pad during 6 weeks of ISO (3mg/kg IP daily) treatment **(A)**. Primary tumor mass after 4 weeks **(B).** Average Number of bones with an osteolytic lesion **(C)** and total area of lesions per mouse **(D)** from analysis of 2D radiographs. Representative Faxitron images **(E)** showing characteristic small 4T1592 bone lesions. Data are plotted as means ±SEM ; ***** p<.05.

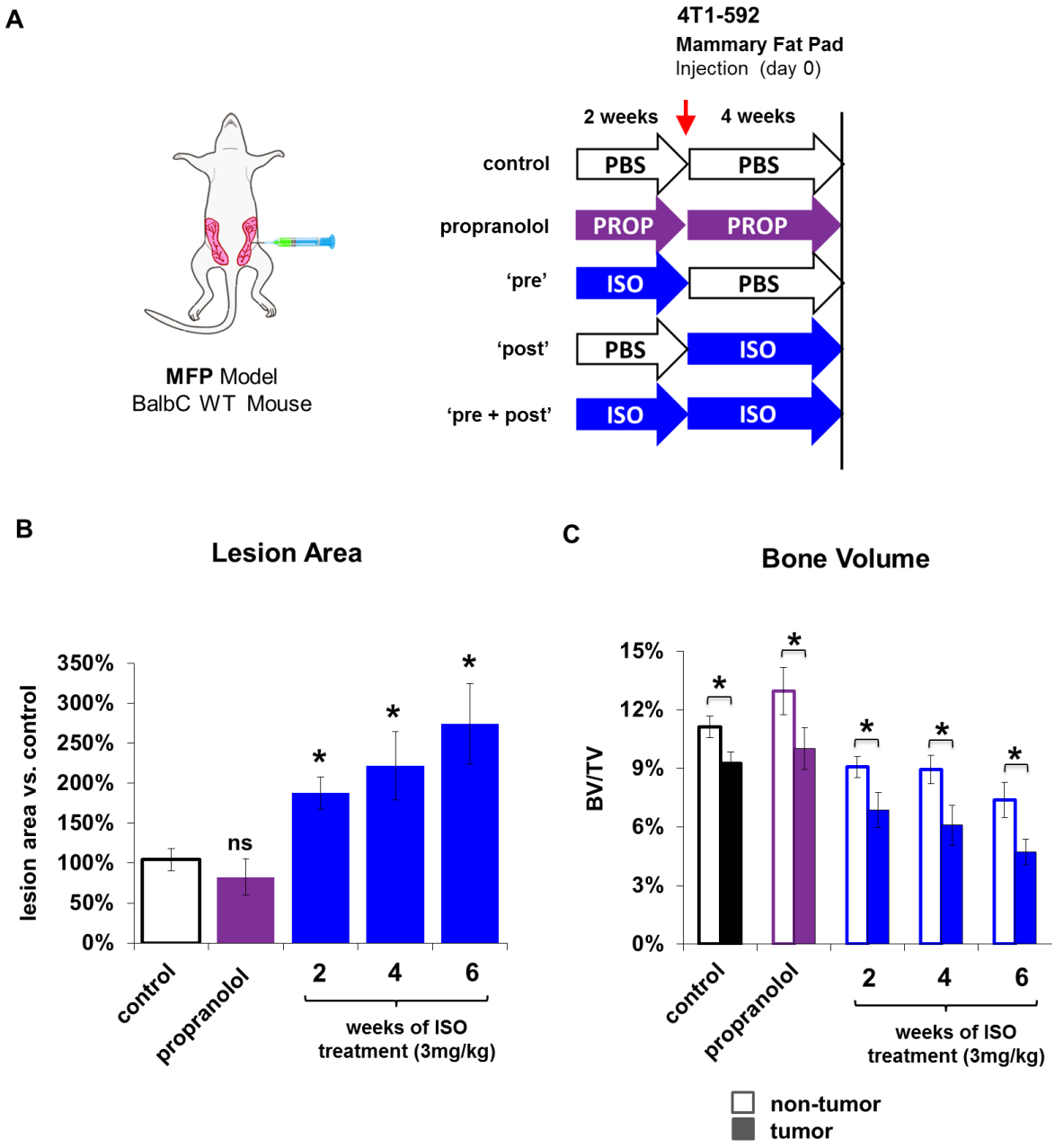

Figure 26. **β-adrenergic signaling exacerbates metastatic bone disease.** Treatment paradigm involved 2 weeks pre-treatment, 4 weeks post treatment, or a combination **(A)** in combination with mammary fat pad injection of 10^6 4T1592 cells. Treatment increased the area of lytic lesions quantified from radiographs **(B)**in a duration dependent fashion . Quantification of μCT data showed a corresponding decrease in BV/TV **(C)** in response to ISO.

suggests that the effects of ISO on bone tumor establishment are mediated through actions on the bone before the arrival of a tumor.

The notion that β-adrenoreceptor signaling can additionally contribute to the progression of cancer-induced bone disease was further tested by altering the duration of ISO treatment. Daily injections of ISO for as few as 2 weeks resulted in a significant increase in total lesion area (Figure 26 A,B) which was further increased with 4 weeks and 6 weeks of treatment (Figure 26 A,B). The increase in lesion area upon ISO treatment corresponds to a decrease in bone volume observed in both tumor and non-tumor bearing bones. This data shows, for the first time, that βAR stimulation can increase bone resorption in the BalbC mouse strain, and that this effect accelerates bone destruction when a tumor is present. As was the case with $Fox^{nu/nu}$ mice, blockade by propranolol of βAR's in non-stressed WT BalbC mice did not produce a significant effect in either lesion area or bone volume (Figure 26 B, C). We suspected that this lack of effect of propranolol on bone resorption and tumor parameters was due to insufficient sympathetic outflow in basal conditions.

Conclusions

We show here that sympathetic outflow alters the cytokine profile of the bone microenvironment to increase metastatic colonization and accelerate the progression of metastatic bone disease by two distinct RANKL-mediated mechanisms. Athymic mice ($Fox^{nu/nu}$) mice under chronic immobilization stress (CIS) showed an increase in bone tumor number, which was be blocked with propranolol, indicating that this was a β-adrenergic-mediated effect, rather than a consequence of chronic HPA outflow. This data was replicated when mice were administered a β-agonist, isoproterenol, confirming that the effect of CIS on increased bone metastasis was mediated via β-adrenergic signaling. We then treated the mice only before the cancer arrived in bone *or* after cells had already been seeded, allowing us to distinguish the early effects of SNS on metastatic establishment from latter acceleration of the vicious cycle. In these experiments we showed that adrenergic stimulation of the bone, in the absence of cancer, changed microenvironment in such a way that more tumors were able to seed, resulting in greater numbers of bone tumors. We further elucidated that the increase in bone metastasis was due adrenergic signaling in osteoblasts which increased soluble factors that increased the migration, but not the growth, of cancer cells. Osteoblast derived RANKL was identified as the factor responsible for β2AR-induced cell migration in vitro and subsequent bone metastatic establishment in vivo.

When β2AR stimulation was given after intracardiac inoculation of tumor cell, we observed a second and distinct effect of ISO on bone metastasis, where bone

tumors increased in size but not number. However, direct stimulation of the β2AR on cancer cells decreased growth in vivo in a subcutaneous tumor model, and in vitro. Instead of a having a direct effect on tumor growth, we showed that ISO and CIS treatment could increase RANKL production via osteoblastic β2AR signaling, resulting in increased resorption and bone destruction, suggesting that acceleration of the 'vicious cycle' is the mechanism by which SNS activity can increase growth of established tumors in bone. Collectively, these data demonstrate that SNS outflow regulates both metastatic colonization and the resultant cancer induced bone disease via distinct mechanisms of osteoblastic β-adrenergic signaling and RANKL on colonization and growth, and imply that β-blockers may be clinically useful in the treatment of metastatic breast cancer

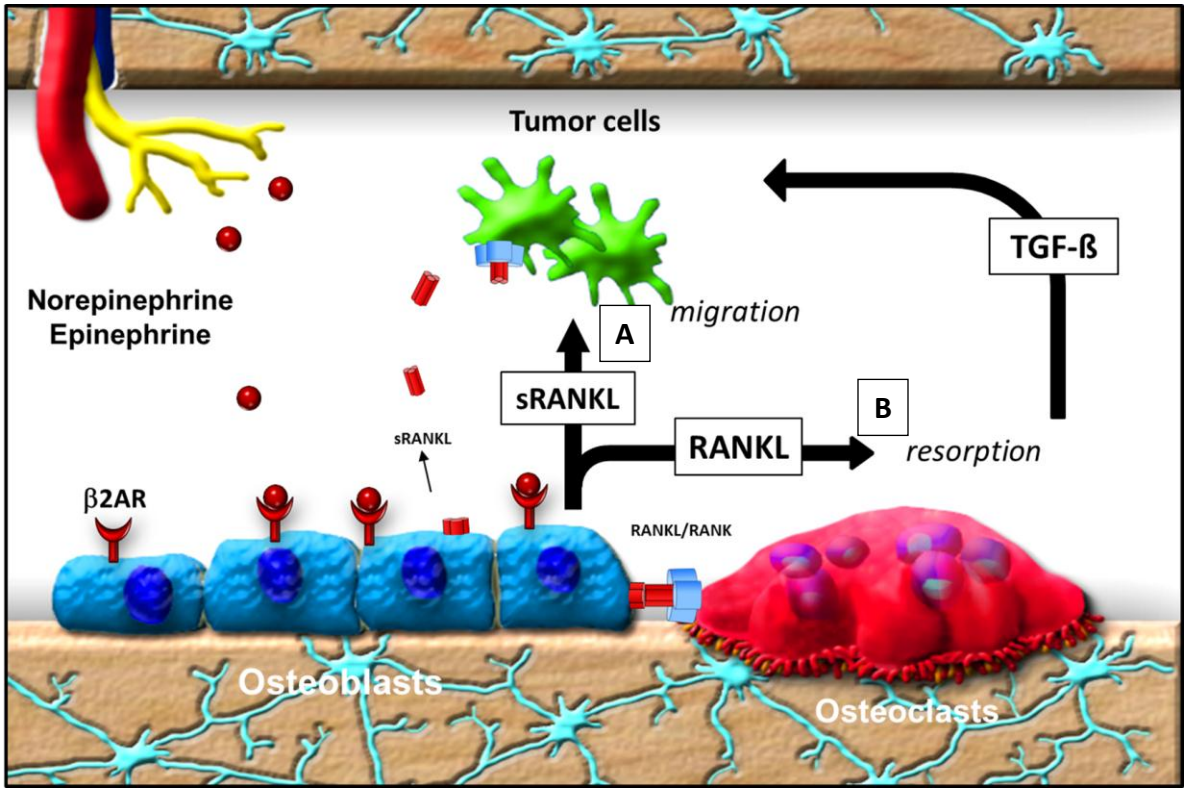

Figure 27 β2AR signaling affects bone metastasis by two distinct RANKL mediated mechanisms (A) sRANKL from the bone stroma increases bone tumor colonization **(B)** RANKL from osteoblasts increases bone resorption and exacerbates cancer induced bone destruction

Discussion and Future Directions

Although the genetic and phenotypic make-up of a tumor determines its metastatic efficiency, a receptive microenvironment is a prerequisite for tumor colonization, establishment and growth in distant sites. In the case of breast cancer, the interaction of cancer cells with the bone microenvironment is crucial for their preferential colonization of bone, as well as their subsequent survival, growth, and osteolysis-promoting activity [85]. Characterization of the conditions and factors that transform the bone microenvironment to a state more favorable for cancer cell colonization, dormancy escape, and growth, is thus of great interest. In these experiments, we show that activation of the sympathetic nervous system, a hallmark of severe stress and depression, promotes breast cancer cell colonization in bone. We demonstrate that this neuronal effect on bone metastasis is mediated via the β2AR in bone-forming cells of the host bone marrow environment, and not by a direct effect on metastatic cancer cells, and furthermore that RANKL, whose expression is induced in osteoblasts by sympathetic activation, mediates this effect *in vitro* and *in vivo* via its pro-migratory activity. Additionally and of clinical importance, we show that reduction of RANKL signaling and the β-blocker propranolol can inhibit the stimulatory effect of endogenous sympathetic activation on breast cancer bone metastasis.

Sympathetic nerves releasing NE are present within bone in the vicinity of bone cells, and the β2AR is broadly expressed in bone cells of the mesenchymal,

monocytic or immune lineages, as well as in several cancer cell lines, including mammary carcinomas [81]. Sympathetic activation can thus directly stimulate the β2AR in metastatic cancer cells to promote their survival during anoikis, their colonization of bone, and their growth following bone establishment. Such direct stimulatory mechanisms have been reported for ovarian [202] and prostate [203] cancer cell lines. The results of our study, however, indicate that β2AR activation in host stromal osteoblasts predominantly accounts for the stimulatory effect of sympathetic activation on MDA-231 breast cancer cell bone colonization. This is supported by the observation that cancer cell inoculation in mice pre-treated for 2 weeks with ISO can increase the number of bone tumors and lesions. In that experimental setting, cancer cells are not directly subjected to ISO stimulation, therefore the stimulatory effect of ISO on breast cancer cell bone metastasis must occur via stimulation of the β2AR in host stromal cells, and not via a direct effect on breast cancer cells. It is further reinforced by the observation that selective deletion of the β2AR in osteoblasts recapitulates the high bone mass induced by global β2AR deletion [204], suggesting that β2AR signaling in osteoblasts, and not vascular cells or immune cells for instance, contributes to the regulation of bone remodeling and of the bone marrow cytokine profile. It is also of note that the increase in RANKL expression induced by ISO was more pronounced in the MC3T3 osteoblastic cell line when compared to BMSCs, suggesting that among the adherent stromal cells constituting the bone marrow, osteoblasts represent the main target for the effect of sympathetic nerves on RANKL expression and breast cancer cell bone colonization. Of interest is that

osteocytes also secrete RANKL [205] and thus might also represent a critical bone mesenchymal cell population associated with the aforementioned sympathetic effect. It is still possible that endothelial cells could be target of sympathetic activation on cancer cell metastasis, as nerves are intimately associated with blood vessels in bone and express the β2AR. An osteoblast-selective and endothelial cell-selective β2AR loss of function approach, initiated in the laboratory, will be necessary to address this question. The evidence that sympathetic activation promotes breast cancer cell metastasis to bone via a host-mediated mechanism has broad implications for other bone malignancies such multiple myeloma. Myeloma is an incurable B-cell malignancy that, like breast cancer bone metastases, causes severe bone resorption and devastatign fractures. Also, like breast cancer, myeloma can participate in a resorptive cycle involving PTHrP and RANKL [206], suggesting that SNS signaling may play a role in this disease since we have shown that β2AR stimulation of osteoblasts exacerbates this vicious cycle. Unlike breast cancer cells, B-cells are *directly* responsive to β2AR signaling in ways that suggest a direct effect of SNS signaling on myeloma progression [207-210] such as increased survival and RANKL secretion, presenting the possibility of both direct and indirect mechanisms to promote myeloma growth and progression. In addition to RANKL, IL-6 is also critical to multiple myeloma [211], and expression of this cytokine is highly increased in bone cells upon ISO stimulation (Figure 28A). These data

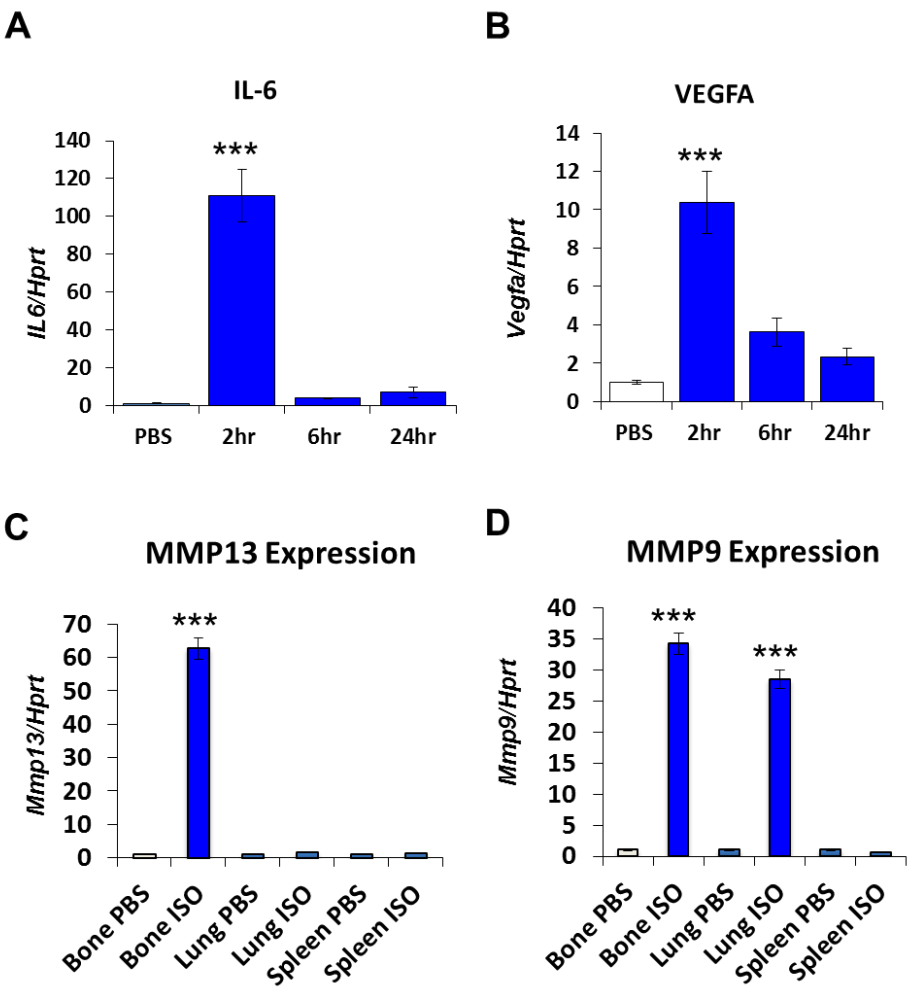

Figure 28 β2AR stimulation increases the expression of multiple metastatic genes. (A) IL6 Expression (B) Vegfa mRNA expression in MC3T3 treated with 10μM ISO as quantified by QPCR. Tissue mRNA levels of MMP 13 and MMP9 **(C and D)**from mice 2 hours after treatment with 3mg/kg ISO. All *in vitro* assays repeated at least 2 times. Data are plotted as means ±SEM ; *p<.05; **p<.01; ******* p<0.001.

suggest that the effecs of chronic stress on disease progression in multiple myeloma could be even more pronounced than in our breast cancer studies.

Though pharmacologic stimulation of β-adrenoreceptors increased bone resorption and bone loss via osteoblasts and RANKL production, endogenous sympathetic outflow from CIS did not have the same effect. We expected that the combination of catecholamine production and glucocorticoid secretion from this model of chronic stress would act in an additive fashion as has been published with dexamethasone treatment [212]. However, CIS induced an increased in RANKL expression but no bone loss. One reason for the lack of bone loss could be desensitization from CIS and subsequent recovery of bone mass, which could be remedied by applying unpredictable stress, or by histological bone examination at earlier time points. Since the effects of restraint stress on bone have not been published, further experiments could provide crucial insights into the neuroendocrone regulation of bone remodeling including possible benefits for SNS outflow and cancer since β2AR stimulation directly decreases tumor size in non bone sites and has a toxic effect *in vitro*.

Since CIS had no effect on BV/TV in non-tumor bearing mice, we turned to other methods of endogenous sympathetic activation that might produce a measurable change in bone and yield further insight into neural signaling in bone and cancer. In contrast to CIS, ISO was able to decrease bone volume by stimulating only βAR, whereas physiological stress releases catecholamines that target both αAR and βAR. Additionally, recent studies have demonstrated the presence of functional alpha adrenergic receptors in bone [213], though those

studies maintain that the β2AR mediates the most profound effects on bone biology. To account for aAR and bAR signaling, we decided to test the effects of an α2 antagonist , atipemazole, on bone. This drug, known by the brand name Antisedan, is routinely used in veterinary practice to awaken animals from sedation, by blocking α2AR centrally and reversing the effects of dexmedetomidine or medetomidine. By blocking central α2 adrenergic receptors, this drug increases noradrenergic signaling and subsequent tachycardia from α1AR stimulation. A similar pharmacologic stress model has been published using yohimbine, but these studies are complicated by yohimbine's additional actions at α1-adrenergic, 5-HT1A, 5-HT1B, 5-HT1D, 5-HT1F, 5-HT2B, and D2 [214, 215] receptors while atipamezole binds only the α2AR, though it is not subtype specific [216]. Thus, this drug could provide a model of endogenous stress, and address the contribution of the αAR and βAR in a more physiologically relevant setting than is the case with ISO or yohimbine, and with fewer technical hurdles than behavioral stress models. However, when given to BalbC wild type mice daily for a month, atipemazole failed to produce a significant change in bone volume (Figure 29A), though a trend was observed which merits further investigation.

Alternatively, we hypothesized that we could decrease sympathetic outflow by stimulation of central α2AR. Since Propranolol did not significantly reduce tumors in non-stressed mice, we speculated that basal levels of adrenergic signaling were too low to see a difference with β-blockade.

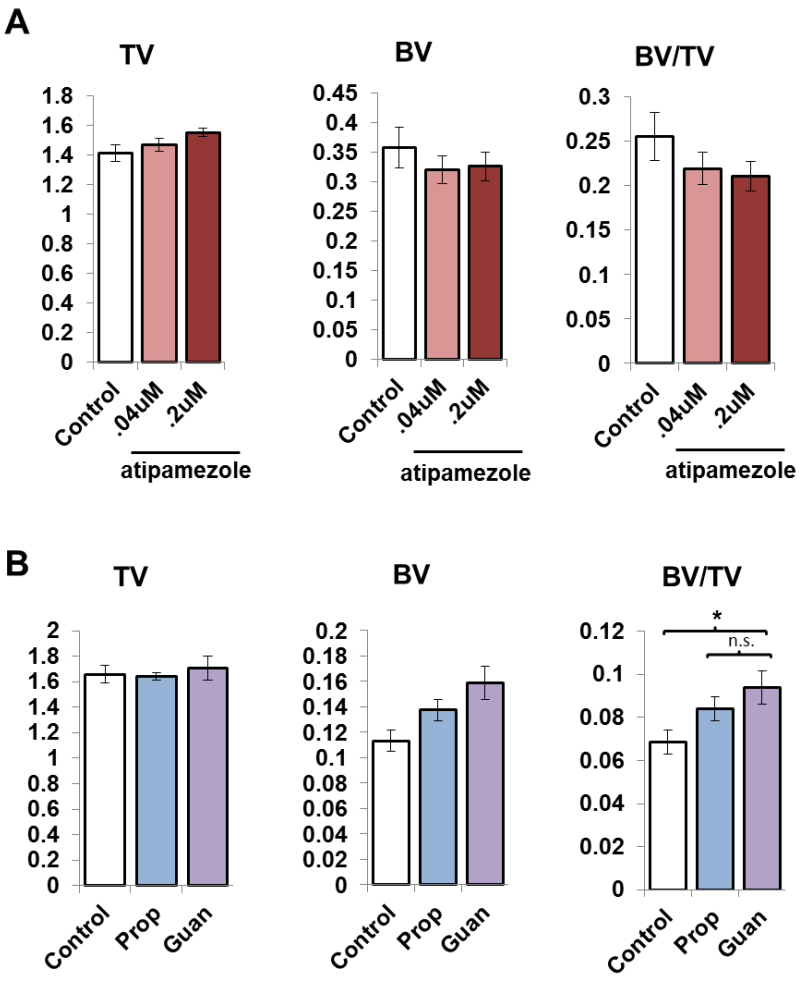

Figure 29. Bone effects of centrally acting α2AR drugs. . Wild type BalbC mice were treated daily with different doses of atipamezole (I.P.). No significant difference was observed in bone parameters as assessed by micro-ct. Athymic mice were treated daily with central $\alpha 2_a$ agonist Guanfacine (guan). No significant difference was observed between propranolol and Guanfacine in bone parameters as assessed by micro-ct. Data are plotted as means ±SEM ; *p<.05

Additionally, different doses of propranolol have different effects on bone phenotypes in rodents [217], and β-blockade has been shown to increase cortisol levels [218], suggesting that there may be some dysregulation of SNS and HPA signaling that could mask any beneficial effects of β-blockade on bone metastasis. We hypothesized that if total SNS and HPA outflow were decreased centrally, meaning lower glucocorticoid levels and less alpha and beta adrenergic signaling, then the effects in bone would be greater than using β-blockers alone. To test this, we chose a frequently prescribed selective $\alpha 2_a$ agonist, guanfacine, sold under the brand name Tenex or Intuniv. Guanfacine decreases systolic and diastolic blood pressure by stimulating the central nervous system $\alpha 2_a$ norepinephrine autoreceptors, resulting in reduced peripheral sympathetic outflow, reduced plasma catecholamines, and reduced plasma cortisol [219] . Although this drug increased bone volume over control, the improvement was not significantly different from propranolol (Figure 29 B). Given its ability to decrease both catecholamines and glucocorticoids, guanfacine could prove to be a useful tool in investigating stress effects in bone and cancer.

During the course of this work we have found that the mammary carcinoma models used in these experiments express α1 and α2 adrenergic receptors. Since bone metastatic tumors from prostate [220] and mammary carcinomas, and bone cells express functional α1 adrenergic receptors [221], this direction may prove fruitful in the investigation of SNS-mediated effects on cancer. Further supporting a role for α-adrenoreceptors in cancer is the fact that norephinephrine, which has been shown to mediate cancer metastasis, is

primarily an α-agonist and α-blockers are used clinically to treat prostatic hyperplasia [222]. If a functional role of these receptors is found in stress-induced metastasis, they could be targeted along with βARs, using dual action adrenergic blockers. The most widely used of these dual action β-blockers is a third generation cardiovascular drug, carvedilol, which targets β2AR and $\alpha 1_b$AR. This drug is more efficacious than drugs that target only the β1 or β2 AR and is likely to be first choice over the β-selective drugs [223]. Carvedilol may have added benefits in adjuvant cancer therapy due to its antioxidant properties in cardiac ischemia studies [224] and in oxidation caused by chemotherapy [225].

Though RANKL mediated two distinct effects in our study (cancer cell promigratory activity and pro-osteoclastogenic activity), we cannot exclude the possibility that sympathetic activation could also influence breast cancer bone colonization by a stimulatory effect on other pro-metastatic cytokines in the stroma that regulate processes like inflammation and angiogenesis, which are critical to metastatic progression [174, 226, 227]. Indeed, we obtained preliminary data demonstrating an increase in osteoblastic IL-6, VEGF, and MMPs (Figure 28 A-D) induced by ISO treatment, which could play a role in the stress-induced metastasis of other breast cancer cell lines to the bone, such as the MDA-231 ATCC clone that has low RANK expression, but still metastasizes to the bone. We also observed that IL6, whose expression is induced by β2AR stimulation, promotes the expression of RANK on MDA231 cells, suggesting that low RANK expressing metastatic breast cancer cells, upon traffic through the bone marrow

and following endogenous sympathetic stress, may upregulate their sensitivity to bone cell-derived RANKL.

The effect of β2AR stimulation in osteoblasts on cancer cell migration was shown to be mediated by soluble RANKL. As RANKL is produced as a membrane-bound molecule, it is still unclear how β2AR stimulation triggers the release of the soluble form of RANKL, which is a necessary step for this cytokine to act as a promigratory homing factor. These results, however, do not exclude the possibility that the membrane-bound form of RANKL could act as an adhesion factor to retain metastatic cancer cells within the bone marrow environment, perhaps promoting cancer cell-osteoblast adhesion and the protective effect of osteoblasts on cancer cells.

Neuronal regulation of bone has been the primary focus of our work up to this point, but other organs, such as lung and lymph glands, are responsive to adrenergic stimulation [228, 229] and common metastatic sites [4], raising the possibility that SNS activation may mediate breast cancer metastasis to non-osseous sites. This is supported by preliminary data showing that ISO treatment increased lung metastasis of 4T1592LM cells in a mammary fat pad model (Figure 30 B). This particular clone, derived from the osteotropic 4T1592, no longer metastasizes to bone and has decreased RANK expression (Figure 30 C) This suggests that other genes besides RANKL mediate the stress-induced metastasis of breast cancer cells to lung, and could relate to metastasis between

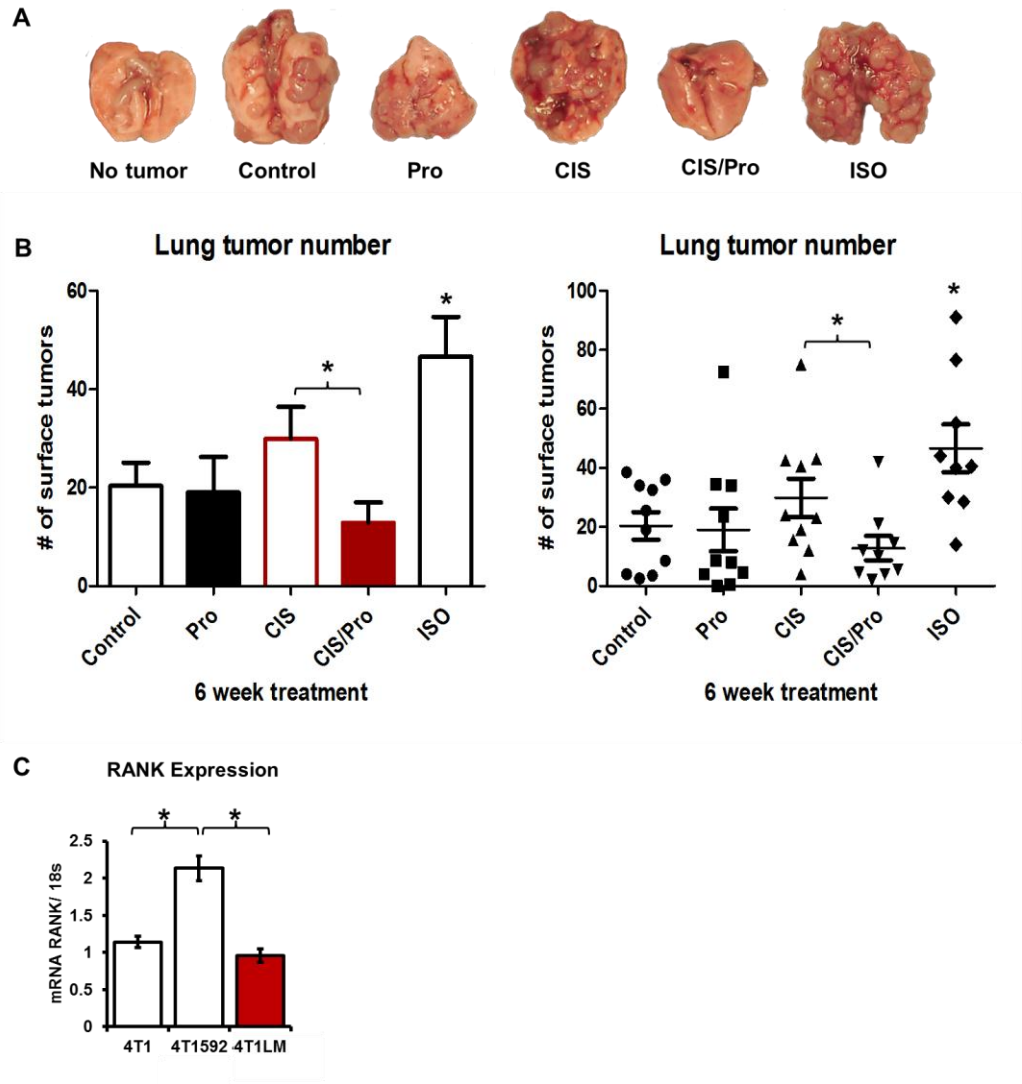

Figure 30. □–adrenergic signaling increases lung metastasis of a low RANK expressing mammary carcinoma (A) Representative images of freshly dissected lungs from WT BalbC mice 6 weeks after mammary fat pad injection of 10^6 4T1VU cells. **(B)** Quantification of surface lung tumor counts. (**C)** Low RANK expressing 4T1 clones do not selectively metastasize to bone. Data are plotted as means ±SEM; *p<.05

distant organs different from the primary cancer site. The metastases could be mediated by a host of other genes, such as matrix metalloproteinase 9 (MMP9), which is upregulated in lung upon ISO treatment (Figure 28 B, D). MMP-9 is associated with aggressive tumors [230], regulates multiple steps of metastasis such as inflammation [231], tumor angiogenesis [232], and invasion [233], and is known to play a role in lung cancer [234] and breast cancer metastasis to the lung [235, 236]. We also found that the combination of CIS and propranolol decreased lung tumor metastasis to level that was significantly lower that control, propranolol treated, or CIS treated mice, suggesting a possible beneficial effect of SNS outflow in this paradigm (Figure 29 B).

RANKL is well known for its osteoclastogenic properties during typical bone turnover. The importance of RANKL in promoting tumor growth in bone and osteolysis induced by metastatic breast cancer cells is also well established [237] and has led to the use of RANKL blockade to prevent fracture in patients with breast and prostate cancer [238]. Over the last few years, it has become increasingly recognized that this cytokine plays a broader role in the process of cancer cell metastasis [239]. The protective effect of RANKL blockade by recombinant OPG on melanoma bone metastasis reported by Jones and collaborators [81] was the first to suggest that RANKL, by promoting the migration of B16F10 melanoma cancer cells, was implicated in promoting metastatic bone colonization and establishment. In our study, the finding that RANK knockdown in metastatic breast cancer cells reduces bone metastasis indicates that this signaling axis is used by metastatic breast cancer cells as well

for their bone metastatic potential, independently of the increased bone turnover induced by sympathetic activation. These findings differ from the Jones' study in that this effect was only observed in mice subjected to β2AR stimulation (and high levels of RANKL in bone), and not in non-challenged mice. Regardless of the pathophysiological factor(s) increasing its expression or activity, our findings indicate that RANKL is one of the important "soil" factors that promote the colonization of bone by breast cancer cells. The derived therapeutic implication is that drugs targeting RANKL, including Denosumab (which is currently only approved for the prevention of bone fracture in patients with breast and prostate cancer), could be efficacious not only to treat the bone symptoms associated with bone cancer metastasis, but also to prevent or limit the initiation and development of the disease itself, by reducing breast cancer bone metastasis and/or the activation of dormant breast cancer cells, if administered as adjuvant therapy.

The links between severe depression, high sympathetic tone, increased RANKL expression in bone, and higher incidence of bone metastasis reported in our study, as well as the poor prognosis of breast cancer patients with high tumor RANK expression [240], provide a possible explanation for the observed correlation between emotional stress and reduced survival of patients with breast cancers [241-243] which will obviously have to be confirmed by further clinical studies. Before any epidemiological studies can take place, it must first be determined which subset of patients would be at risk of increased metastasis due to stress.

Numerous pathophysiological states are associated with both elevated SNS activity and cancer morbidity. Metabolic conditions such as obesity [244] and diabetes are linked to depression, known to increase catecholamine levels [245-247] and are associated with increased mortality and metastatic spread in multiple cancers [248, 249]. As with conditions of psychosocial stress, these metabolic disorders are linked to exacerbation of an existing malignancy rather than causation [250, 251]. These relationships are further complicated by the common comorbidity of metabolic disorders with hypertension [252] and cardiac failure [253] and the fact that many cancer therapies have adverse cardiovascular side effects [254].

Prospective clinical trials will be needed to ascertain the efficacy of β-blockers or RANKL blockers to decrease recurrence or increase survival in breast cancer patients. Currently, these kinds of trials may prove difficult and expensive since the vast majority of breast cancers are removed at early stages with a 99% 10 year survival rate. Because PTHrP and other cytokines converge on the RANKL pathway once tumor load increases, the effect of sympathetic activation on RANKL expression by host bone marrow osteoblasts is likely to be most relevant to the early phases of bone metastasis, when tumor load is minimal. The use of β-blockers may have similar effects to RANKL blockade and could represent an alternative to the current standard of care, with a possible milder effect on bone turnover and a proven safety profile. Given our preliminary data on adrenergic stimulation of other pro-metastatic genes such as IL-6, MMP-9, MMP12, and MMP13 in the bone (Figure 27A-D), it is possible that β-blockers

could be of even greater benefit as adjuvant therapy than treatments that target only RANKL. This is compelling when considering preventative treatments and thus long-term use, and when taking into account the current economical context, as drug “repositioning” is gaining more and more interest as an alternative to drug development. Importantly, three recent studies [241-243] reported a beneficial effect of β-blocker drug therapy on secondary breast cancer formation and patient survival. These clinical studies support the contribution of sympathetic signaling to the bone metastatic process, and the use of β-blockers as possible adjuvant therapy for breast cancer patients, especially in combination with chemotherapy [255].

REFERENCES

1. Fuchs, E., *Das Sarkom des Uvealtractus.* Graefe's Archiv für Ophthalmologie, 1882. **XII**(2).
2. Paget, S., *The distribution of secondary growths in cancer of the breast. 1889.* Cancer Metastasis Rev, 1989. **8**(2): p. 98-101.
3. Coleman, R.E. and R.D. Rubens, *The clinical course of bone metastases from breast cancer.* Br J Cancer, 1987. **55**(1): p. 61-6.
4. Altekruse SF, K.C., Krapcho M, Neyman N, Aminou R, Waldron W, Ruhl J, Howlader N, Tatalovich Z, Cho H, Mariotto A, Eisner MP, Lewis DR, Cronin K, Chen HS, Feuer EJ, Stinchcomb DG, Edwards BK, *SEER Cancer Statistics Review 1975-2007*, M. National Cancer Institute. Bethesda, Editor. 2009.
5. Hortobagyi, G.N., *Chemotherapy of breast cancer: a historical perspective.* Semin Oncol, 1997. **24**(5 Suppl 17): p. S17-1-S17-4.
6. Kang, Y., et al., *A multigenic program mediating breast cancer metastasis to bone.* Cancer Cell, 2003. **3**(6): p. 537-49.
7. Gupta, G.P. and J. Massague, *Cancer metastasis: building a framework.* Cell, 2006. **127**(4): p. 679-95.
8. Studebaker, A.W., et al., *Fibroblasts isolated from common sites of breast cancer metastasis enhance cancer cell growth rates and invasiveness in an interleukin-6-dependent manner.* Cancer Res, 2008. **68**(21): p. 9087-95.
9. Lee, Y.J., et al., *Differential effects of VEGFR-1 and VEGFR-2 inhibition on tumor metastases based on host organ environment.* Cancer Res, 2010. **70**(21): p. 8357-67.
10. Deering, R.E., et al., *Morphometric quantitation of stroma in human benign prostatic hyperplasia.* Urology, 1994. **44**(1): p. 64-70.
11. Bremnes, R.M., et al., *The role of tumor stroma in cancer progression and prognosis: emphasis on carcinoma-associated fibroblasts and non-small cell lung cancer.* J Thorac Oncol, 2011. **6**(1): p. 209-17.
12. Suetsugu, A., et al., *The cyan fluorescent protein nude mouse as a host for multicolor-coded imaging models of primary and metastatic tumor microenvironments.* Anticancer Res, 2012. **32**(1): p. 31-8.
13. Wels, J., et al., *Migratory neighbors and distant invaders: tumor-associated niche cells.* Genes Dev, 2008. **22**(5): p. 559-74.
14. Trimboli, A.J., et al., *Pten in stromal fibroblasts suppresses mammary epithelial tumours.* Nature, 2009. **461**(7267): p. 1084-91.
15. Tubiana, M. and A. Courdi, *Cell proliferation kinetics in human solid tumors: relation to probability of metastatic dissemination and long-term survival.* Radiother Oncol, 1989. **15**(1): p. 1-18.
16. Gentili, C., O. Sanfilippo, and R. Silvestrini, *Cell proliferation and its relationship to clinical features and relapse in breast cancers.* Cancer, 1981. **48**(4): p. 974-9.

17. Tahan, S.R., et al., *Prediction of early relapse and shortened survival in patients with breast cancer by proliferating cell nuclear antigen score.* Cancer, 1993. **71**(11): p. 3552-9.
18. Magno, W.B., et al., *Correlation of proliferative index (PCNA reactivity and Ki-67 reactivity) in primary breast carcinoma with hormone status, lymph node status, and disease-free survival.* Conn Med, 1992. **56**(12): p. 667-9.
19. Ananthanarayanan, V., et al., *Alteration of proliferation and apoptotic markers in normal and premalignant tissue associated with prostate cancer.* BMC Cancer, 2006. **6**: p. 73.
20. Olumi, A.F., et al., *Carcinoma-associated fibroblasts direct tumor progression of initiated human prostatic epithelium.* Cancer Res, 1999. **59**(19): p. 5002-11.
21. Martinez-Outschoorn, U.E., et al., *Stromal–epithelial metabolic coupling in cancer: Integrating autophagy and metabolism in the tumor microenvironment.* The International Journal of Biochemistry & Cell Biology, 2011. **43**(7): p. 1045-1051.
22. Liao, D., et al., *Cancer Associated Fibroblasts Promote Tumor Growth and Metastasis by Modulating the Tumor Immune Microenvironment in a 4T1 Murine Breast Cancer Model.* PLoS One, 2009. **4**(11): p. e7965.
23. Lin, E.Y., et al., *Macrophages regulate the angiogenic switch in a mouse model of breast cancer.* Cancer Res, 2006. **66**(23): p. 11238-46.
24. Wagner, A.J., M.B. Small, and N. Hay, *Myc-mediated apoptosis is blocked by ectopic expression of Bcl-2.* Mol Cell Biol, 1993. **13**(4): p. 2432-40.
25. Callahan, R., *p53 mutations, another breast cancer prognostic factor.* J Natl Cancer Inst, 1992. **84**(11): p. 826-7.
26. Kozbor, D. and C.M. Croce, *Amplification of the c-myc oncogene in one of five human breast carcinoma cell lines.* Cancer Res, 1984. **44**(2): p. 438-41.
27. Mahadevan, V. and I.R. Hart, *Metastasis and angiogenesis.* Acta Oncol, 1990. **29**(1): p. 97-103.
28. Wang, R., et al., *Glioblastoma stem-like cells give rise to tumour endothelium.* Nature, 2010. **468**(7325): p. 829-833.
29. Folkman, J., *The role of angiogenesis in tumor growth.* Semin Cancer Biol, 1992. **3**(2): p. 65-71.
30. Mizukami, Y., et al., *Abnormal tumor vasculatures and bone marrow-derived pro-angiogenic cells in cancer.* Int J Hematol, 2012. **95**(2): p. 125-30.
31. Finke, J., et al., *MDSC as a mechanism of tumor escape from sunitinib mediated anti-angiogenic therapy.* Int Immunopharmacol, 2011. **11**(7): p. 856-61.
32. Mantovani, A., et al., *Role of tumor-associated macrophages in tumor progression and invasion.* Cancer Metastasis Rev, 2006. **25**(3): p. 315-22.
33. Jones, P.A. and Y.A. DeClerck, *Destruction of extracellular matrices containing glycoproteins, elastin, and collagen by metastatic human tumor cells.* Cancer Res, 1980. **40**(9): p. 3222-7.
34. Iurlaro, M., et al., *Angiogenesis extent and expression of matrix metalloproteinase-2 and -9 correlate with upgrading and myometrial invasion in endometrial carcinoma.* Eur J Clin Invest, 1999. **29**(9): p. 793-801.

35. Wong, S.Y. and R.O. Hynes, *Lymphatic or hematogenous dissemination: how does a metastatic tumor cell decide?* Cell Cycle, 2006. **5**(8): p. 812-7.
36. Cooper, C.R., et al., *Stromal factors involved in prostate carcinoma metastasis to bone.* Cancer, 2003. **97**(3 Suppl): p. 739-47.
37. Wyckoff, J.B., et al., *Direct visualization of macrophage-assisted tumor cell intravasation in mammary tumors.* Cancer Res, 2007. **67**(6): p. 2649-56.
38. Salmi, M., et al., *Tumor endothelium selectively supports binding of IL-2-propagated tumor-infiltrating lymphocytes.* J Immunol, 1995. **154**(11): p. 6002-12.
39. Hosaka, S., M. Suzuki, and H. Sato, *Leucocyte-like motility of cancer cells, with reference to the mechanism of extravasation in metastasis.* Gann, 1979. **70**(4): p. 559-61.
40. Redondo-Munoz, J., et al., *MMP-9 in B-cell chronic lymphocytic leukemia is up-regulated by alpha4beta1 integrin or CXCR4 engagement via distinct signaling pathways, localizes to podosomes, and is involved in cell invasion and migration.* Blood, 2006. **108**(9): p. 3143-51.
41. Gassmann, P., et al., *CXCR4 regulates the early extravasation of metastatic tumor cells in vivo.* Neoplasia, 2009. **11**(7): p. 651-61.
42. Ben-Baruch, A., *Organ selectivity in metastasis: regulation by chemokines and their receptors.* Clin Exp Metastasis, 2008. **25**(4): p. 345-56.
43. McCarthy, J.B., et al., *Tumor cell adhesive mechanisms and their relationship to metastasis.* Semin Cancer Biol, 1991. **2**(3): p. 155-67.
44. Morris, V.L., et al., *Effects of the disintegrin eristostatin on individual steps of hematogenous metastasis.* Exp Cell Res, 1995. **219**(2): p. 571-8.
45. Rice, G.E. and M.P. Bevilacqua, *An inducible endothelial cell surface glycoprotein mediates melanoma adhesion.* Science, 1989. **246**(4935): p. 1303-6.
46. Lafrenie, R.M., M.R. Buchanan, and F.W. Orr, *Adhesion molecules and their role in cancer metastasis.* Cell Biophys, 1993. **23**(1-3): p. 3-89.
47. Zolotareva, A.G., et al., *[Selective adhesion of tumor cells to the endothelium of the target organ in metastasis].* Eksp Onkol, 1986. **8**(6): p. 28-32.
48. Rucci, N., P. Sanita, and A. Angelucci, *Roles of metalloproteases in metastatic niche.* Curr Mol Med, 2011. **11**(8): p. 609-22.
49. Shiozawa, Y., K.J. Pienta, and R.S. Taichman, *Hematopoietic stem cell niche is a potential therapeutic target for bone metastatic tumors.* Clin Cancer Res, 2011. **17**(17): p. 5553-8.
50. Kim, M., et al., *CXCR4 signaling regulates metastasis of chemoresistant melanoma cells by a lymphatic metastatic niche.* Cancer Res, 2010. **70**(24): p. 10411-21.
51. Yasuda, T., et al., *Chemokines CCL19 and CCL21 promote activation-induced cell death of antigen-responding T cells.* Blood, 2007. **109**(2): p. 449-56.
52. Delk, N.A. and M.C. Farach-Carson, *Interleukin-6: a bone marrow stromal cell paracrine signal that induces neuroendocrine differentiation and modulates autophagy in bone metastatic PCa cells.* Autophagy, 2012. **8**(4): p. 650-63.

53. Azim, H.A., N.S. Kamal, and H.A. Azim, Jr., *Bone metastasis in breast cancer: The story of RANK-Ligand.* J Egypt Natl Canc Inst, 2012. **24**(3): p. 107-14.
54. Handschuhmacher, C.P. and H.J. Maurer, *[Incidence of metastasis to the lungs and skeleton in breast carcinoma and carcinoma of the female genitalia].* Strahlentherapie, 1957. **104**(1): p. 55-70.
55. Rozin, D.L., *[on the Incidence of Osteolytic and Osteoblastic Manifestations of Cancer Metastases from the Mammary Glands to Bones].* Klin Khir, 1965. **12**: p. 61-2.
56. Koizumi, M., et al., *An open cohort study of bone metastasis incidence following surgery in breast cancer patients.* BMC Cancer, 2010. **10**: p. 381.
57. Suva, L.J., et al., *Bone metastasis: mechanisms and therapeutic opportunities.* Nat Rev Endocrinol, 2011. **7**(4): p. 208-18.
58. Disibio, G. and S.W. French, *Metastatic patterns of cancers: results from a large autopsy study.* Arch Pathol Lab Med, 2008. **132**(6): p. 931-9.
59. Ibrahim, T., et al., *Role of RANK, RANKL, OPG, and CXCR4 tissue markers in predicting bone metastases in breast cancer patients.* Clin Breast Cancer, 2011. **11**(6): p. 369-75.
60. Powell, G.J., et al., *Localization of parathyroid hormone-related protein in breast cancer metastases: increased incidence in bone compared with other sites.* Cancer Res, 1991. **51**(11): p. 3059-61.
61. Bonewald, L.F., *Primer on the metabolic bone diseases and disorders of mineral metabolism (Rosen, C. J. ed.)*. 7th ed, ed. C.J. Rosen. Vol. Rosen, C. J. ed. 2008, Washington D.C: American Society for Bone and Mineral

Research. .
62. Bonewald, L.F., *The amazing osteocyte.* J Bone Miner Res, 2011. **26**(2): p. 229-38.
63. Kong, Y.Y., et al., *OPGL is a key regulator of osteoclastogenesis, lymphocyte development and lymph-node organogenesis.* Nature, 1999. **397**(6717): p. 315-23.
64. Fata, J.E., et al., *The osteoclast differentiation factor osteoprotegerin-ligand is essential for mammary gland development.* Cell, 2000. **103**(1): p. 41-50.
65. Bachmann, M.F., et al., *TRANCE, a tumor necrosis factor family member critical for CD40 ligand-independent T helper cell activation.* J Exp Med, 1999. **189**(7): p. 1025-31.
66. Onal, M., et al., *Receptor Activator of Nuclear Factor kappaB Ligand (RANKL) Protein Expression by B Lymphocytes Contributes to Ovariectomy-induced Bone Loss.* J Biol Chem, 2012. **287**(35): p. 29851-60.
67. Fuller, K., et al., *TRANCE is necessary and sufficient for osteoblast-mediated activation of bone resorption in osteoclasts.* J Exp Med, 1998. **188**(5): p. 997-1001.
68. Nakashima, T., M. Hayash, and H. Takayanagi, *[Regulation of bone resorption by osteocytes].* Clin Calcium, 2012. **22**(5): p. 685-96.
69. Riegel, A., et al., *Human polymorphonuclear neutrophils express RANK and are activated by its ligand, RANKL.* Eur J Immunol, 2012. **42**(4): p. 975-81.

70. Takahashi, N., N. Udagawa, and T. Suda, *A new member of tumor necrosis factor ligand family, ODF/OPGL/TRANCE/RANKL, regulates osteoclast differentiation and function.* Biochem Biophys Res Commun, 1999. **256**(3): p. 449-55.
71. Lacey, D.L., et al., *Osteoprotegerin ligand modulates murine osteoclast survival in vitro and in vivo.* Am J Pathol, 2000. **157**(2): p. 435-48.
72. Burgess, T.L., et al., *The ligand for osteoprotegerin (OPGL) directly activates mature osteoclasts.* J Cell Biol, 1999. **145**(3): p. 527-38.
73. Willard, D., et al., *Expression, purification, and characterization of the human receptor activator of NF-kappaB ligand (RANKL) extracellular domain.* Protein Expr Purif, 2000. **20**(1): p. 48-57.
74. Kanazawa, K. and A. Kudo, *Self-assembled RANK induces osteoclastogenesis ligand-independently.* J Bone Miner Res, 2005. **20**(11): p. 2053-60.
75. Wong, B.R., et al., *The TRAF Family of Signal Transducers Mediates NF-κB Activation by the TRANCE Receptor.* Journal of Biological Chemistry, 1998. **273**(43): p. 28355-28359.
76. Jones, D.H., Y.Y. Kong, and J.M. Penninger, *Role of RANKL and RANK in bone loss and arthritis.* Ann Rheum Dis, 2002. **61 Suppl 2**: p. ii32-9.
77. Singh, P.P., et al., *Membrane-bound receptor activator of NFkappaB ligand (RANKL) activity displayed by osteoblasts is differentially regulated by osteolytic factors.* Biochem Biophys Res Commun, 2012. **422**(1): p. 48-53.
78. Lum, L., et al., *Evidence for a Role of a Tumor Necrosis Factor-α (TNF-α)-converting Enzyme-like Protease in Shedding of TRANCE, a TNF Family Member Involved in Osteoclastogenesis and Dendritic Cell Survival.* Journal of Biological Chemistry, 1999. **274**(19): p. 13613-13618.
79. Kanamaru, F., et al., *Expression of membrane-bound and soluble receptor activator of NF-κB ligand (RANKL) in human T cells.* Immunology Letters, 2004. **94**(3): p. 239-246.
80. Armstrong, A.P., et al., *RANKL acts directly on RANK-expressing prostate tumor cells and mediates migration and expression of tumor metastasis genes.* Prostate, 2008. **68**(1): p. 92-104.
81. Jones, D.H., et al., *Regulation of cancer cell migration and bone metastasis by RANKL.* Nature, 2006. **440**(7084): p. 692-6.
82. Zhang, L., et al., *C-Src-mediated RANKL-induced breast cancer cell migration by activation of the ERK and Akt pathway.* Oncol Lett, 2012. **3**(2): p. 395-400.
83. *Denosumab and bone metastases. No better than a bisphosphonate.* Prescrire Int, 2012. **21**(130): p. 204-6.
84. Russell, R.G., et al., *Mechanisms of action of bisphosphonates: similarities and differences and their potential influence on clinical efficacy.* Osteoporos Int, 2008. **19**(6): p. 733-59.
85. Guise, T.A., et al., *Evidence for a causal role of parathyroid hormone-related protein in the pathogenesis of human breast cancer-mediated osteolysis.* J Clin Invest, 1996. **98**(7): p. 1544-9.
86. Sterling, J.A., et al., *Advances in the biology of bone metastasis: how the skeleton affects tumor behavior.* Bone, 2011. **48**(1): p. 6-15.

87. Yoneda, T., A. Sasaki, and G.R. Mundy, *Osteolytic bone metastasis in breast cancer.* Breast Cancer Res Treat, 1994. **32**(1): p. 73-84.
88. Johnson, R.W., et al., *TGF-beta promotion of Gli2-induced expression of parathyroid hormone-related protein, an important osteolytic factor in bone metastasis, is independent of canonical Hedgehog signaling.* Cancer Res, 2011. **71**(3): p. 822-31.
89. Li, X., et al., *Loss of TGF-beta Responsiveness in Prostate Stromal Cells Alters Chemokine Levels and Facilitates the Development of Mixed Osteoblastic/Osteolytic Bone Lesions.* Mol Cancer Res, 2012.
90. Yoneda, T., et al., *Actions of bisphosphonate on bone metastasis in animal models of breast carcinoma.* Cancer, 2000. **88**(12 Suppl): p. 2979-88.
91. Rose, A.A., et al., *Osteoactivin promotes breast cancer metastasis to bone.* Mol Cancer Res, 2007. **5**(10): p. 1001-14.
92. Oyajobi, B.O., et al., *Dual effects of macrophage inflammatory protein-1alpha on osteolysis and tumor burden in the murine 5TGM1 model of myeloma bone disease.* Blood, 2003. **102**(1): p. 311-9.
93. Bouxsein, M.L., et al., *Guidelines for assessment of bone microstructure in rodents using micro–computed tomography.* Journal of Bone and Mineral Research, 2010. **25**(7): p. 1468-1486.
94. Hurrell, D.J., *The Nerve Supply of Bone.* J Anat, 1937. **72**(Pt 1): p. 54-61.
95. Calvo, W., *The innervation of the bone marrow in laboratory animals.* Am J Anat, 1968. **123**(2): p. 315-28.
96. Duncan, C.P. and S.S. Shim, *J. Edouard Samson Address: the autonomic nerve supply of bone. An experimental study of the intraosseous adrenergic nervi vasorum in the rabbit.* J Bone Joint Surg Br, 1977. **59**(3): p. 323-30.
97. Gajda, M., et al., *Development of rat tibia innervation: colocalization of autonomic nerve fiber markers with growth-associated protein 43.* Cells Tissues Organs, 2010. **191**(6): p. 489-99.
98. Antonacci, M.D., D.R. Mody, and M.H. Heggeness, *Innervation of the human vertebral body: a histologic study.* J Spinal Disord, 1998. **11**(6): p. 526-31.
99. Wang, J., et al., *Bone marrow mesenchymal stem cells promote cell proliferation and neurotrophic function of Schwann cells in vitro and in vivo.* Brain Res, 2009. **1262**: p. 7-15.
100. Thomas, S.A., A.M. Matsumoto, and R.D. Palmiter, *Noradrenaline is essential for mouse fetal development.* Nature, 1995. **374**(6523): p. 643-646.
101. Bjurholm, A., et al., *Neuropeptide Y-, tyrosine hydroxylase- and vasoactive intestinal polypeptide-immunoreactive nerves in bone and surrounding tissues.* J Auton Nerv Syst, 1988. **25**(2-3): p. 119-25.
102. Elefteriou, F., *Neuronal signaling and the regulation of bone remodeling.* Cell Mol Life Sci, 2005. **62**(19-20): p. 2339-49.
103. Takeda, S., et al., *Leptin regulates bone formation via the sympathetic nervous system.* Cell, 2002. **111**(3): p. 305-17.
104. Elefteriou, F., et al., *Leptin regulation of bone resorption by the sympathetic nervous system and CART.* Nature, 2005. **434**(7032): p. 514-20.

105. Fu, L., et al., *The molecular clock mediates leptin-regulated bone formation.* Cell, 2005. **122**(5): p. 803-15.
106. Bonnet, N., et al., *Severe bone alterations under beta2 agonist treatments: bone mass, microarchitecture and strength analyses in female rats.* Bone, 2005. **37**(5): p. 622-33.
107. Bonnet, N., et al., *Low dose beta-blocker prevents ovariectomy-induced bone loss in rats without affecting heart functions.* J Cell Physiol, 2008. **217**(3): p. 819-27.
108. Katayama, Y., et al., *Signals from the sympathetic nervous system regulate hematopoietic stem cell egress from bone marrow.* Cell, 2006. **124**(2): p. 407-21.
109. Sousa, D.M., et al., *Neuropeptide Y Y1 receptor antagonism increases bone mass in mice.* Bone, 2012. **51**(1): p. 8-16.
110. Baldock, P.A., et al., *Hypothalamic regulation of cortical bone mass: opposing activity of y2 receptor and leptin pathways.* J Bone Miner Res, 2006. **21**(10): p. 1600-7.
111. Lundberg, P., et al., *Greater bone formation of Y2 knockout mice is associated with increased osteoprogenitor numbers and altered Y1 receptor expression.* J Biol Chem, 2007. **282**(26): p. 19082-91.
112. Igwe, J.C., et al., *Neuropeptide Y is expressed by osteocytes and can inhibit osteoblastic activity.* J Cell Biochem, 2009. **108**(3): p. 621-30.
113. de Vries, F., et al., *Use of beta-blockers and the risk of hip/femur fracture in the United Kingdom and The Netherlands.* Calcif Tissue Int, 2007. **80**(2): p. 69-75.
114. Tam, J., et al., *Involvement of neuronal cannabinoid receptor CB1 in regulation of bone mass and bone remodeling.* Mol Pharmacol, 2006. **70**(3): p. 786-92.
115. Ma, Y., et al., *β2-Adrenergic Receptor Signaling in Osteoblasts Contributes to the Catabolic effect of Glucocorticoids on Bone.* J. Biol. Chem., 2011. **in press**.
116. Yirmiya, R., et al., *Depression induces bone loss through stimulation of the sympathetic nervous system.* Proc Natl Acad Sci U S A, 2006. **103**(45): p. 16876-81.
117. Cizza, G., et al., *Depression: a major, unrecognized risk factor for osteoporosis?* Trends Endocrinol Metab, 2001. **12**(5): p. 198-203.
118. Hinoi, E., et al., *The sympathetic tone mediates leptin's inhibition of insulin secretion by modulating osteocalcin bioactivity.* J Cell Biol, 2008. **183**(7): p. 1235-42.
119. Oury, F., et al., *Endocrine Regulation of Male Fertility by the Skeleton.* Cell, 2011.
120. H, L., *The Stress of Life. Hans Selye, M.D. New York, McGraw-Hill Book Company, Inc. 1956. $5.95.* The Journal of Bone & Joint Surgery, 1957. **39**(2): p. 479-b.
121. Dhabhar, F.S., et al., *Stress-induced redistribution of immune cells-From barracks to boulevards to battlefields: A tale of three hormones - Curt Richter Award Winner.* Psychoneuroendocrinology, 2012. **37**(9): p. 1345-68.
122. Atanackovic, D., et al., *Acute psychological stress alerts the adaptive immune response: stress-induced mobilization of effector T cells.* J Neuroimmunol, 2006. **176**(1-2): p. 141-52.
123. Kotelevtsev, Y., et al., *11β-Hydroxysteroid dehydrogenase type 1 knockout mice show attenuated glucocorticoid-inducible responses and resist hyperglycemia on*

obesity or stress. Proceedings of the National Academy of Sciences, 1997. **94**(26): p. 14924-14929.
124. Guyton, A.C., *Textbook of Medical Physiology*. 2006, Philadelphia, PA: Elsevier Inc. 1116.
125. Schulze, S., et al., *Effect of prednisolone on the systemic response and wound healing after colonic surgery.* Arch Surg, 1997. **132**(2): p. 129-35.
126. Samuelson, W.M. and A.O. Davies, *Hydrocortisone-induced reversal of beta-adrenergic receptor uncoupling.* Am Rev Respir Dis, 1984. **130**(6): p. 1023-6.
127. Violin, J.D., et al., *beta2-adrenergic receptor signaling and desensitization elucidated by quantitative modeling of real time cAMP dynamics.* J Biol Chem, 2008. **283**(5): p. 2949-61.
128. Hoffman, B.B., D. Mullikin-Kilpatrick, and R.J. Lefkowitz, *Desensitization of beta-adrenergic stimulated adenylate cyclase in turkey erythrocytes.* J Cyclic Nucleotide Res, 1979. **5**(5): p. 355-66.
129. Andrews, M.H., et al., *Acute glucocorticoid administration rapidly suppresses basal and stress-induced hypothalamo-pituitary-adrenal axis activity.* Endocrinology, 2012. **153**(1): p. 200-11.
130. Lund, D.D., et al., *Compensatory recovery of parasympathetic control of heart rate after unilateral vagotomy in rabbits.* Am J Physiol, 1992. **262**(4 Pt 2): p. H1122-7.
131. Li, Q., et al., *Effect of electric foot shock and psychological stress on activities of murine splenic natural killer and lymphokine-activated killer cells, cytotoxic T lymphocytes, natural killer receptors and mRNA transcripts for granzymes and perforin.* Stress, 2005. **8**(2): p. 107-16.
132. Meerson, F.Z., et al., *[Prevention of depression of the natural killer activity and myocardial contractile function during long-term stress by using preliminary body adaptation to short stress exposures].* Dokl Akad Nauk SSSR, 1984. **274**(1): p. 241-3.
133. Pare, W.P., *The Effect of Chronic Environmental Stress on Stomach Ulceration, Adrenal Function, and Consummatory Behavior in the Rat.* J Psychol, 1964. **57**: p. 143-51.
134. Camps Bansell, J. and J. Prieto Valtuena, *[Chronic fatigue syndrome].* An Med Interna, 1990. **7**(10): p. 497-9.
135. Kita, T., et al., *[Abnormal ECG and adrenaline-induced arrhythmias in restraint and water immersion stressed mice and effects of oxprenolol].* Nihon Yakurigaku Zasshi, 1984. **83**(5): p. 373-82.
136. *Therapy for hypercholesterolemia; standardization of cholesterol measurements.* JAMA, 1990. **263**(3): p. 375-6.
137. Garcia Tamayo, F., L.I. Terrazas Valdes, and N. Malpica Lopez, *Zinc administration prevents wasting in stressed mice.* Arch Med Res, 1996. **27**(3): p. 319-25.
138. Larkins, R.G., *Problems facing the teaching hospitals.* Med J Aust, 1990. **153**(8): p. 438-40.

139. Veith Rc, L.N.L.O.A. and et al., *Sympathetic nervous system activity in major depression: Basal and desipramine-induced alterations in plasma norepinephrine kinetics.* Archives of General Psychiatry, 1994. **51**(5): p. 411-422.
140. Suls, J. and J. Bunde, *Anger, anxiety, and depression as risk factors for cardiovascular disease: the problems and implications of overlapping affective dispositions.* Psychol Bull, 2005. **131**(2): p. 260-300.
141. Kendler, K.S. and L.J. Halberstadt, *The road not taken: life experiences in monozygotic twin pairs discordant for major depression.* Mol Psychiatry, 2012.
142. Kubzansky, L.D., et al., *Shared and unique contributions of anger, anxiety, and depression to coronary heart disease: a prospective study in the normative aging study.* Ann Behav Med, 2006. **31**(1): p. 21-9.
143. Holsen, L.M., et al., *Brain hypoactivation, autonomic nervous system dysregulation, and gonadal hormones in depression: a preliminary study.* Neurosci Lett, 2012. **514**(1): p. 57-61.
144. Cyranowski, J.M., et al., *Psychosocial Features Associated with Lifetime Comorbidity of Major Depression and Anxiety Disorders among a Community Sample of Mid-Life Women: The Swan Mental Health Study.* Depress Anxiety, 2012.
145. Meng, X. and C. D'Arcy, *Common and unique risk factors and comorbidity for 12-month mood and anxiety disorders among canadians.* Can J Psychiatry, 2012. **57**(8): p. 479-87.
146. Young, E.A., et al., *HPA axis activation in major depression and response to fluoxetine: a pilot study.* Psychoneuroendocrinology, 2004. **29**(9): p. 1198-1204.
147. Young, E. and A. Korszun, *Stress, the HPA Axis and Depressive Illness*, in *Encyclopedia of Neuroscience*, R.S. Editor-in-Chief: Larry, Editor. 2009, Academic Press: Oxford. p. 543-548.
148. Balardin, J.B., et al., *Subjective mild depressive symptoms are associated with abnormal diurnal cycle of salivary cortisol in older adults.* J Geriatr Psychiatry Neurol, 2011. **24**(1): p. 19-22.
149. Kunugi, H., et al., *[The hypothalamic-pituitary-adrenal axis and depressive disorder: recent progress].* Nihon Shinkei Seishin Yakurigaku Zasshi, 2012. **32**(4): p. 203-9.
150. Herbert, J., et al., *Interaction between the BDNF gene Val/66/Met polymorphism and morning cortisol levels as a predictor of depression in adult women.* Br J Psychiatry, 2012.
151. Barton, D.A., et al., *Sympathetic activity in major depressive disorder: identifying those at increased cardiac risk?* Journal of Hypertension, 2007. **25**(10): p. 2117-2124 10.1097/HJH.0b013e32829baae7.
152. Chida, Y., et al., *Do stress-related psychosocial factors contribute to cancer incidence and survival?* Nature Clinical Practice Oncology, 2008. **5**(8): p. 466-475.
153. Oei, N.Y.L., et al., *Propranolol reduces emotional distraction in working memory: A partial mediating role of propranolol-induced cortisol increases?* Neurobiology of Learning and Memory, 2010. **93**(3): p. 388-395.

154. Bali, S.J., et al., *Evaluation of major depressive disorder in patients receiving chronic treatment with topical timolol.* Ophthalmologica, 2011. **226**(3): p. 157-60.
155. Wohleb, E.S., et al., *beta-Adrenergic receptor antagonism prevents anxiety-like behavior and microglial reactivity induced by repeated social defeat.* J Neurosci, 2011. **31**(17): p. 6277-88.
156. Adamec, R., et al., *Activation patterns of cells in selected brain stem nuclei of more and less stress responsive rats in two animal models of PTSD - predator exposure and submersion stress.* Neuropharmacology, 2012. **62**(2): p. 725-36.
157. Adamec, R.E. and T. Shallow, *Lasting effects on rodent anxiety of a single exposure to a cat.* Physiol Behav, 1993. **54**(1): p. 101-9.
158. Adamec, R.E., T. Shallow, and J. Budgell, *Blockade of CCK(B) but not CCK(A) receptors before and after the stress of predator exposure prevents lasting increases in anxiety-like behavior: implications for anxiety associated with posttraumatic stress disorder.* Behav Neurosci, 1997. **111**(2): p. 435-49.
159. Do Monte, F.H., et al., *New perspectives on beta-adrenergic mediation of innate and learned fear responses to predator odor.* J Neurosci, 2008. **28**(49): p. 13296-302.
160. Agrawal, A., A.S. Jaggi, and N. Singh, *Pharmacological investigations on adaptation in rats subjected to cold water immersion stress.* Physiol Behav, 2011. **103**(3-4): p. 321-9.
161. Tarpy, R.M., M.K. Walsh, and C. Van Toller, *Effects of cold stress on body temperature of immunosympathectomized mice.* Physiol Behav, 1973. **11**(3): p. 411-3.
162. Johnson, D.G., et al., *Plasma norepinephrine responses of man in cold water.* J Appl Physiol, 1977. **43**(2): p. 216-20.
163. Mos, L., J. Vriend, and W. Poley, *Effects of light environment on emotionality and endocrine system of inbred mice.* Physiol Behav, 1974. **12**(6): p. 981-9.
164. Vernikos-Danellis, J., C.M. Winget, and N.W. Hetherington, *Diurnal rhythm of the pituitary-adrenocortical response to stress: effect of constant light and constant darkness.* Life Sci Space Res, 1970. **8**: p. 240-6.
165. Weltman, A.S., A.M. Sachler, and S.B. Sparber, *Endocrine, metabolic and behavioral aspects of isolation stress on female albino mice.* Aerosp Med, 1966. **37**(8): p. 804-10.
166. Essman, W.B., *Gastric ulceration in differentially housed mice.* Psychol Rep, 1966. **19**(1): p. 173-4.
167. Raab, W., et al., *Isolation, stress, myocardial electrolytes, and epinephrine cardiotoxicity in rats.* Proc Soc Exp Biol Med, 1968. **127**(1): p. 142-7.
168. Badowska-Szalewska, E., et al., *The influence of acute and chronic open-field exposure on the hippocampal formation: an immunohistochemical study.* Folia Morphol (Warsz), 2006. **65**(4): p. 343-51.
169. Breschi, M.C., et al., *Morphofunctional changes in the noradrenergic innervation of the rat cardiovascular system after varying duration of noise stress.* Int J Neurosci, 1994. **75**(1-2): p. 73-81.

170. Reynolds, R.P., et al., *Noise in a laboratory animal facility from the human and mouse perspectives.* J Am Assoc Lab Anim Sci, 2010. **49**(5): p. 592-7.
171. Paul, M.I., et al., *Immobilization stress induced changes in adrenocortical and medullary cyclic AMP content in the rat.* Endocrinology, 1971. **88**(2): p. 338-44.
172. Kasuga, S., et al., *[Effect of aged garlic extract (AGE) on hyperglycemia induced by immobilization stress in mice].* Nihon Yakurigaku Zasshi, 1999. **114**(3): p. 191-7.
173. Peres, G., et al., *[Research on the effects of restraint in rats].* Arch Sci Physiol (Paris), 1965. **19**(3): p. 295-320.
174. Thaker, P.H., et al., *Chronic stress promotes tumor growth and angiogenesis in a mouse model of ovarian carcinoma.* Nat Med, 2006. **12**(8): p. 939-44.
175. Liao, M.J., et al., *Daphnetin prevents chronic unpredictable stress-induced cognitive deficits.* Fundam Clin Pharmacol, 2012.
176. Mineur, Y.S., C. Belzung, and W.E. Crusio, *Effects of unpredictable chronic mild stress on anxiety and depression-like behavior in mice.* Behav Brain Res, 2006. **175**(1): p. 43-50.
177. Johns, C., et al., *Models of experimental hypertension in mice.* Hypertension, 1996. **28**(6): p. 1064-9.
178. Amador-Arjona, A., et al., *Susceptibility to stress in transgenic mice overexpressing TrkC, a model of panic disorder.* Journal of Psychiatric Research, 2010. **44**(3): p. 157-167.
179. Seasholtz, A.F., et al., *Mouse models of altered CRH-binding protein expression.* Peptides, 2001. **22**(5): p. 743-751.
180. Oh-hashi, Y., et al., *Elevated sympathetic nervous activity in mice deficient in alphaCGRP.* Circ Res, 2001. **89**(11): p. 983-90.
181. Henn, F.A. and B. Vollmayr, *Stress models of depression: forming genetically vulnerable strains.* Neurosci Biobehav Rev, 2005. **29**(4-5): p. 799-804.
182. Graham, J., et al., *Stressful life experiences and risk of relapse of breast cancer: observational cohort study.* BMJ, 2002. **324**(7351): p. 1420.
183. Thaker, P.H., et al., *Chronic stress promotes tumor growth and angiogenesis in a mouse model of ovarian carcinoma.* Nature Medicine, 2006. **12**(8): p. 939-944.
184. Sloan, E.K., et al., *The Sympathetic Nervous System Induces a Metastatic Switch in Primary Breast Cancer.* Cancer Research, 2010. **70**(18): p. 7042-7052.
185. Mendez-Ferrer, S., et al., *Haematopoietic stem cell release is regulated by circadian oscillations.* Nature, 2008. **452**(7186): p. 442-7.
186. Barbieri, F., et al., *CXC receptor and chemokine expression in human meningioma: SDF1/CXCR4 signaling activates ERK1/2 and stimulates meningioma cell proliferation.* Ann N Y Acad Sci, 2006. **1090**: p. 332-43.
187. Arya, M., et al., *The importance of the CXCL12-CXCR4 chemokine ligand-receptor interaction in prostate cancer metastasis.* J Exp Ther Oncol, 2004. **4**(4): p. 291-303.
188. Mirisola, V., et al., *CXCL12/SDF1 expression by breast cancers is an independent prognostic marker of disease-free and overall survival.* Eur J Cancer, 2009. **45**(14): p. 2579-87.

189. Tang, Z.N., et al., *RANKL-induced migration of MDA-MB-231 human breast cancer cells via Src and MAPK activation.* Oncol Rep, 2011. **26**(5): p. 1243-50.
190. Mikami, S., et al., *Increased RANKL expression is related to tumour migration and metastasis of renal cell carcinomas.* J Pathol, 2009. **218**(4): p. 530-9.
191. Yoneda, T., et al., *Inhibition of osteolytic bone metastasis of breast cancer by combined treatment with the bisphosphonate ibandronate and tissue inhibitor of the matrix metalloproteinase-2.* J Clin Invest, 1997. **99**(10): p. 2509-17.
192. Friedman, M.J., *Toward rational pharmacotherapy for posttraumatic stress disorder: an interim report.* Am J Psychiatry, 1988. **145**(3): p. 281-5.
193. Veith, R.C., et al., *Sympathetic nervous system activity in major depression. Basal and desipramine-induced alterations in plasma norepinephrine kinetics.* Arch Gen Psychiatry, 1994. **51**(5): p. 411-22.
194. Yan, H.C., et al., *Behavioral animal models of depression.* Neurosci Bull, 2010. **26**(4): p. 327-37.
195. Conway, W.D., et al., *Absorption and elimination profile of isoproterenol. 3. The metabolic fate of dl-isoproterenol-7-3H in the dog.* J Pharm Sci, 1968. **57**(7): p. 1135-41.
196. Fogelman, F. and H.F. Grundy, *A comparison of the cardiovascular actions of AQ 110 with those of isoprenaline and salbutamol.* Br J Pharmacol, 1970. **38**(2): p. 416-32.
197. Santini, D., et al., *Expression pattern of receptor activator of NFkappaB (RANK) in a series of primary solid tumors and related bone metastases.* J Cell Physiol, 2011. **226**(3): p. 780-4.
198. Bataille, C., et al., *Different sympathetic pathways control the metabolism of distinct bone envelopes.* Bone, 2012. **50**(5): p. 1162-72.
199. Skrabanek, P., *Catecholamines cause the hypercalciuria and hypercalcaemia in phaeochromocytoma and in hyperthyroidism.* Med Hypotheses, 1977. **3**(2): p. 59-62.
200. Lipski, S., *Effect of beta-adrenergic stimulation by isoprenaline on proliferation and differentation of mouse bone marrow cells in vivo.* Pol J Pharmacol Pharm, 1980. **32**(3): p. 281-7.
201. Thomas, T., *[New actors in bone remodelling: a role for the immune system].* Bull Acad Natl Med, 2010. **194**(8): p. 1493-503; discussion 1503-4.
202. Sood, A.K., et al., *Stress hormone-mediated invasion of ovarian cancer cells.* Clin Cancer Res, 2006. **12**(2): p. 369-75.
203. Sastry, K.S.R., et al., *Epinephrine Protects Cancer Cells from Apoptosis via Activation of cAMP-dependent Protein Kinase and BAD Phosphorylation.* Journal of Biological Chemistry, 2007. **282**(19): p. 14094-14100.
204. Kajimura, D., et al., *Genetic determination of the cellular basis of the sympathetic regulation of bone mass accrual.* J Exp Med, 2011. **208**(4): p. 841-51.
205. Killock, D., *Bone: Osteocyte RANKL in bone homeostasis: a paradigm shift?* Nat Rev Rheumatol, 2011. **7**(11): p. 619.
206. Kitazawa, R., et al., *Expression of parathyroid hormone-related protein (PTHrP) in multiple myeloma.* Pathol Int, 2002. **52**(1): p. 63-8.

207. Sanders, V.M., *The beta2-adrenergic receptor on T and B lymphocytes: do we understand it yet?* Brain Behav Immun, 2012. **26**(2): p. 195-200.
208. Kin, N.W. and V.M. Sanders, *It takes nerve to tell T and B cells what to do.* J Leukoc Biol, 2006. **79**(6): p. 1093-104.
209. Sanders, V.M., *The role of norepinephrine and beta-2-adrenergic receptor stimulation in the modulation of Th1, Th2, and B lymphocyte function.* Adv Exp Med Biol, 1998. **437**: p. 269-78.
210. Abe, M., et al., *Osteoclasts enhance myeloma cell growth and survival via cell-cell contact: a vicious cycle between bone destruction and myeloma expansion.* Blood, 2004. **104**(8): p. 2484-91.
211. Terpos, E., E. Kastritis, and M.A. Dimopoulos, *Prevention and Treatment of Myeloma Bone Disease.* Curr Hematol Malig Rep, 2012.
212. Ma, Y., et al., *beta2-Adrenergic receptor signaling in osteoblasts contributes to the catabolic effect of glucocorticoids on bone.* Endocrinology, 2011. **152**(4): p. 1412-22.
213. Huang, H.H., et al., *Functional alpha1- and beta2-adrenergic receptors in human osteoblasts.* J Cell Physiol, 2009. **220**(1): p. 267-75.
214. Millan, M.J., et al., *Agonist and antagonist actions of yohimbine as compared to fluparoxan at α2-adrenergic receptors (AR)s, serotonin (5-HT)1A, 5-HT1B, 5-HT1D and dopamine D2 and D3 receptors. Significance for the modulation of frontocortical monoaminergic transmission and depressive states.* Synapse, 2000. **35**(2): p. 79-95.
215. Arthur, J.M., S.J. Casanas, and J.R. Raymond, *Partial agonist properties of rauwolscine and yohimbine for the inhibition of adenylyl cyclase by recombinant human 5-HT1A receptors.* Biochem Pharmacol, 1993. **45**(11): p. 2337-41.
216. Pertovaara, A., et al., *Pharmacological properties, central nervous system effects, and potential therapeutic applications of atipamezole, a selective alpha2-adrenoceptor antagonist.* CNS Drug Rev, 2005. **11**(3): p. 273-88.
217. Bonnet, N., et al., *Dose effects of propranolol on cancellous and cortical bone in ovariectomized adult rats.* J Pharmacol Exp Ther, 2006. **318**(3): p. 1118-27.
218. Lewis, M.J., et al., *The effects of propranolol and acebutolol on the overnight plasma levels of anterior pituitary and related hormones.* Br J Clin Pharmacol, 1981. **12**(5): p. 737-42.
219. Dura Trave, T., et al., *[Sensitivity of the clonidine and guanfacine tests (alpha-2-adrenergic agonists) as pharmacologic stimulants of growth hormone. Effects on plasma cortisol].* An Esp Pediatr, 1996. **45**(6): p. 575-8.
220. Gray, K., J. Short, and S. Ventura, *The alpha1A-adrenoceptor gene is required for the alpha1L-adrenoceptor-mediated response in isolated preparations of the mouse prostate.* Br J Pharmacol, 2008. **155**(1): p. 103-9.
221. Cuscito, C., et al., *Adrenergic stimulation decreases osteoblast oxytocin synthesis.* Ann N Y Acad Sci, 2011. **1237**: p. 53-7.
222. Hori, Y., et al., *Naftopidil, a selective {alpha}1-adrenoceptor antagonist, suppresses human prostate tumor growth by altering interactions between tumor cells and stroma.* Cancer Prev Res (Phila), 2011. **4**(1): p. 87-96.

223. DiNicolantonio, J.J. and D.G. Hackam, *Carvedilol: a third-generation beta-blocker should be a first-choice beta-blocker.* Expert Rev Cardiovasc Ther, 2012. **10**(1): p. 13-25.
224. Arumanayagam, M., et al., *Antioxidant properties of carvedilol and metoprolol in heart failure: a double-blind randomized controlled trial.* J Cardiovasc Pharmacol, 2001. **37**(1): p. 48-54.
225. Rodrigues, M.A., et al., *Carvedilol protects against cisplatin-induced oxidative stress, redox state unbalance and apoptosis in rat kidney mitochondria.* Chem Biol Interact, 2011. **189**(1-2): p. 45-51.
226. Yang, E.V., et al., *Norepinephrine upregulates VEGF, IL-8, and IL-6 expression in human melanoma tumor cell lines: implications for stress-related enhancement of tumor progression.* Brain Behav Immun, 2009. **23**(2): p. 267-75.
227. Yang, E.V., et al., *Norepinephrine up-regulates the expression of vascular endothelial growth factor, matrix metalloproteinase (MMP)-2, and MMP-9 in nasopharyngeal carcinoma tumor cells.* Cancer Res, 2006. **66**(21): p. 10357-64.
228. Giron, L.T., Jr., K.A. Crutcher, and J.N. Davis, *Lymph nodes--a possible site for sympathetic neuronal regulation of immune responses.* Ann Neurol, 1980. **8**(5): p. 520-5.
229. Felten, D.L., et al., *Noradrenergic and peptidergic innervation of lymphoid tissue.* J Immunol, 1985. **135**(2 Suppl): p. 755s-765s.
230. Himelstein, B.P., et al., *Metalloproteinases in tumor progression: the contribution of MMP-9.* Invasion Metastasis, 1994. **14**(1-6): p. 246-58.
231. Ahrens, D., et al., *Expression of matrix metalloproteinase 9 (96-kd gelatinase B) in human rheumatoid arthritis.* Arthritis Rheum, 1996. **39**(9): p. 1576-87.
232. Thorgeirsson, U.P., et al., *Breast cancer; tumor neovasculature and the effect of tissue inhibitor of metalloproteinases-1 (TIMP-1) on angiogenesis.* In Vivo, 1996. **10**(2): p. 137-44.
233. Stetler-Stevenson, W.G., *Type IV collagenases in tumor invasion and metastasis.* Cancer Metastasis Rev, 1990. **9**(4): p. 289-303.
234. Kao, S.J., et al., *Osthole inhibits the invasive ability of human lung adenocarcinoma cells via suppression of NF-kappaB-mediated matrix metalloproteinase-9 expression.* Toxicol Appl Pharmacol, 2012. **261**(1): p. 105-15.
235. Iwata, H., et al., *[The expression of MMPs and TIMPs in human breast cancer tissues and importance of their balance in cancer invasion and metastasis].* Nihon Rinsho, 1995. **53**(7): p. 1805-10.
236. Ibrahim, A., et al., *Effect of curcumin and Meriva on the lung metastasis of murine mammary gland adenocarcinoma.* In Vivo, 2010. **24**(4): p. 401-8.
237. Canon, J.R., et al., *Inhibition of RANKL blocks skeletal tumor progression and improves survival in a mouse model of breast cancer bone metastasis.* Clin Exp Metastasis, 2008. **25**(2): p. 119-29.
238. Ellis, G.K., et al., *Randomized trial of denosumab in patients receiving adjuvant aromatase inhibitors for nonmetastatic breast cancer.* J Clin Oncol, 2008. **26**(30): p. 4875-82.

239. Yoneda, T., *[Anti-RANKL antibody for the management of bone metastasis].* Gan To Kagaku Ryoho, 2011. **38**(9): p. 1439-45.
240. Zhang, L., et al., *Receptor activator for nuclear factor kappa B expression predicts poor prognosis in breast cancer patients with bone metastasis but not in patients with visceral metastasis.* J Clin Pathol, 2011.
241. Powe, D.G., et al., *Beta-blocker drug therapy reduces secondary cancer formation in breast cancer and improves cancer specific survival.* Oncotarget, 2010. **1**(7): p. 628-38.
242. Melhem-Bertrandt, A., et al., *Beta-blocker use is associated with improved relapse-free survival in patients with triple-negative breast cancer.* J Clin Oncol, 2011. **29**(19): p. 2645-52.
243. Barron, T.I., et al., *Beta blockers and breast cancer mortality: a population- based study.* J Clin Oncol, 2011. **29**(19): p. 2635-44.
244. Alvarez, G.E., et al., *Sympathetic Neural Activation in Visceral Obesity.* Circulation, 2002. **106**(20): p. 2533-2536.
245. Lambert, E.A., N.E. Straznicky, and G.W. Lambert, *A sympathetic view of human obesity.* Clin Auton Res, 2012.
246. Champaneri, S., et al., *Biological basis of depression in adults with diabetes.* Curr Diab Rep, 2010. **10**(6): p. 396-405.
247. Esler, M., et al., *Sympathetic nervous system and insulin resistance: from obesity to diabetes.* Am J Hypertens, 2001. **14**(11 Pt 2): p. 304S-309S.
248. Connolly, G.C., et al., *Diabetes Mellitus Is Associated With the Presence of Metastatic Spread at Disease Presentation in Hepatocellular Carcinoma.* Cancer Invest, 2012.
249. Vucenik, I. and J.P. Stains, *Obesity and cancer risk: evidence, mechanisms, and recommendations.* Ann N Y Acad Sci, 2012. **1271**: p. 37-43.
250. Campbell, P.T., et al., *Diabetes and cause-specific mortality in a prospective cohort of one million u.s. Adults.* Diabetes Care, 2012. **35**(9): p. 1835-44.
251. Redaniel, M.T., et al., *Associations of type 2 diabetes and diabetes treatment with breast cancer risk and mortality: a population-based cohort study among British women.* Cancer Causes Control, 2012. **23**(11): p. 1785-95.
252. Nguyen, T. and D.C. Lau, *The obesity epidemic and its impact on hypertension.* Can J Cardiol, 2012. **28**(3): p. 326-33.
253. Giles, T.D., *The patient with diabetes mellitus and heart failure: at-risk issues.* Am J Med, 2003. **115 Suppl 8A**: p. 107S-110S.
254. Daher, I.N. and E.T. Yeh, *Vascular complications of selected cancer therapies.* Nat Clin Pract Cardiovasc Med, 2008. **5**(12): p. 797-805.
255. Pasquier, E., et al., *Propranolol potentiates the anti-angiogenic effects and anti-tumor efficacy of chemotherapy agents: implication in breast cancer treatment.* Oncotarget, 2011. **2**(10): p. 797-809.